



DE84013781

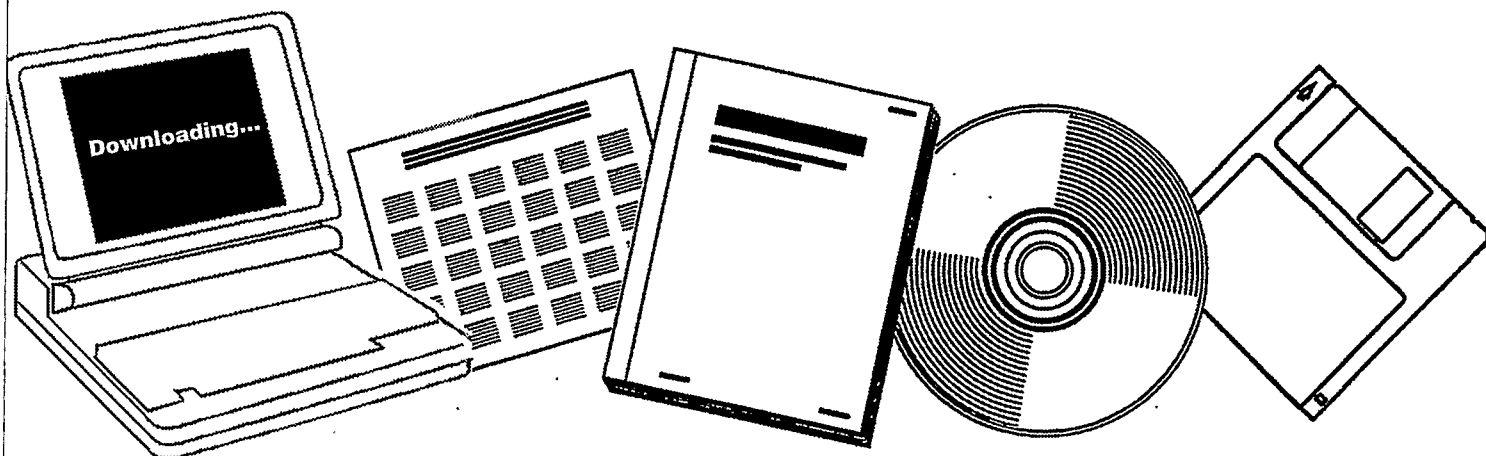
NTIS

One Source. One Search. One Solution.

IMPACT OF HYDRODYNAMICS ON COAL LIQUEFACTION. FINAL TECHNICAL REPORT

INTERNATIONAL COAL REFINING CO.
ALLENTOWN, PA

SEP 1983



U.S. Department of Commerce
National Technical Information Service

DE84013781



DOE/OR/03054-63

(DE84013781)

Distribution Category UC-89

IMPACT OF HYDRODYNAMICS ON COAL LIQUEFACTION

Final Technical Report

By
D. Kang
D. H. S. Ying
E. N. Givens

International Coal Refining Company
Allentown, Pennsylvania

TABLE OF CONTENTS

	<u>Page</u>
ABSTRACT	v
EXECUTIVE SUMMARY	1
BACKGROUND	2
Reactor Model Development	2
Effect of Laboratory Reactor Design	3
Use of CSTRs	5
Use of Tubular Reactors	6
DEVELOPMENT OF TUBULAR REACTOR DESIGN BASIS	8
Computer Simulation of the Effects of Hydrodynamics on Liquefaction	8
Tubular Reactor Design Criteria and Configuration	15
Design Criteria	15
Reactor Configuration	19
Cold-Flow Study of the Reactor Simulator	19
Preliminary Considerations	19
Experimental Procedures	25
Results and Discussion	31
Residence Time Distribution and Dispersion Analyses	34
LIQUEFACTION STUDY OF PLUG-FLOW TUBULAR REACTOR	46
Process Runs	46
Materials	53
Coal	53
Solvent	53
Results and Discussion	53
Predictability of the Sequential Reaction Model for Yield Distribution	62
Utility of Plug-Flow Reactor	70
CONCLUSIONS	73
LITERATURE CITED	75

TABLE OF CONTENTS (Continued)

	<u>Page</u>
APPENDIX A-1: DERIVATION OF THE TUBULAR REACTOR DESIGN CORRELATIONS	76
APPENDIX A-2: COLD-FLOW FLUID-DYNAMIC DATA SUMMARY FOR THE PLUG-FLOW REACTOR SIMULATOR	81
APPENDIX A-3: OPERATING AND MATERIAL-BALANCE DATA SUMMARY FOR THE PLUG-FLOW REACTOR	100
APPENDIX A-4: RELATIONSHIP OF NOMINAL LIQUID RESIDENCE TIMES TO TRUE LIQUID RESIDENCE TIME	126

ABSTRACT

This report summarizes R&D work performed in support of SRC-I plant design on the effect of reactor hydrodynamics on yield distribution. The work was initiated by Air Products, and later supported by the Department of Energy under program 12.1.5. A bench-scale tubular reactor was built to study the effect of a plug-flow fluid dynamic regime on coal liquefaction. Computer simulation and extensive cold-flow hydrodynamic studies were performed to support the reactor design. Data from the tubular reactor were compared with coal liquefaction data from a continuous stirred-tank reactor to determine how conversion and product distribution were affected.

EXECUTIVE SUMMARY

This is the final report under program area 12.1.5, the Effect of Tubular Reactor Configuration on Coal Liquefaction. This program was initiated under project 87-7-3004, Exploratory Process Studies, an ICRC internally funded research effort, and was conducted with DOE funding for a period of only three months. This report covers both the ICRC- and DOE-funded work.

The overall objectives of this program were to:

- Develop a plug-flow reactor for exploratory process studies
- Confirm or improve APCI/ICRC's existing sequential kinetic reactor model prediction
- Determine the impact of reactor hydrodynamics on coal dissolution
- Provide guidelines defining optimum reactor configurations.

In this program, a bench-scale tubular reactor was built that performed coal liquefaction in the plug-flow fluid dynamic regime. An extensive cold-flow simulation study and a computer simulation of reactor performances at various configurations were conducted to support the design of the plug-flow reactor.

Coal liquefaction data obtained from the plug-flow reactor were compared with data from a continuous stirred-tank reactor (CSTR). The plug-flow configuration enhanced coal conversion 6%, preasphaltene conversion 10%, and oil conversion 10%.

Interfacing the CSTR and plug-flow reactor yield data on a common fluid dynamic basis using APCI/ICRC's sequential kinetic model revealed that the model requires improvement. Predicted plug-flow yields deviated considerably from actually measured values. Having both plug-flow and CSTR data bases is important for developing a sound model and for determining the effects of reactor hydrodynamics on coal liquefaction in a direct way.

BACKGROUND

In order to evaluate design options and determine operating conditions for an optimized coal liquefaction plant, an understanding of the reaction sequence in the dissolver is essential. One of the key efforts in designing the 6,000-ton-per-day SRC-I Demonstration Plant was development of mathematical correlations describing dissolver behavior.

REACTOR MODEL DEVELOPMENT

Design of the demonstration plant dissolver was based on data available from laboratory and pilot-plant reactors. However, relating such data to the demonstration-plant scale was difficult because of the different hydrodynamic behaviors in the reactor systems. Simulation of coal liquefaction in laboratory reactors involves equipment having geometries that give different flow velocities, interfacial phase contacts, length-to-diameter ratios, wall relationships, and ratios of reactant phases than larger demonstration-sized units. These factors affect heat- and mass-transfer behavior, as well as residence time and solid accumulation behavior. Satisfactory laboratory simulation of large reactors is especially critical for upflow slurry reactors.

Considerable effort was expended by APCI, and later by ICRC, to ensure that the laboratory reactors used for coal liquefaction experiments would effectively simulate larger reactors. Many of the questions regarding dissolver and preheater design were addressed in cold-flow studies on both laboratory and larger scale simulators.

Understanding hydrodynamic behavior allowed us to address the impact that reactor design would have on the relative reaction scheme. Most of our work in the laboratory coal process development unit (CPDU) had been conducted in backmixed reactors. In order to complete our understanding of the impact of reactor hydrodynamics on the liquefaction reaction, a brief study was conducted to determine the effect of plug-flow hydrodynamics on liquefaction.

A laboratory tubular reactor was designed and fabricated to conduct these experiments. One serious problem in designing a laboratory reactor was the need to keep liquid and gas velocities, as well as residence time, within the range required for the large reactor. The relationship between gas and liquid superficial velocities for various dissolver sizes is illustrated in Table 1. Only Exxon's 250-tpd coal liquefaction pilot plant (ECLP) reactor approached the actual velocities that would be experienced in a demonstration-sized unit. All the others were off by at least a factor of three.

EFFECT OF LABORATORY REACTOR DESIGN

Obviously, the geometric dimensions of small-scale reactors impose considerable limitations on developing a meaningful simulation of demonstration-scale units, because of the widely different degrees of liquid backmixing, gas hold-up, solids accumulation, and other hydrodynamically induced behavior. For example, unacceptably large amounts of solids accumulation were often found in the dissolvers at the Wilsonville and Ft. Lewis pilot plants, which hindered data analyses. Withdrawal of accumulated solids from the bottom of the Wilsonville dissolver was only a partial solution.

Thus, an R&D program was initiated to decouple the hydrodynamic effects from the overall coal liquefaction reaction in a small laboratory reactor. Most of the SRC-I reaction data were generated from an ideal reaction system in a continuous stirred-tank reactor (CSTR). The scale-up data to address the impact of hydrodynamics on reactor performance largely depended upon various tubular columns, ranging in size from a few inches to 6 ft in diameter. Results from cold-flow studies answered many key questions regarding scale-up in the area of hydrodynamics.

The overall process data based on CSTR runs provided an indirect way to evaluate reactor performance. However, using the CSTR data to predict reactor yields at another fluid dynamic condition is valid only if the pseudocomponents defined for the reactor yields are uniquely identifiable and free from the history of reaction conditions. State-of-the-art analytical characterization methods have not yet validated

Table 1

Relationship between Gas and Liquid Superficial Velocities
for Various Dissolver Sizes

Plant	Capacity (tons/day)	Volume (ft ³)	Diameter (ft)	Height (ft)	Superficial velocities (ft/sec)	
					Liquid	Gas
Wilsonville	6	18.6	1	23	0.012	0.074
Ft. Lewis	50	106.8	2	34	0.017	0.10
ECLP (EDS) ^a	250	2,764	2	220 ^c	0.052	0.32
SRC-I Demo Plant	6,000	10,454	11	110	0.06	0.36
CPDU (CSTR) ^b	0.05	0.035	0.3	0.5	0.005	0.031

^aECLP, Exxon Coal Liquefaction Plant; EDS, Exxon donor solvent.

^bCSTR, continuous stirred tank reactor.

^cRepresents total length for all four reactors.

this underlying assumption nor is it likely to be clarified in the near future. Thus, supplementing the CSTR data with plug-flow data provided a direct way to assess the effect of hydrodynamic behavior on coal dissolution and also minimized the risks associated with a plant design based only on CSTR data, especially since coal liquefaction chemistry is so elusive.

Plug-flow data were also developed to help choose the optimum reactor configuration. A variety of options with different degrees of backmixing were available. The EDS process uses four reactor in series, and two reactors in series or in parallel were considered for the SRC-I process.

In the process of designing and fabricating the pilot-plant plug-flow reactor, an extensive cold-flow study was performed in a simply prepared piece of laboratory equipment. The equipment was designed to simulate actual reactor conditions so that gas hold-up and dispersion correlations could be developed to confirm that plug-flow behavior occurred in the pilot-plant reactor.

Data developed from the pilot-plant plug-flow reactor showed a better product yield distribution than predicted by ICRC/APCI's sequential kinetic model and also provided the key information needed to improve the kinetic correlation.

USE OF CSTRs

CSTRs were widely used for laboratory coal liquefaction studies to support development of large-scale tubular bubble column reactors. The major advantage in using a CSTR is the well-defined mixing and residence-time behavior of its liquid phase. Because of the simple reactor hydrodynamics, the data generated from a CSTR can be conveniently manipulated to develop kinetic and other process correlations. The kinetic correlations can be translated to predict the performance of reactors with different hydrodynamics, if the hydrodynamics of those reactors are known. This allows prediction of product distribution and reactor performance for the large-scale reactors, whose hydrodynamics may be intermediate between complete plug-flow and backmixed states.

A major difficulty in using the CSTR to simulate the gas-phase residence time behavior of tubular reactors is the CSTR's low length-to-diameter (L/D) ratio. Also, the very short gas-phase residence time inherent to a CSTR results in imprecise simulation of the gas-to-liquid reactant distribution, which impacts gas-to-liquid mass transfer in the reaction. Whether this is a major problem for the reaction in question can be determined through use of a tubular reactor in laboratory simulation.

Still another problem associated with simulating coal liquefaction in a CSTR is that the coal dissolves in the presence of the ultimate reaction products. In contrast, in large-scale operation, all of the dissolution occurs in the preheater. Use of a tubular reactor can prevent the distortion of results that may occur during dissolution in the presence of ultimate products.

USE OF TUBULAR REACTORS

Others have used tubular reactors to develop liquefaction data, including Exxon and Gulf in support of the EDS and SRC-II processes, respectively. However, use of tubular reactors is not completely free of complications. In order to use a laboratory tubular reactor correctly for simulation, both residence time and mixing behavior of the various phases in the reactor should be accurately determined, in order to separate hydrodynamic effects and intrinsic reaction kinetics from the observed reaction data. Undoubtedly, a major drawback of a tubular reactor system is its less definitive hydrodynamics, which casts considerable uncertainty upon the data analysis. Thus, the laboratory tubular reactor is practical only if its fluid dynamic characteristics are similar to a plug-flow reactor. Even with a plug-flow reactor, its void space must be accurately measured at various flow conditions in order to determine the liquid residence time. Therefore, cold-flow studies on any laboratory tubular simulator are necessary in order to develop a correlation for void space (residence time) over the desired operating ranges of gas and liquid velocities. These data are needed to confirm the plug-flow characteristics of the reactor in that range of operating conditions (operating window).

CSTR data can be transformed to predict the performance of other nonideal reactors having different fluid dynamic conditions only when both the kinetic correlations from the CSTR and the hydrodynamic correlations from cold-flow simulation of its counterpart reactors are accurately developed. Both correlations are bound to involve considerable uncertainties. Unfortunately, state-of-the-art methods for characterizing coal liquefaction products cannot provide data accurate enough to lead to accurate kinetic correlations. Uncertainties also plague the hydrodynamic correlations, because of the many unknowns involved. When combined with CSTR data, plug-flow liquefaction data can provide a direct way to determine the effects of fluid dynamics on coal liquefaction and to interpolate reaction kinetic data to other fluid dynamic conditions, rather than extrapolating from either plug-flow or CSTR data alone. Certainly, this direct combination of CSTR and plug-flow data offers both a feasible and precise way to develop reaction kinetics and process data correlations, compared to conventional approaches. In addition, CSTR/plug-flow liquefaction data can provide better guidelines to use in searching for the optimum reactor configuration, because the largest fluid dynamic effects on liquefaction exist between the two reaction systems.

DEVELOPMENT OF TUBULAR REACTOR DESIGN BASIS

COMPUTER SIMULATION OF THE EFFECTS OF HYDRODYNAMICS ON LIQUEFACTION

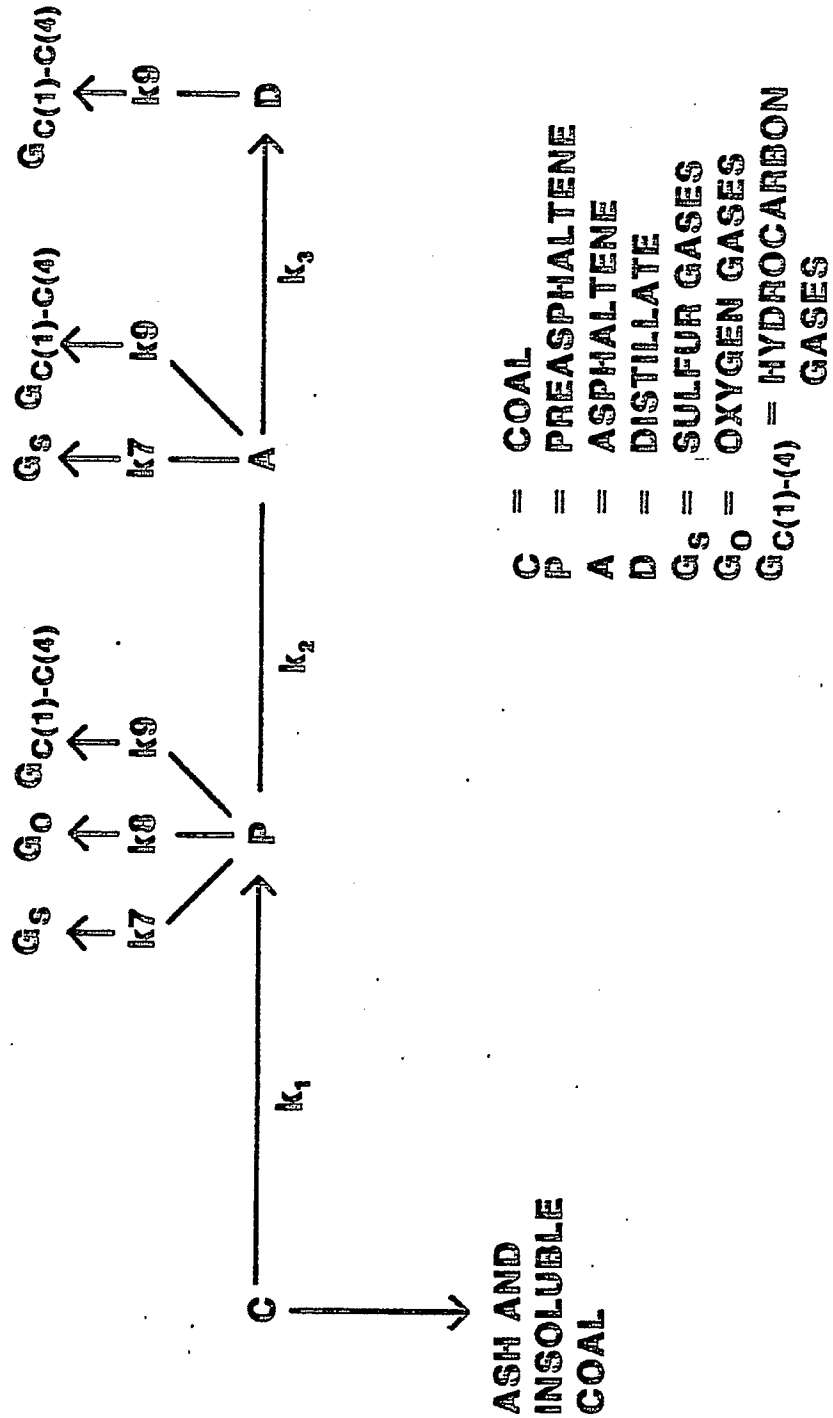
A computer simulation study was conducted using the APCI/ICRC sequential kinetic reaction model (Martin, 1979) to predict the impact of hydrodynamics on yield distribution, and to determine the design of the proposed plug-flow experimental tubular reactor. The sequential model (shown in Figure 1) assumes that coal converts to preasphaltenes, preasphaltenes to asphaltenes, and asphaltenes to distillate. Gas forms from all of the intermediate products. This model, supported by the CSTR data base, was used extensively to evaluate dissolver performance during SRC-I Demonstration Plant design. The model's adequacy can unquestionably be improved as more data accumulate. However, use of this model was sufficient for the current study.

Figures 2-6 summarize the results, based on the Kentucky #9 Pyro coal data base. The residence time was 40 min and temperatures covered the demonstration plant operating range of 760-850°F.

Reactor hydrodynamics were predicted to impact preasphaltene and asphaltene yields the most. For example, at 840°F, compared to the CSTR, the plug-flow reactor was predicted to yield 16% fewer preasphaltenes (from 32 to 16%) (Figure 2), 17% more asphaltenes (from 32% to 49%) (Figure 3), 3% more coal converted (from 93% to 96%) (Figure 4), and 4% more oils (from 23 to 27%) (Figure 5). At 815°F, a crossover in oil yields occurs, with a decline in oil yield predicted for the plug-flow reactor. Insignificant differences in the gas yields were predicted (Figure 6).

Figures 2-6 also compare the yield distributions predicted for 10 CSTRs in series with those for a single CSTR and a plug-flow reactor. The performance of 10 CSTRs in series closely resembles that of the plug-flow reactor, but differs distinctively from that of the single CSTR; that is, the conversion of coal and the oil and gas yields become nearly identical to those for the plug-flow reactor, whereas preas-

FIGURE 1
SEQUENTIAL REACTION MODEL



- C = COAL
- P = PREASPHALTENE
- A = ASPHALTENE
- D = DISTILLATE
- G_s = SULFUR GASES
- G_o = OXYGEN GASES
- $G_{C(1)-(4)}$ = HYDROCARBON GASES

FIGURE 2
EFFECT OF FLUID DYNAMICS
ON PREASPHALTENE YIELDS
BASIS—40 MINUTES AND KY#9 PYRO COAL DATA BASE

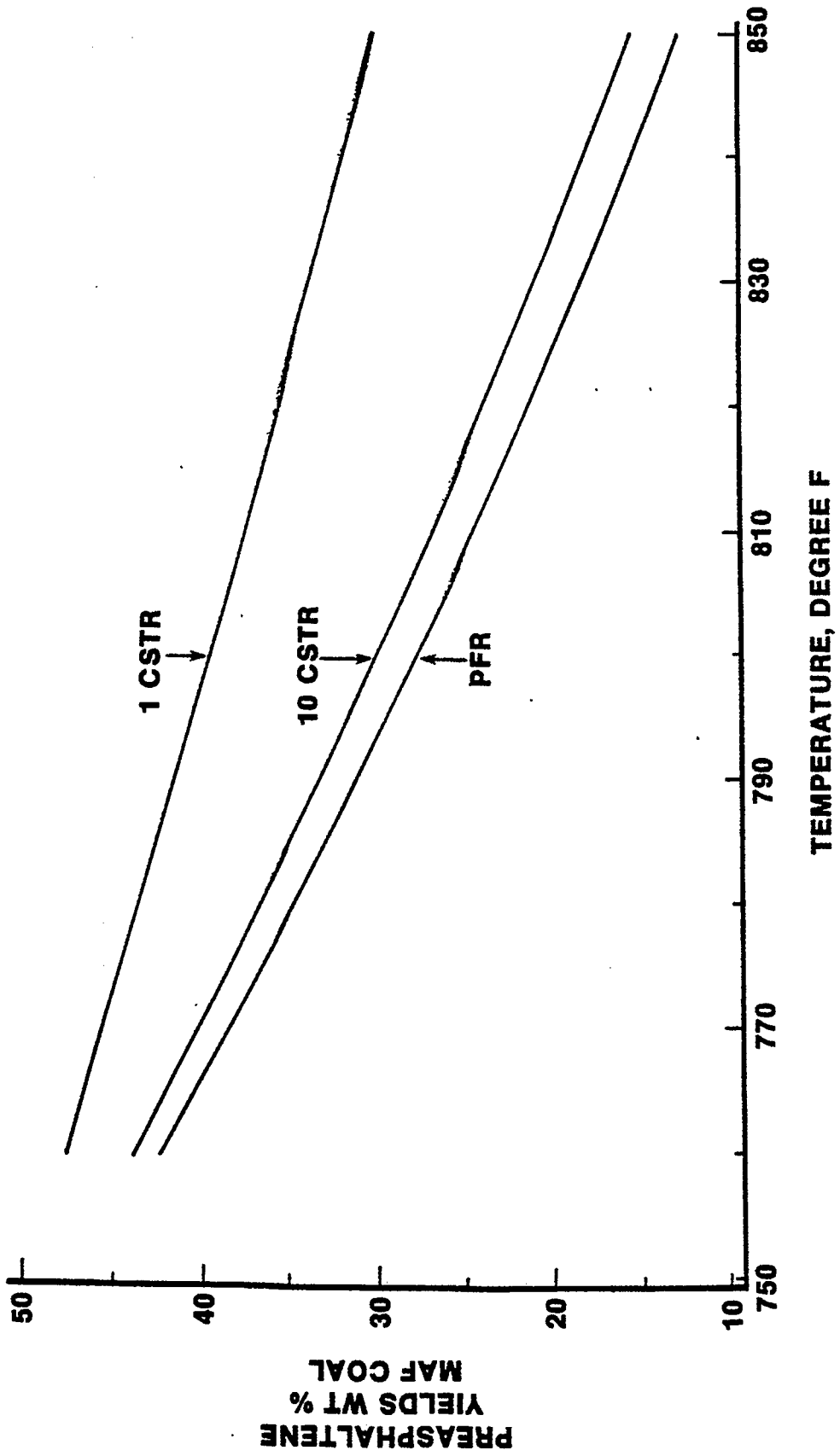


FIGURE 3
EFFECT OF FLUID DYNAMICS
ON ASPHALTENE YIELDS
BASIS--40 MINUTES AND KY#9 PYRO COAL DATA BASE

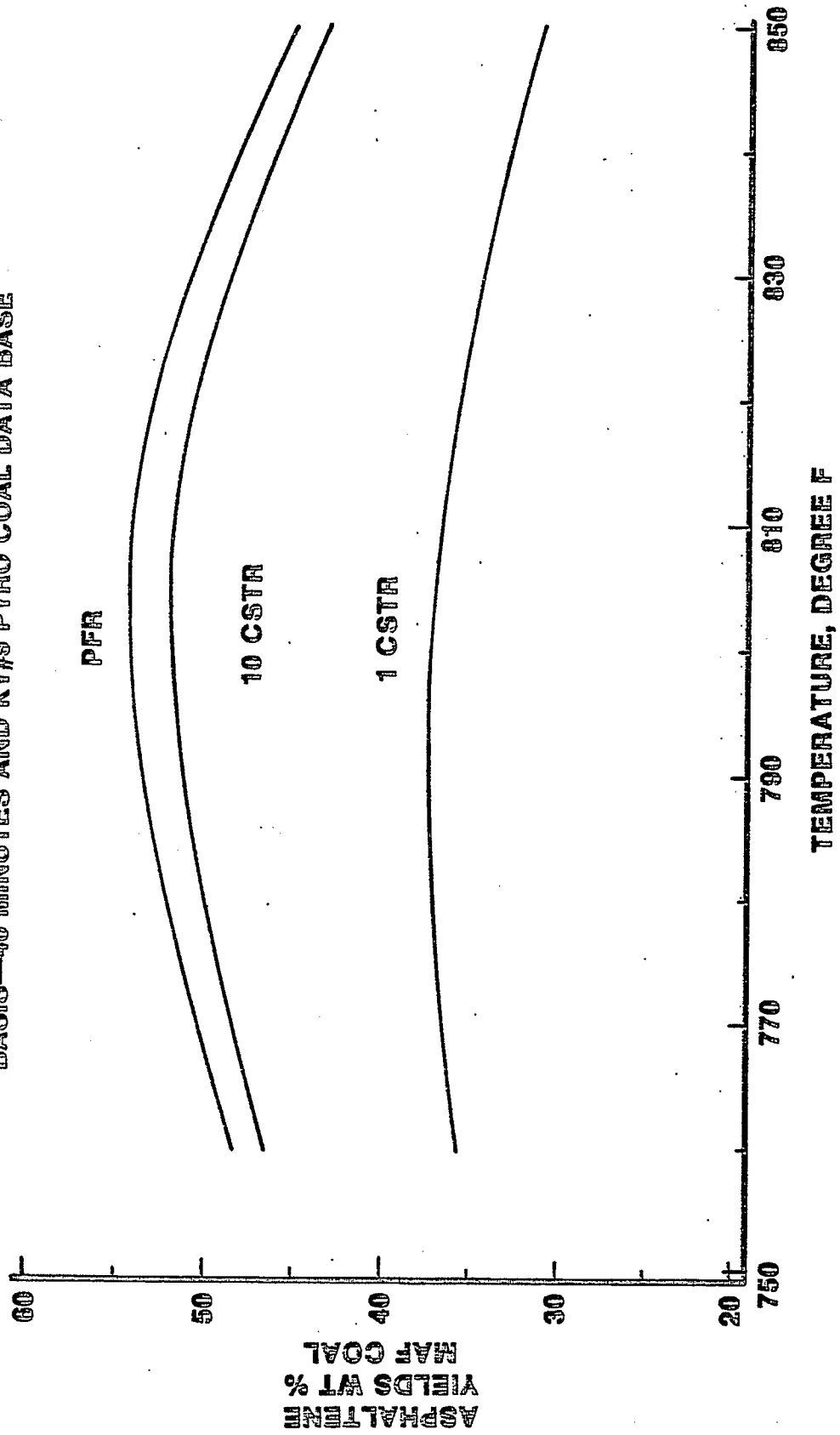


FIGURE 4
EFFECT OF FLUID DYNAMICS ON CONVERSION
BASIS—40 MINUTES AND KY#9 PYRO COAL DATA BASE

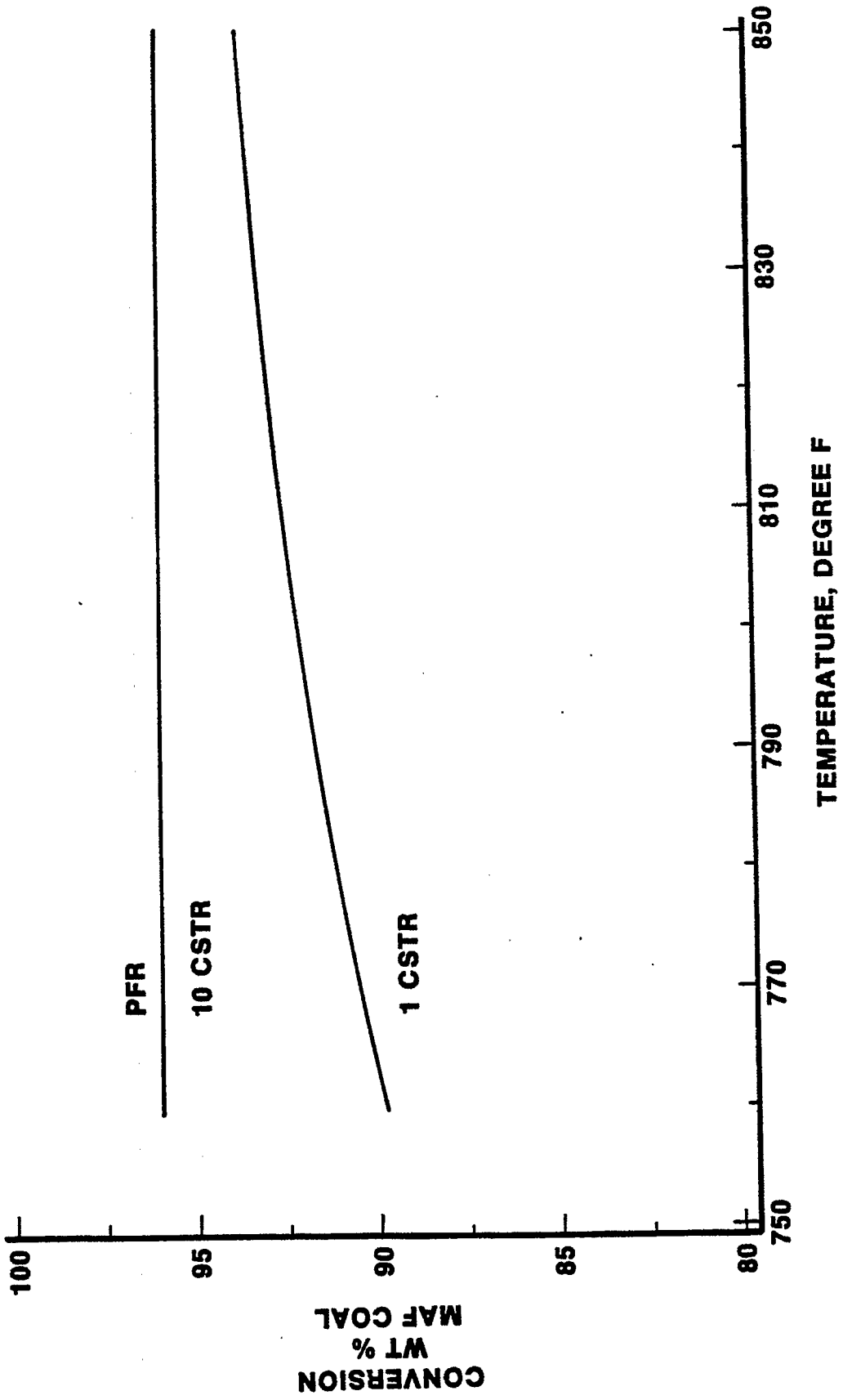


FIGURE 5
EFFECT OF FLUID DYNAMICS ON OIL YIELDS
BASIS—40 MINUTES AND KY/S PYRO COAL DATA BASE

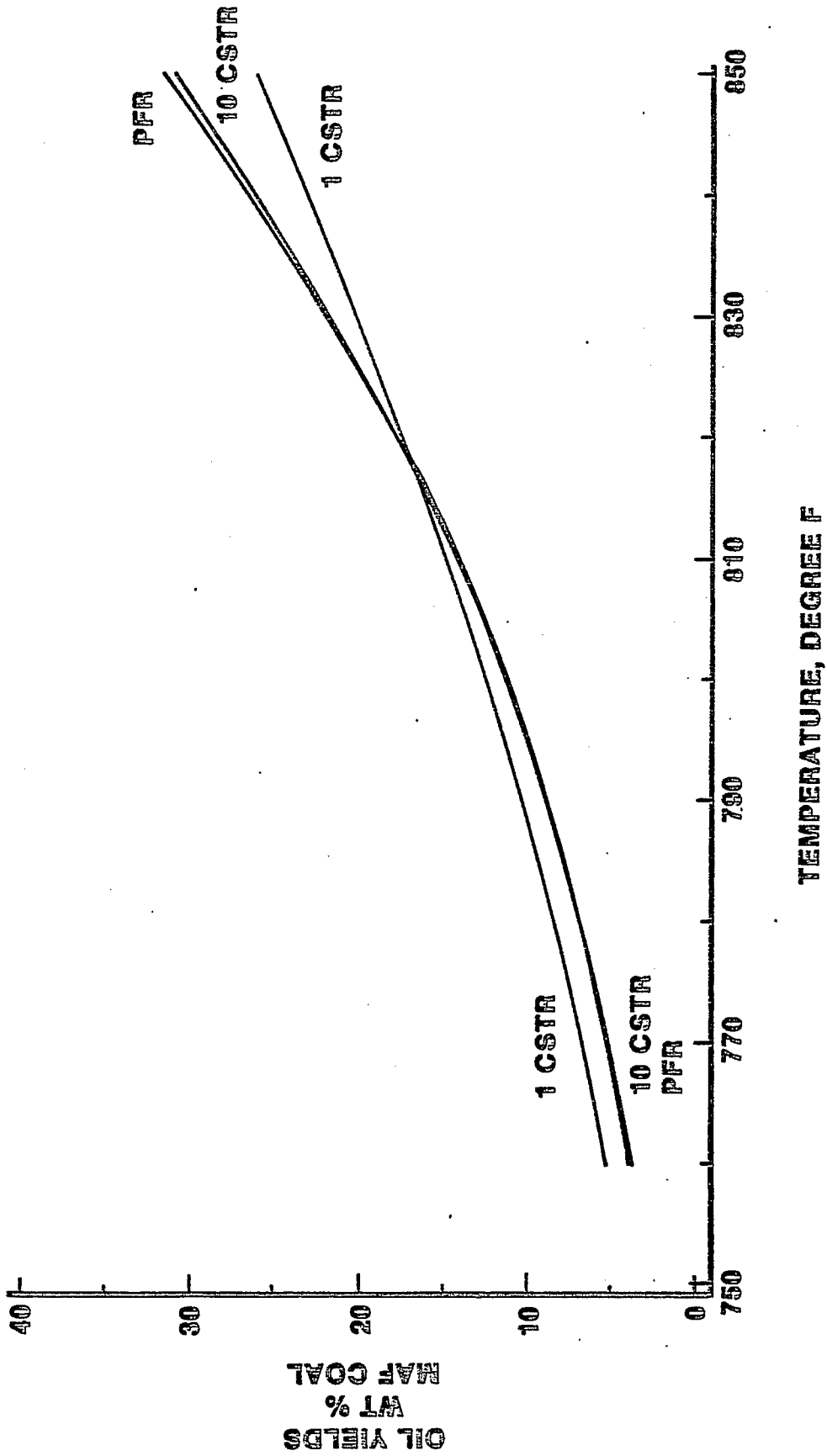
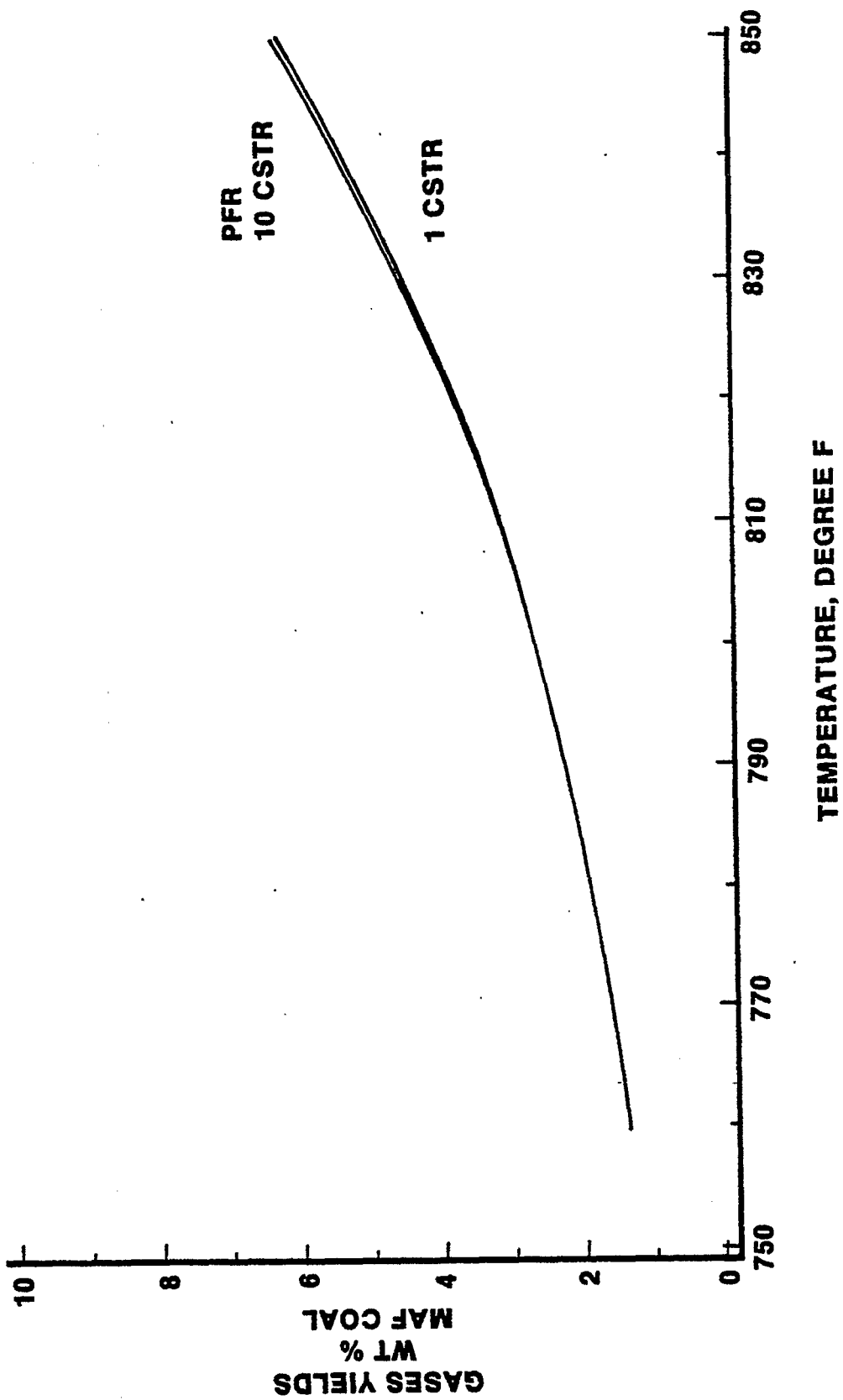


FIGURE 6
EFFECT OF FLUID DYNAMICS ON GASES YIELDS
BASIS—40 MINUTES AND KY#9 PYRO COAL DATA BASE



phaltene and asphaltene yields do not differ by more than 3% from those of the plug-flow reactor. Increasing the number of CSTRs to 20 caused less than 1.5% deviation in preasphaltene and asphaltene yields, within the operating temperatures of the plug-flow reactor. Since such small differences cannot be measured with current analytical techniques, the performance of 20 CSTRs in series is considered virtually identical to that of the plug-flow reactor.

TUBULAR REACTOR DESIGN CRITERIA AND CONFIGURATION

Design Criteria

Since our CPDUs were typically equipped with 1-L reactors, a 1-L volume was chosen as the size for the new experimental tubular reactor to maintain consistency. On the basis of this capacity, Peclet numbers (which define the extent of backmixing as predicted by the axial dispersion model) were correlated with the reactor diameters (see Figure 7). Derivations of these correlations are detailed in Appendix A-1.

According to this correlation, Peclet numbers (which relate directly to the plug-flow characteristics of the reactor) will increase rapidly at smaller reactor diameters. Operating residence time also impacts the Peclet numbers, but to a lesser degree.

By merging a tanks-in-series model and an axial dispersion model (Levenspiel and Bischoff, 1963), reaction kinetics and reactor hydrodynamics could be easily related. Residence time/distribution curves were plotted for various reactors, in dimensionless concentration vs. dimensionless residence time scales (local concentration and local residence time normalized to total concentration and to mean residence time, respectively), as predicted by both models (Figures 8 and 9). As the number of CSTRs increased, the degree of backmixing decreased, as indicated by the sharper residence time/distribution curves, resulting ultimately in a plug-flow reactor configuration. Similarly, as backmixing in the reactors decreased, the Peclet numbers became larger until they ultimately approached infinity at the perfect plug-flow reactor condition.

FIGURE 7
PREDICTED MIXING CHARACTERISTICS OF A
DESIGN TUBULAR REACTOR AS FUNCTIONS
OF ITS GEOMETRY AND RESIDENCE TIME

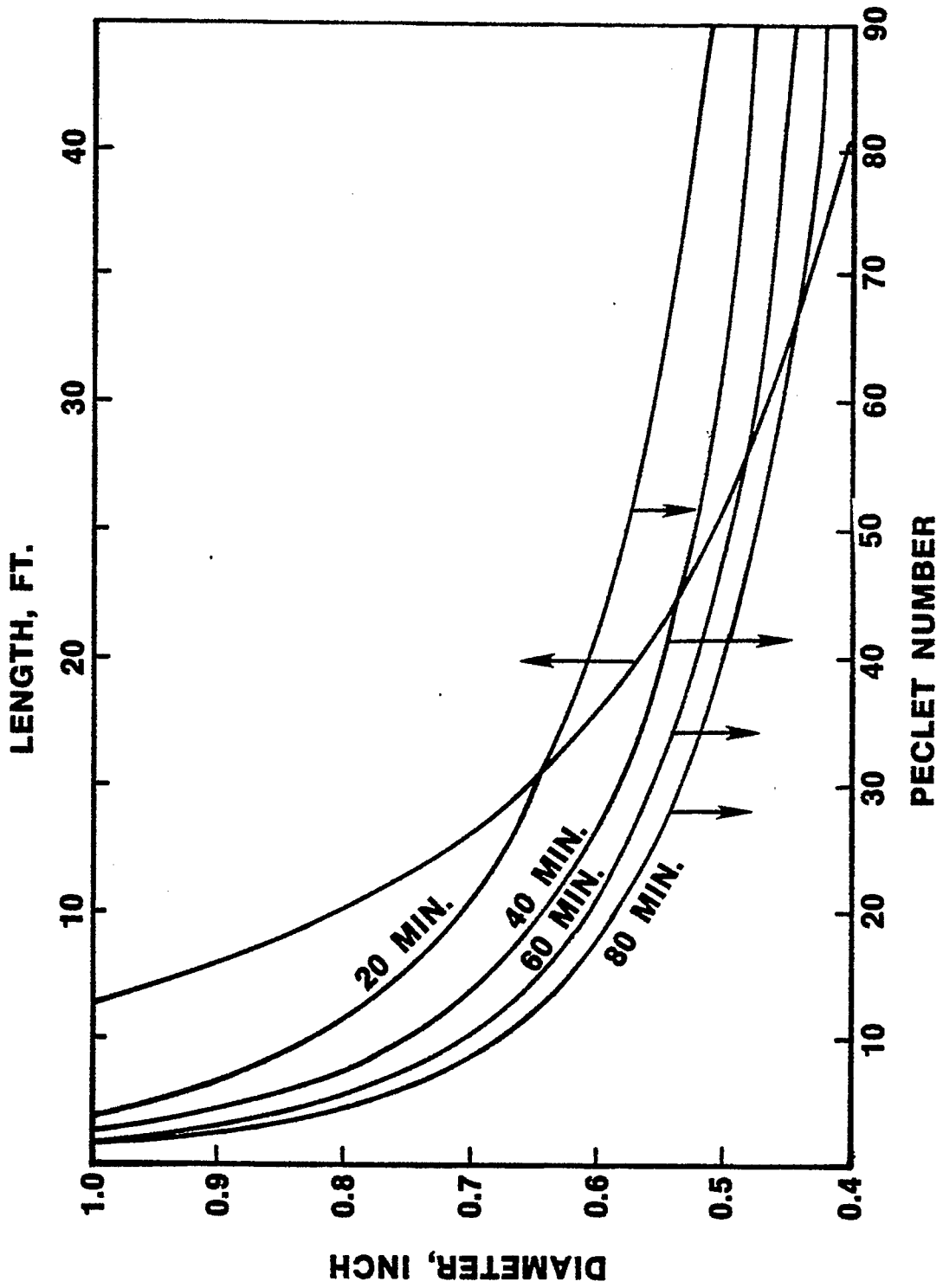
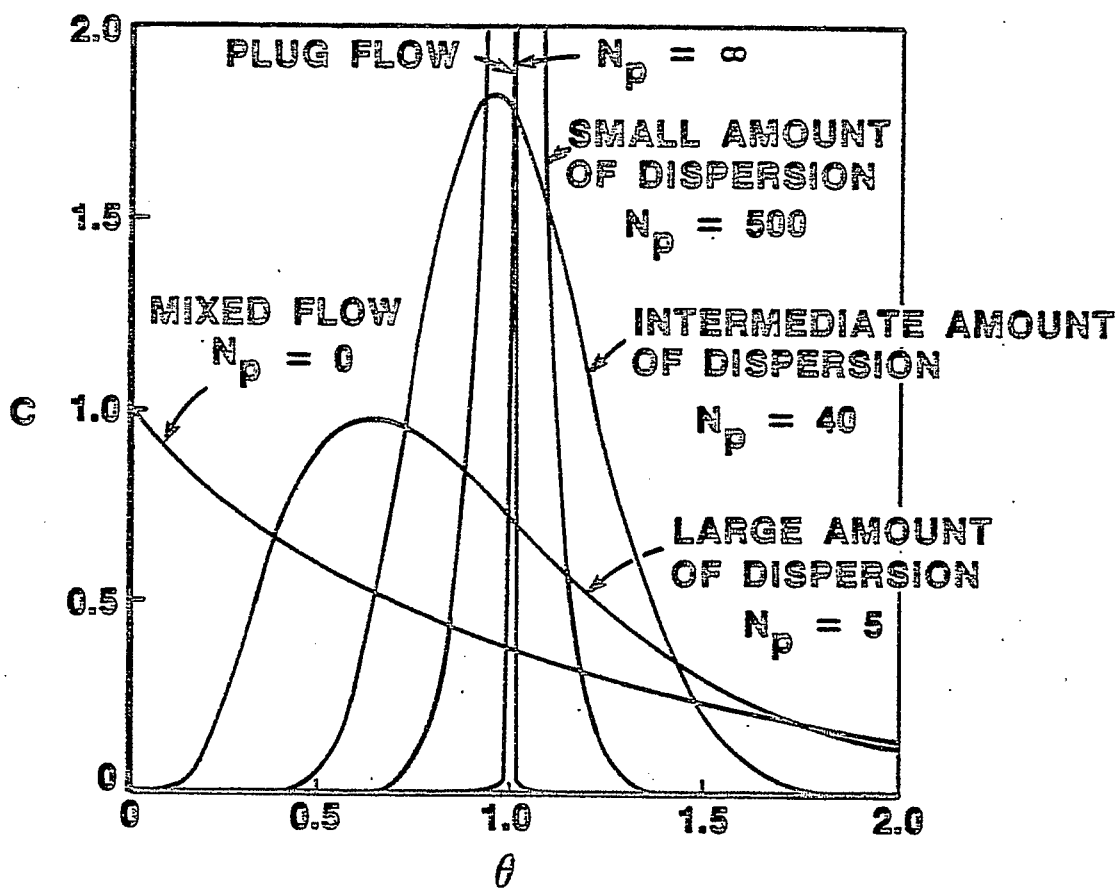
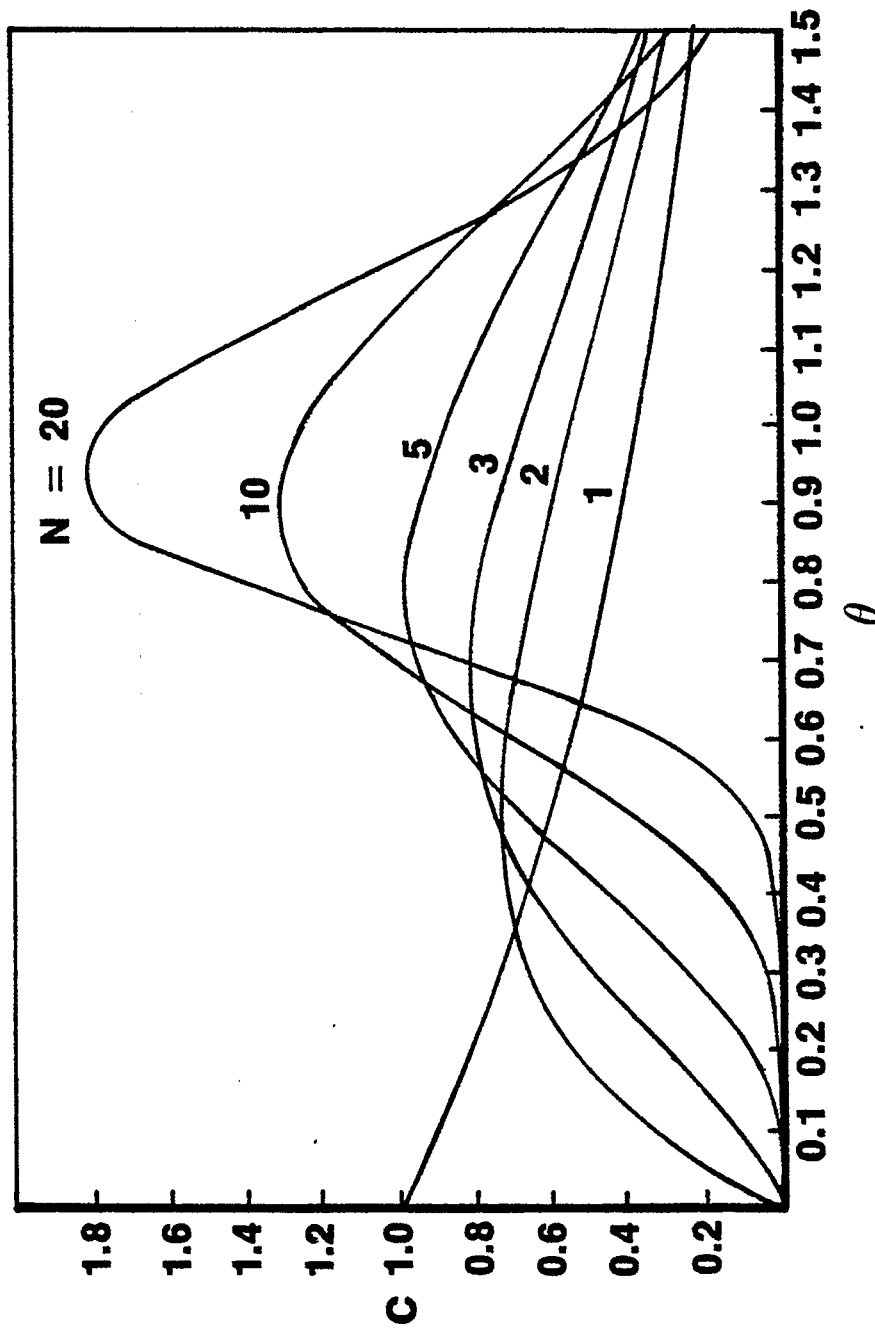


FIGURE 8
C CURVES IN CLOSED VESSELS FOR VARIOUS
EXTENTS OF BACKMIXING AS PREDICTED BY
THE DISPERSION MODEL



N_p = PÉCLET NUMBER
 C = NORMALIZED CONCENTRATION
 θ = DIMENSIONLESS RESIDENCE TIME

FIGURE 9
C CURVE FOR TANKS IN SERIES MODEL



N = NUMBER OF TANKS IN SERIES
C = NORMALIZED CONCENTRATION
 θ = DIMENSIONLESS RESIDENCE TIME

Our computer simulation had predicted that reactors with mixing equivalent to 10 or 20 CSTRs would perform close to the plug-flow regime, so that preasphaltene and asphaltene yields would deviate by less than 3 and 1.5%, respectively, from the perfect plug-flow regime. Ten and twenty CSTRs in series would give Peclet numbers of about 20 and 40, respectively.

Reactor Configuration

The preceding analyses indicated that the internal diameter for a practical plug-flow reactor with a Peclet number above 40 and a residence time of up to 80 min should be slightly larger than 0.5 in. Thus, based on the availability of materials and practical limitations on the tubing length, tubes with inside diameters of 0.56 in. (9/16 in.) were used to fabricate the actual reactor.

The reactor consisted of seven tubular sections, each approximately 4-ft long (excluding a preheater section with identical dimension), which were interconnected by downcomers. The "s"-shaped downcomer segments had tubular diameters of 0.203 in. i.d. (13/16 in.), and the fittings between the tubes and downcomers were streamlined to minimize backmixing of media within the fittings and downcomers.

Specific dimensions and sizes are shown in Figures 10 and 11 and Table 2. The entire reactor system was submerged into a sand bath for accurate temperature control under isothermal conditions. The general layout of the unit is shown in Figure 12. Other facets of the unit are the same as used in prior experimental programs.

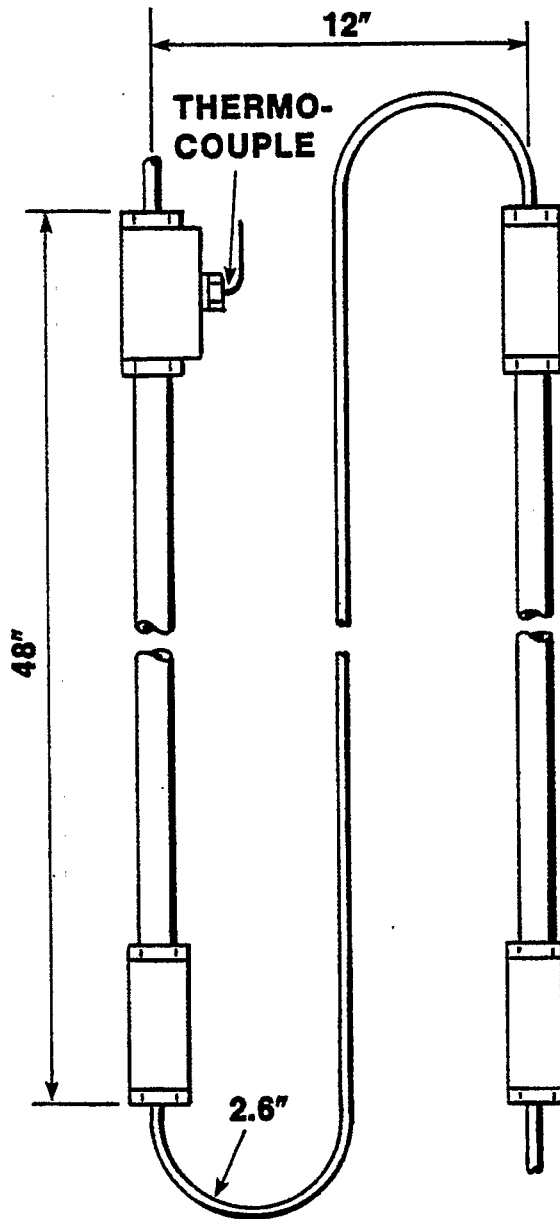
COLD-FLOW STUDY OF THE REACTOR SIMULATOR

Preliminary Considerations

A meaningful cold-flow study requires selection of fluid media having physical properties that can best represent actual reactor contents. Unfortunately, accurate physical properties of liquefied coal at reaction conditions were unavailable. Also, the physical properties of reactor fluids are not constant, but vary as the reaction progresses. Figure 13 illustrates how coal slurry viscosities are predicted to change as the reaction progresses through the preheater and dissolver.

**FIGURE 10
PREHEATER AND REACTOR SIDE VIEWS**

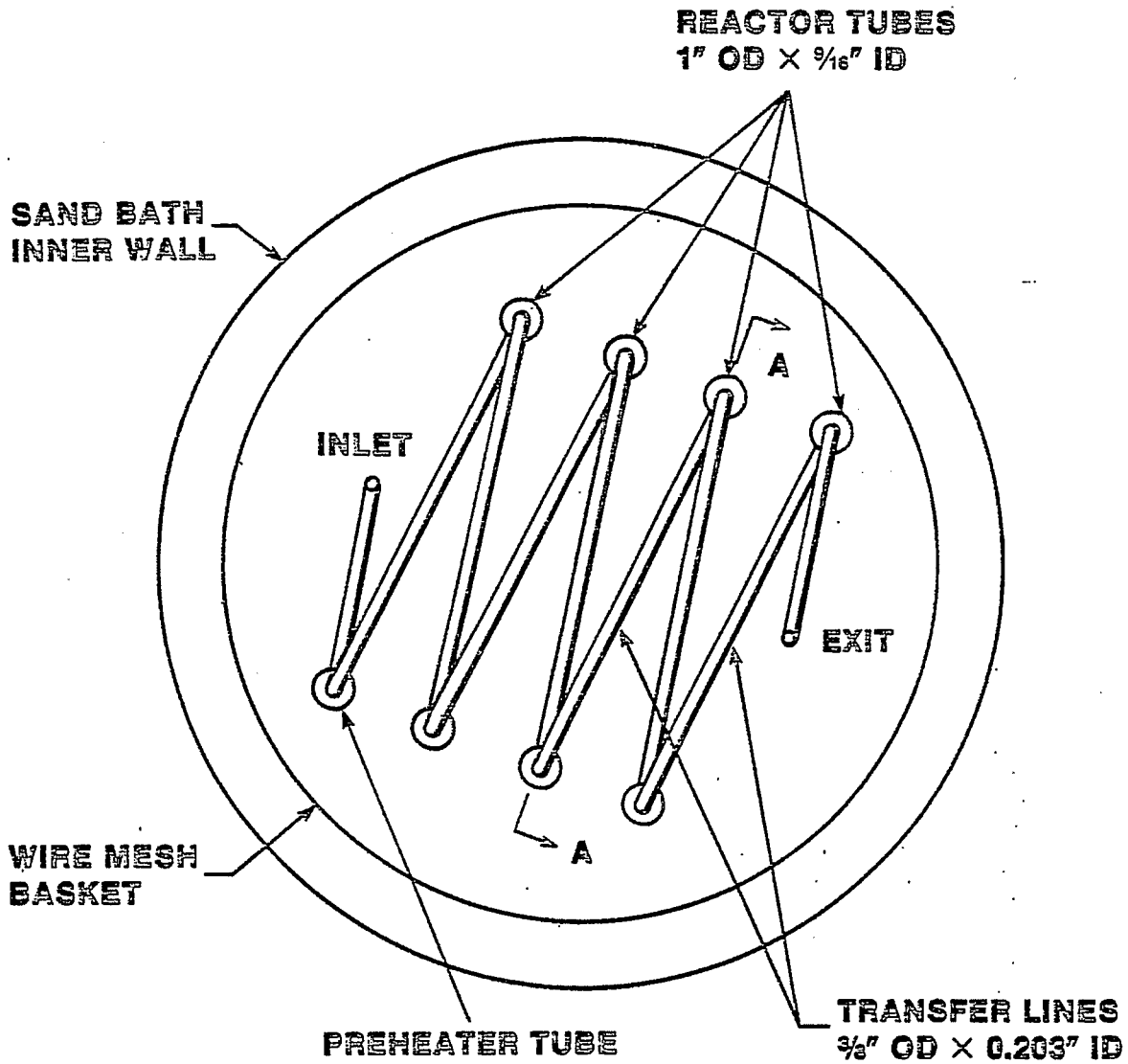
SECTION A-A



REACTOR TUBE ASSEMBLY

SCALE - 1/5

FIGURE 11
TUBULAR REACTOR BUNDLE
TOP VIEW



SCALE = 1/5

Table 2
Detailed Dimension Data for the Tubular Reactor System

Tube			Downcomer		
No.	Diameter (in.)	Length (in.) ^a	No.	Diameter (in.)	Length (in.) ^a
Preheater	9/16	(45.46)	P-1	0.203	(78.00)
1	9/16	45.44	1-2	0.203	77.74
2	9/16	45.38	2-3	0.203	77.93
3	9/16	45.41	3-4	0.203	77.93
4	9/16	45.38	4-5	0.203	78.11
5	9/16	45.44	5-6	0.203	78.18
6	9/16	45.41	6-7	0.203	78.11
7	9/16	45.81			
	Total	318.25 (363.71)	Total =	468.00 (546.00)	
		= 26.52 ft (30.31 ft)	=	39 ft (45.5 ft)	

Excluding Preheater

Reactor volume of tube sections = 1,296 mL
 Reactor volume of downcomer sections = 249 mL
 Total volume = 1,545 mL

Including Preheater

Reactor volume of tube sections = 1,481 mL
 Reactor volume of downcomer sections = 291 mL
 Total volume = 1,772 mL

^aIncluding extended sections in fittings; numbers in parentheses include preheater section.

FIGURE 12
SCHEMATIC DIAGRAM OF TUBULAR REACTION
SYSTEM

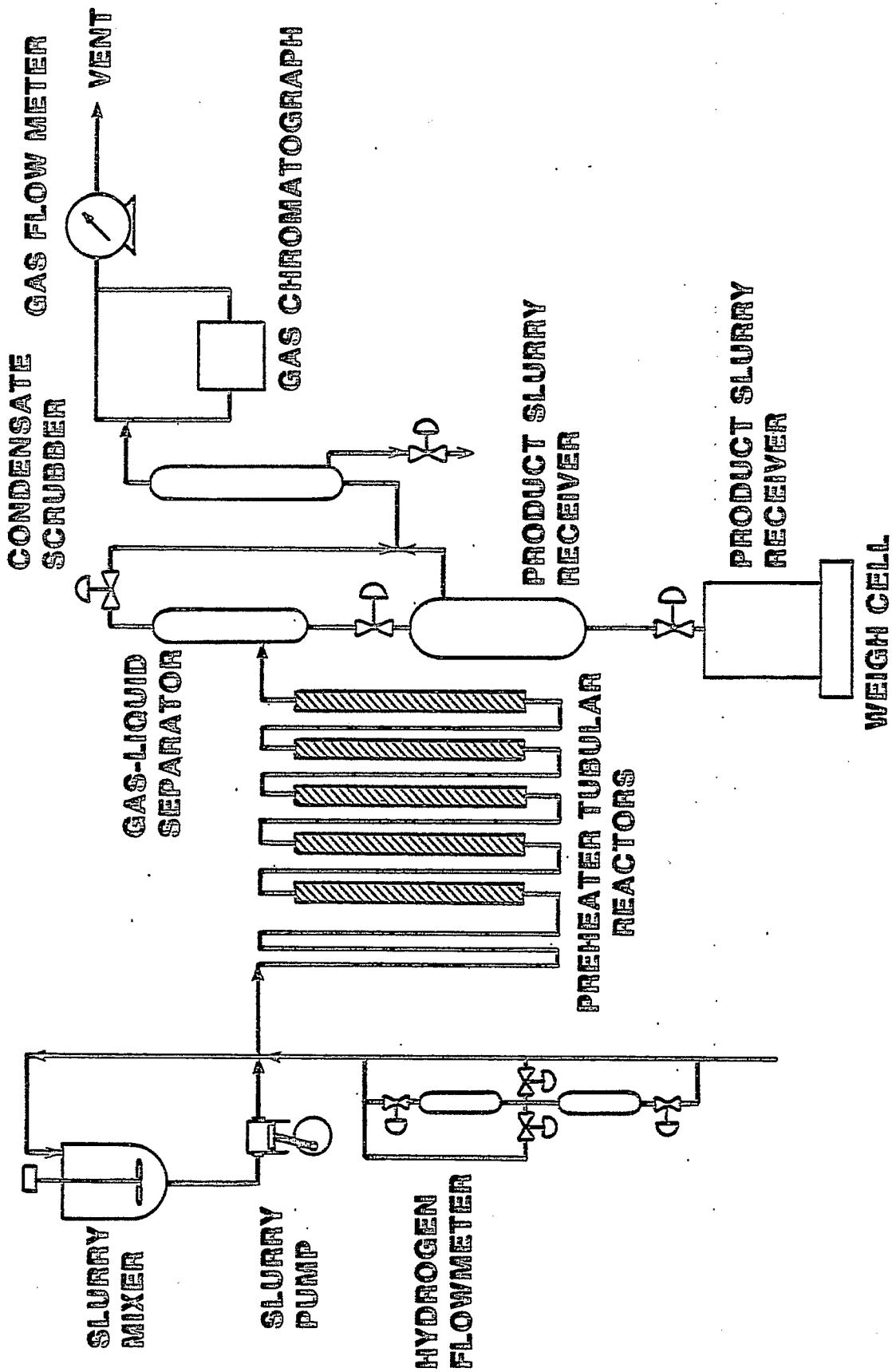
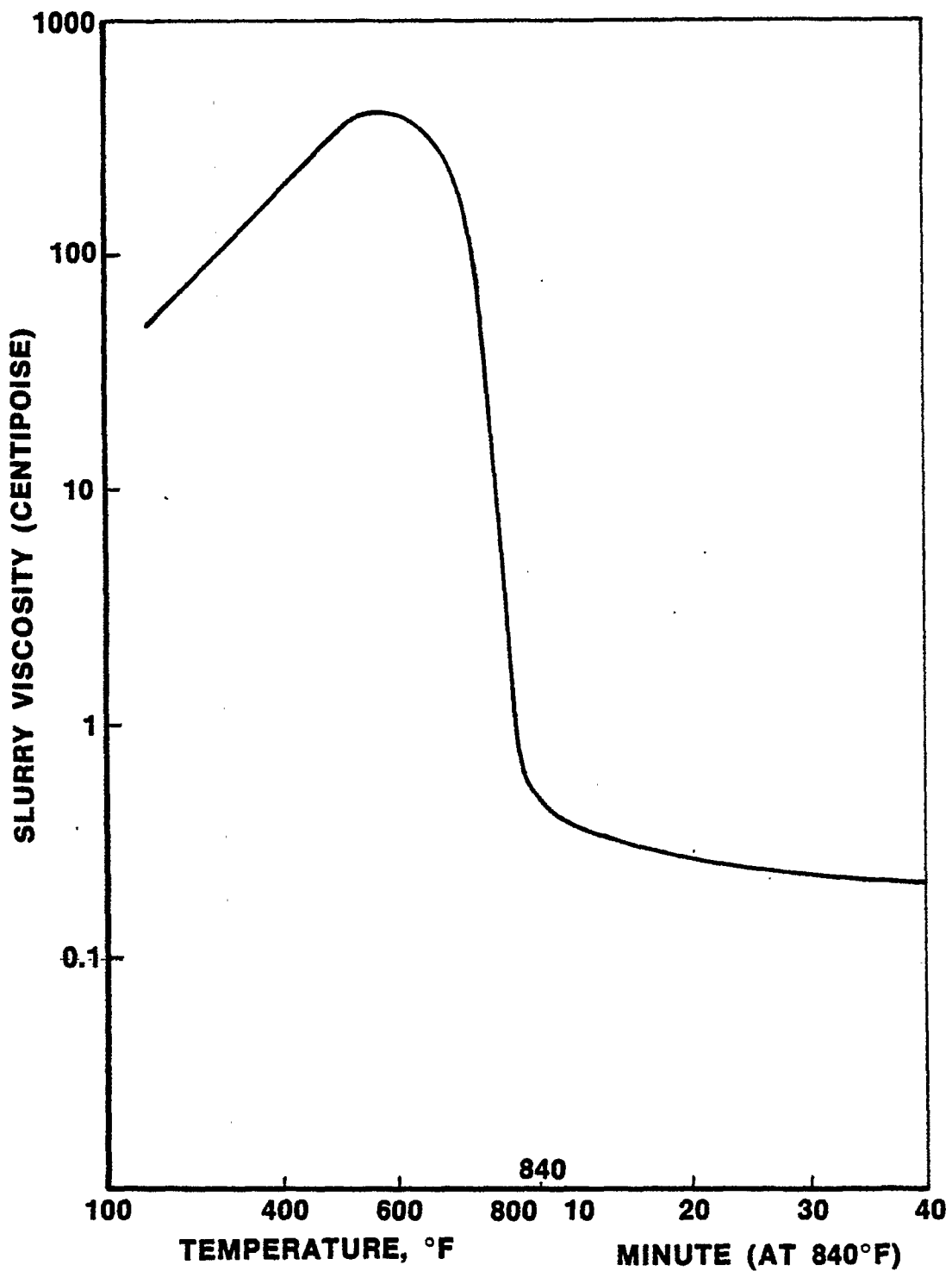


FIGURE 13
SLURRY VISCOSITY VS. TEMPERATURE AND
RESIDENCE TIME



However, we assumed that the changes of the liquid viscosity in the reactor are relatively small after the coal slurry passes from the preheater; we estimated the changes to be in the range of 0.2 to ~1 cP at typical demonstration plant conditions.

Likewise, we can reasonably assume that other major physical properties that are known to impact residence time and mixing characteristics, such as density and surface tension, will not vary unexpectedly throughout the reactor. Table 3 summarizes the ranges of three major physical properties (viscosity, density, and surface tension) typical of reactor fluids at demonstration plant conditions. The table also compares these properties with those of the model fluids considered for the study. Understanding the effect of changing physical properties on fluid dynamic characteristics is desirable in order to gauge the impact of varying properties of the reactor contents. Unfortunately, due to time constraints, only water and methanol were used for our cold-flow simulation, and nitrogen was the only gas-phase model compound tested. The density of nitrogen gas is considerably lower than the gas-phase density predicted to exist at reactor conditions, but heavier gases such as Freon could not be tested because of manpower and time constraints.

However, when the effect of gas density on void space was evaluated using a modified Hughmark (1967) correlation (modified by replacing the liquid-phase density with the differential density between liquid and gas phases), the change of void space within the range of the projected operating conditions is marginal (about 5-6% lower in the nitrogen simulation system than in the projected dense vapor phase in the reactor). The diameter we selected for the simulator (about 0.56-0.63 in.) is much smaller than Hughmark's experimental range (based on columns larger than 1 in. in diameter). Thus, experimental verification of gas-density effects on the void space, preferably using heavy gases, should be performed in order to clarify the uncertainty associated with this simulation study.

Experimental Procedures

Two model simulators with nearly identical geometry to the tubular reactor system were constructed to characterize the reactor hydrodynamics. A Plexiglas simulator was used to study water/nitrogen and a

Table 3

Comparison of Predicted Physical Properties of Reactor
Effluents and Cold-Flow Model Fluids

Basis 840°F, 2,000 psig

Slurry phase			
Viscosity		0.2-0.6 cP	
Surface tension		~15 dyne/cm	
Density		~0.8 g/cm ³	
Vapor phase			
Density		0.045 g/cm ³	
Density of hydrogen		4.6 x 10 ⁻³ g/cm ³	

System	Surface tension (dyne/cm)	Viscosity (cP)	Density (g/cm ³)
H ₂ O/air at 25°C	71.97	0.89	0.997
Acetone/air at 25°C	22.67	0.31	0.785
MeOH/air at 25°C	22.25	0.55	0.786
Density of air at 250°C and 1 atm		1.14 x 10 ⁻³ g/cm ³	
Density of nitrogen at 25°C and 1 atm		1.18 x 10 ⁻³ g/cm ³	

glass simulator was made for methanol/nitrogen and glass bead/methanol/nitrogen systems. A schematic diagram of the apparatus and detailed dimensions of the tubular columns and transfer-line segments are shown in Figure 14 and Tables 4 and 5. The simulators comprised, in sequence, a pressurized liquid feed tank, a nitrogen inlet system, a flow controller plus a flow meter for each liquid and gas feed system, a high-pressure tracer injection syringe, a column assembly, a gas/liquid separator, a letdown valve with a back-pressure regulator, a tracer detector probe, and a recorder, with a liquid receiving tank.

Steady liquid and gas flows were established using the inlet flow controllers and the back-pressure regulator for the gas/liquid separator at the exit of the column assembly. After a steady flow was established, the inlet ball valve was rapidly closed to cut gas/liquid flow into the columns and to entrap the liquid retained in the columns.

Gas holdup was determined by measuring the void fraction of the columns occupied by nitrogen. The pressure drop through the columns was about 6 to 12 psig, depending on the flow rates. The gas flow rates were measured using a gas flow meter based on the inlet pressure of the system. A correction was made for the average gas flow rate using the pressure drops for the whole column.

The residence time distribution was obtained by injecting a pulse of tracer at the simulator inlet and then detecting the response of tracer at the exit. The tracers used were sodium chloride for the H_2O/N_2 experiment and potassium chloride for the methanol/ N_2 experiment.

To determine solid residence time distribution, a predetermined amount of glass beads was placed in the first column. Then the solid particles were fluidized with flowing nitrogen gas at the desired rate. After the gas rate was adjusted to the desired experimental condition, liquid (methanol) was passed into the simulator at the predetermined flow rate. After liquid flow was initiated, samples were taken sequentially at 2-min intervals, until all the solid particles in the column were completely eluted. Total mass recovery was attained. For each sample, concentrations of both KCl tracer and solid particles in the liquid were determined for the residence time distribution analysis. Because accurate coordination in the sequence of operations was required to execute this procedure, the operator's skill was developed until meaningful data could be taken.

FIGURE 14
A SCHEMATIC FLOW DIAGRAM OF
THE COLD FLOW REACTOR SIMULATOR

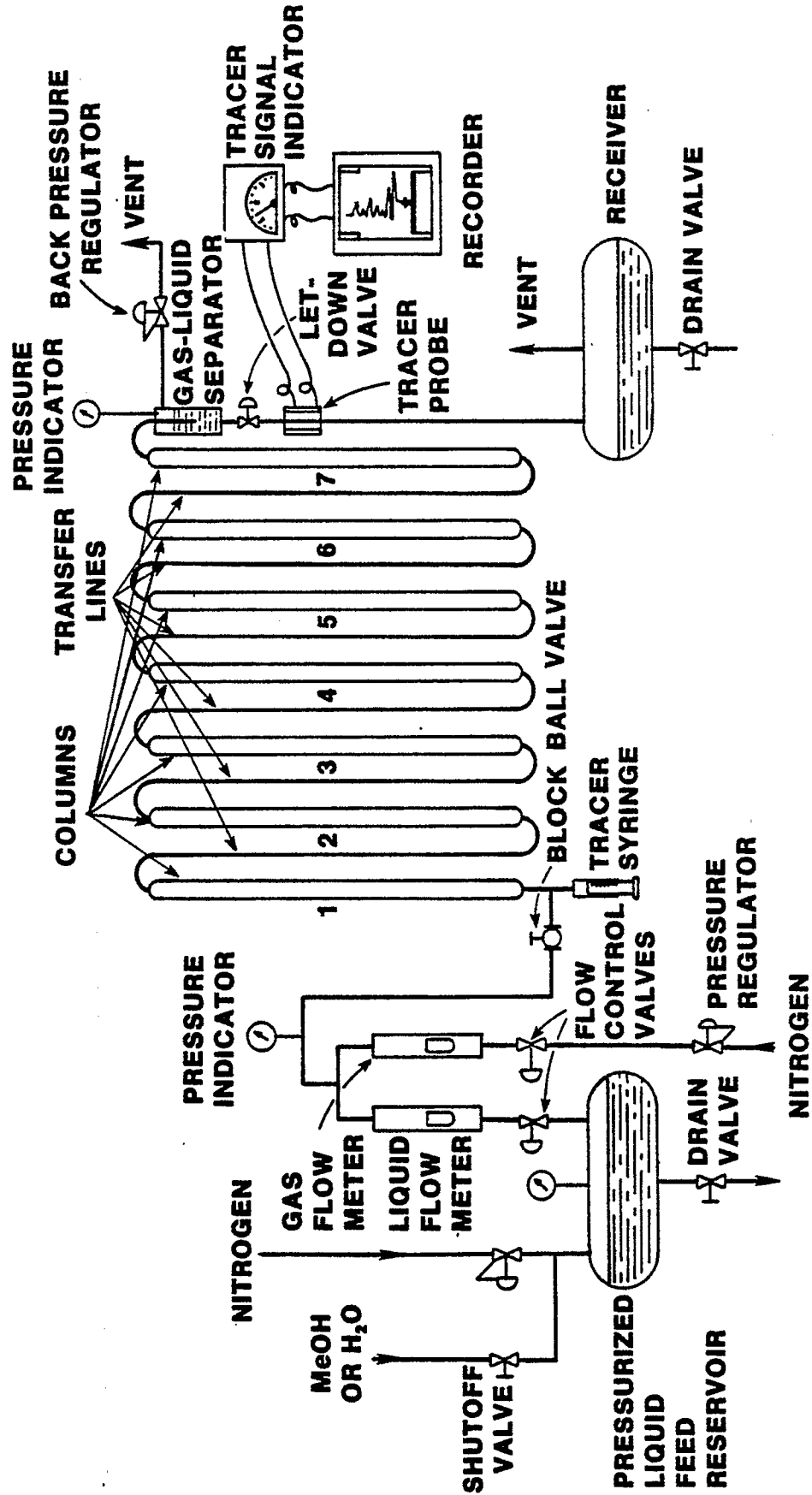


Table 4

Dimensions of Plexiglas Columns and Transfer Lines

Columns			Transfer lines		
No.	Diameter (in.)	Length (in.)	No.	Diameter (in.)	Length (in.)
1	0.625	50.13	1-2	0.25	75.94
2	0.625	50.00	2-3	0.25	73.78
3	0.625	49.88	3-4	0.25	74.03
4	0.625	50.00	4-5	0.25	75.78
5	0.625	49.88	4-6	0.25	73.75
6	0.625	50.06	6-7	0.25	73.56
7	0.625	49.88			
		349.81 (29.2 ft)			446.84 (37.2 ft)
Total volume of columns			1,759 mL		
Total volume of transfer lines			359 mL		
Total volume			2,118 mL		

Table 5

Dimensions of Glass Columns and Transfer Lines

Columns			Transfer lines		
No.	Diameter (cm.)	Length (in.)	No.	Diameter (cm.)	Length (in.)
1	9/16	48.2	1-2	0.5	65.94
2	9/16	48.2	2-3	0.5	66.19
3	9/16	48.2	3-4	0.5	66.32
4	9/16	48.2	4-5	0.5	65.44
5	9/16	48.2	4-6	0.5	66.44
6	9/16	48.2	6-7	0.5	65.07
7	9/16	48.2			
Total		337.40 (28.12 ft)			395.40 (32.95 ft)
Total column section volume		1,374 mL			
Total transfer line volume		197 mL			
Total volume		1,572 mL			

The glass beads used in these experiments were smaller than 200 mesh (Tyler) (75 μm), which is typical of the standard particle size of coal routinely used in our coal process development unit.

The purpose of this simplified slurry experiment was to ensure that solid accumulation would not occur under the operating conditions of the coal liquefaction study. The absence of accumulation would insure that the residence time characteristics of the solids would be similar to those of the liquid, which is a necessary condition for the tubular reactor study.

Various data obtained from the cold-flow studies are detailed in Appendix A-2.

Results and Discussion

Figure 15 depicts the flow patterns observed while operating in the experimental range. The liquid flow patterns in the tubular reactor were in the "slug-flow regime," in which bullet-shaped gas bubbles, followed by swarms of tiny bubbles at the tails, rose through the slowly moving liquid slugs. The gas/liquid interface of the bullet-shaped bubbles was unstable and formed rapidly propagating ripples, which transformed into vortices at the tails. This pattern of gas flow is near plug flow. Both gas and liquid flow patterns in the transfer lines were nearly perfect plug-flow, as indicated by the formation of sharp phase boundaries, with one slug successively followed by another.

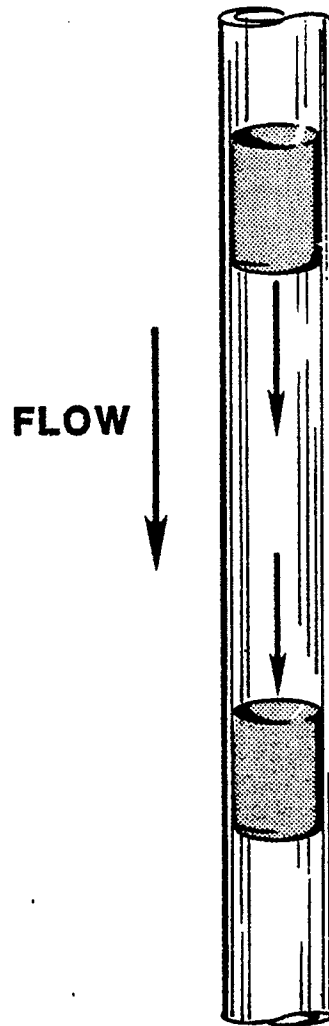
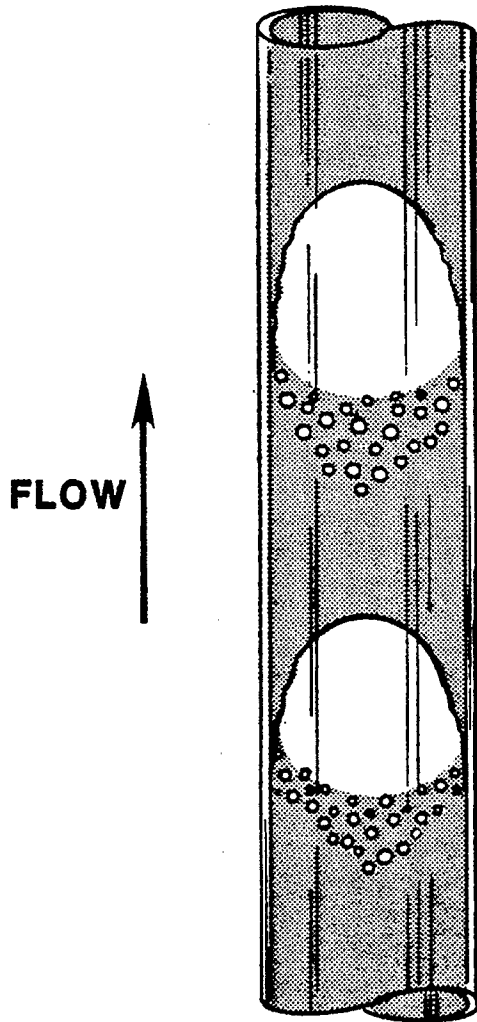
Gas holdup was measured for a wide range of flow conditions, far exceeding the projected liquefaction conditions of the tubular reactor. As shown in Figure 16, liquid flow rates from 0.004 to 0.044 ft/sec and superficial gas flow rates from 0.017 to 0.470 ft/sec were studied. Gas holdup was independent of liquid velocity, but strongly dependent on the gas flow rates. As Figure 16 shows, gas holdup was considerably higher than the values predicted by the Akita and Yoshida correlation (1973).

Unexpectedly, the gas holdups in water and methanol, which have considerably different physical properties, were found to be similar, within the experimental error ranges. Methanol does generate a higher gas holdup (about 15%) in the larger bubble columns. This insensitivity of holdup behavior with fluids having significantly different physical properties is a very desirable property of the tubular reactor that was

FIGURE 15 FLOW PATTERNS

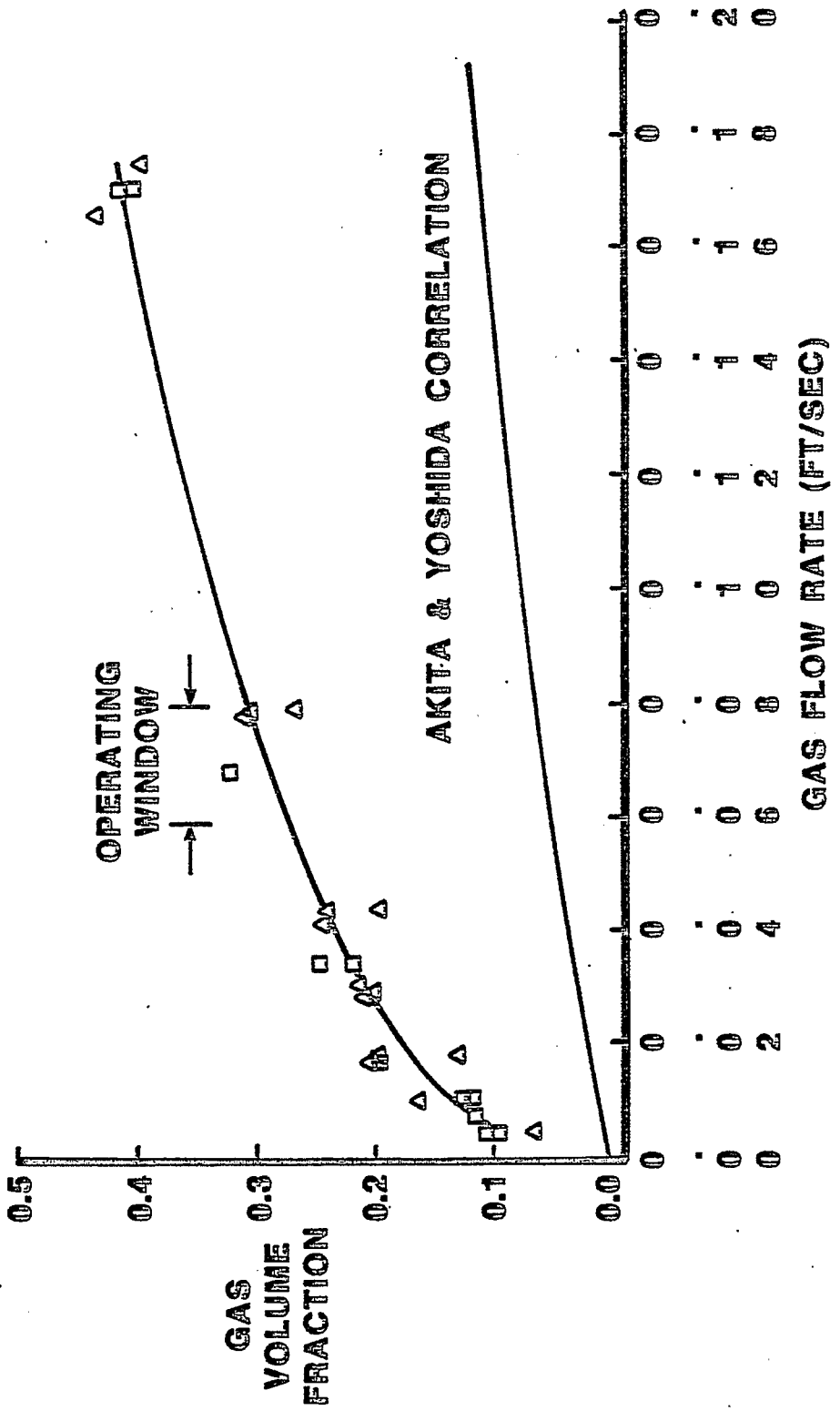
SLUG FLOW

PLUG FLOW



REACTOR TUBE DOWNCOMER TUBE

FIGURE 16
EFFECT OF GAS VELOCITY ON GAS HOLDUP
WATER (Δ) AND METHANOL (\square)/NITROGEN SYSTEM



used in our liquefaction study, because the physical properties of fluids in the reactor progressively changed within the range, as discussed earlier. Undoubtedly, the wall proximity effect in such a small tube may have created the insensitivity in fluid properties and shifted the holdup to a different regime from that observed for large bubble columns.

Under actual process conditions, the void space in the reactor segments (excluding the transfer lines) should be about 30%, based on this cold-flow study, whereas the transfer lines' void fraction is over 80%. The mean residence time of the slurry would be reduced with increasing gas velocity, due to the increased gas holdup (this will be detailed in the following residence time analysis).

An empirical correlation of gas holdup as a function of gas velocity was developed, as shown by the following equations:

$$E = 0.902U_G^{0.415} \quad (\text{correlation coefficient} = 0.98) \quad (1)$$

where E is the fractional gas void fraction of the reactor section and U_G is gas velocity in ft/sec. The void fraction of the transfer line is:

$$E_L = U_G / (U_L + U_G) \quad (2)$$

where U_L is the liquid velocity in ft/sec.

Equation 2 holds because of the continuity of both gas and liquid flowing in the transfer line under plug-flow conditions. Therefore, the total void fraction is:

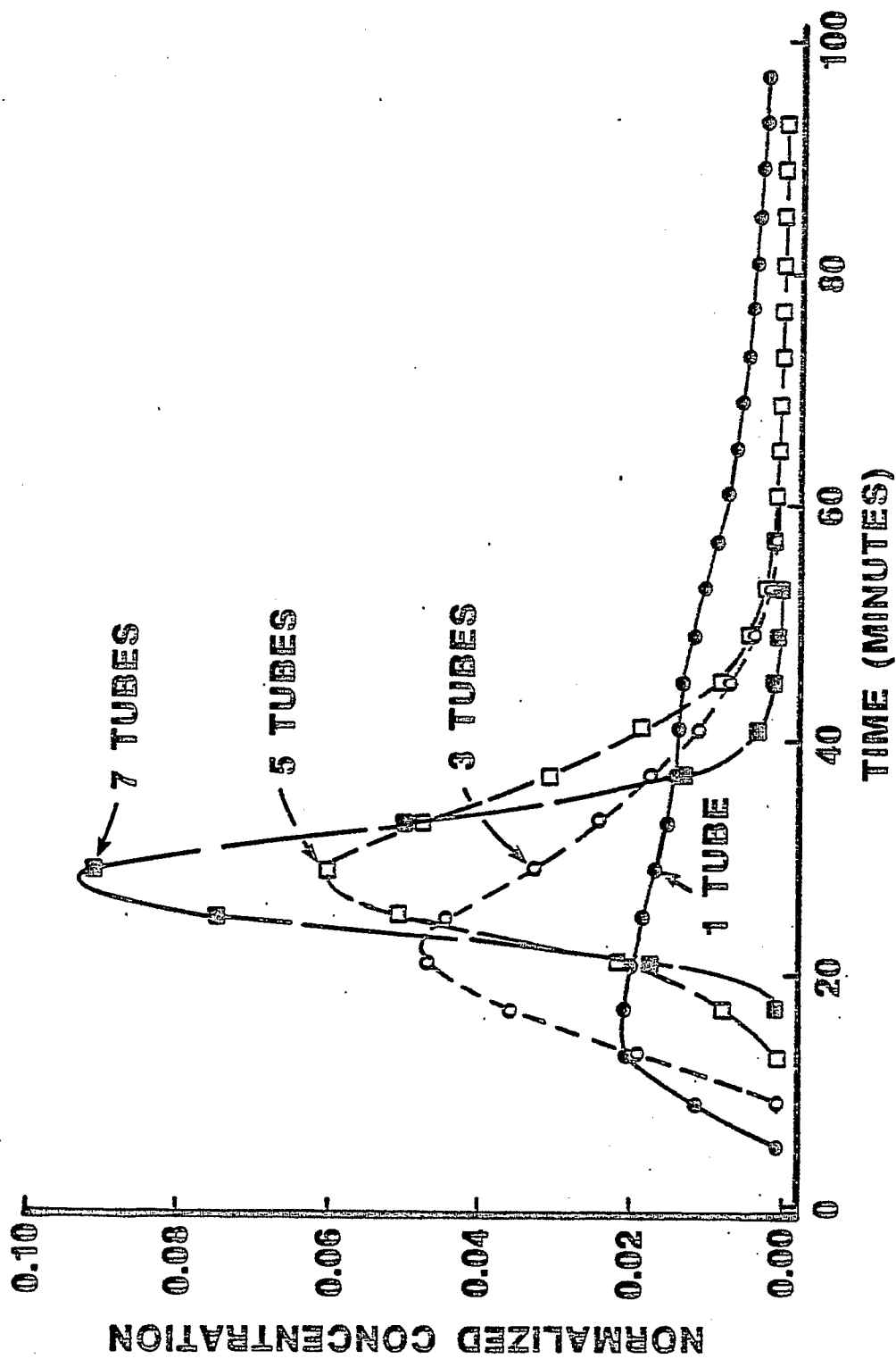
$$E_T = \frac{VE + V_L E_L}{V_T} + \frac{V}{V_T} (0.902U_G^{0.415}) + \frac{V_L}{V_T} \frac{U_G}{U_L + U_G} \quad (3)$$

where V is the volume of the tubular column segments in ft^3 , V_L is the volume of the transfer-line segment in ft^3 , and $V_T = V + V_L$, the total reactor volume.

Residence Time Distribution and Dispersion Analyses

Figure 17 compares the liquid residence time/distribution curves determined from the methanol/nitrogen cold-flow simulation using four different tubular reactor configurations. The tubes were the same size

FIGURE 17
RESIDENCE TIME DISTRIBUTION
AT VARIOUS TUBE CONFIGURATIONS



as those used for the actual experimental tubular reactor (0.56 in. i.d.), but the number of columns was varied--either one, three, five, or seven tubes in series. Liquid and gas flow conditions were chosen to simulate liquefaction flow-rate conditions, in order to give identical mean residence times (30 min).

The residence time/distribution curve of the single-tube configuration was flat and skewed, with extensive tailing far beyond 100 min, indicating considerable dispersion of the liquid phase. As the number of tubes increased, the curve rapidly became narrow and normally distributed. This demonstrates quite dramatically how dispersion decreased with more tubes.

The residence time/distribution obtained from the tubular reactor simulator with seven tubes in series was analyzed to derive the Peclet number and the corresponding number of CSTRs in series using the axial dispersion model and the tanks-in-series model, respectively. For a closed vessel, the dispersion model gives the following relation between variance of the residence time distribution curve and the Peclet number:

$$\sigma^2 = 2\left(\frac{1}{P}\right) - 2\left(\frac{1}{P}\right)[1 - \exp(-P)] \quad (4)$$

where the Peclet number is defined as $P = U_L L / E_{zL}$, U = liquid velocity, L = length of column, and E_{zL} = liquid dispersion coefficient.

In contrast, the tanks-in-series model gives:

$$\sigma^2 = 1/N \quad (5)$$

where N is the number of CSTRs and σ is the nondimensional variance of the normalized residence time/distribution curve.

Tables 6 and 7 summarize data evaluated at the various flow conditions for water/nitrogen and methanol/nitrogen, respectively. The Peclet number decreases (increases backmixing or dispersion number) with increasing gas velocities at fixed liquid flow rates. In contrast, the Peclet number increases with increasing liquid flow rate at a fixed gas velocity. The mean residence time determined from the residence time/distribution curves varies significantly with the change of gas flow rate, which is caused by the consequent change of gas holdup. Mean

Table 6
Gas Holdup and Liquid Dispersion Results^a

U_G (ft/sec)	\bar{t} (min)	σ^2	N	P	E_T	E	E_L	$\bar{t}/(1 - E)$
1. <u>Water/N₂ System</u>								
a. $U_L = 0.004265$ ft/sec								
0	169.4	0.0866	11.5	23	-			
0.018	85.3	0.0485	20.6	41	0.297	0.198	0.806	106.4
0.028	89.7	0.0624	16.0	32	0.319	0.212	0.868	113.8
0.044	80.2	0.0670	14.9	30	0.315	0.198	0.912	100.0
0.080	73.6	0.0747	13.4	27	0.380	0.268	0.949	100.6
0.175	59.9	0.0711	13.0	26	0.492	0.398	0.976	99.5
0.315	47.1	0.0771	13.0	26	0.596	0.520	0.987	98.1
0.446	47.5	0.1063	9.4	19	0.653	0.586	0.991	114.7
b. $U_L = 0.007218$ ft/sec								
0	101.4	0.0684	14.6	29				
0.018	60.5	0.03	33.3	67				
0.029	56.2	0.0362	27.7	55				
0.042	53.6	0.0415	24.1	48				
0.089	45.7	0.0485	20.6	41				
0.179	41.6	0.0559	17.9	36				
0.320	33.7	0.0675	14.8	30				
0.483	32.0	0.086	11.6	23				
c. $V_L = 0.01083$ ft/sec								
0	71.6	0.0685	14.6	29	-	-	-	-
0.017	45.4	0.0232	43.2	86	0.273	0.206	0.616	57.2
0.030	40.1	0.029	34.3	69	0.300	0.216	0.732	51.2
0.041	37.2	0.0396	25.2	50	0.334	0.245	0.790	49.3
0.078	34.2	0.029	34.5	69	0.404	0.311	0.878	49.6
0.170	28.0	0.0465	21.5	43	0.491	0.403	0.940	46.9
0.311	24.3	0.057	17.5	35	0.571	0.494	0.966	48.0
0.470	19.7	0.0526	19.0	38	0.657	0.594	0.978	48.5
d. $U_L = 0.02198$ ft/sec								
0	34.8	0.0769	13.0	26				
0.017	20.5	0.0124	81.0	162				
0.026	20.5	0.0152	66.0	132				
0.041	19.5	0.017	59.7	119				
0.086	17.2	0.0245	40.7	82				
0.180	15.0	0.0302	33.1	66				
0.309	12.1	0.0388	25.8	52				
0.460	10.9	0.045	22.2	44				

Table 6 (Continued)

U_G (ft/sec)	\bar{t} (min)	σ^2	N	P	E_T	E	E_L	$\bar{t}/(1 - E)$
e. $U_L = 0.04364$ ft/sec								
0	10.4	0.05514	18.1	36	-			
0.004	9.6	0.00214	467.1	934	0.068	0.066	0.075	10.3
0.010	8.6	0.00486	205.8	412	0.164	0.163	0.173	10.3
0.018	8.3	0.00555	180.1	360	0.155	0.132	0.271	9.6
0.029	7.9	0.00627	159.4	319	0.232	0.203	0.379	9.9
0.044	7.6	0.00566	88.3	177	0.285	0.242	0.503	10.0
0.079	7.1	0.00595	84.0	168	0.360	0.305	0.644	10.2
0.175	5.7	0.01484	67.4	135	0.463	0.397	0.801	9.5
0.166	5.4	0.00924	108	216	0.492	0.436	0.777	9.6
0.334	4.7	0.01439	69.5	139	0.547	0.482	0.875	9.1
0.508	3.5	0.02125	47.1	94	0.621	0.564	0.915	8.0
2. <u>Methanol/N₂ System</u>								
a. $U_L = 0.0092$ ft/sec								
0.00341	47.7	47.3	0.01478	67.7	0.126	0.105	0.270	134.3
0.00682	48.8	46.7	0.02757	36.3	0.153	0.114	0.426	71.5
0.0102	49.1	46.3	0.03334	30.0	0.168	0.117	0.526	59.0
0.0171	44.1	41.4	0.04035	24.8	0.254	0.197	0.650	48.5
0.0341	40.8	37.3	0.05134	19.5	0.315	0.247	0.788	37.9
0.0682	37.9	35.6	0.04943	20.2	0.392	0.322	0.881	39.4
0.1705	34.0	31.5	0.06296	15.9	0.479	0.412	0.949	30.7
b. $V_L = 0.00614$ ft/sec								
0.00341	81.5	78.3	0.02316	43.2	0.128	0.095	0.357	85.3
0.0102	74.3	70.1	0.03950	25.3	0.188	0.125	0.624	49.6
0.0341	70.6	64.8	0.06292	15.9	0.296	0.217	0.847	30.8
0.1705	55.5	49.4	0.07924	12.6	0.473	0.402	0.965	24.2
c. $U_L = 0.03649$ ft/sec								
0.00341	24.4	24.1	0.002271	440	0.063	0.0595	0.085	879.7

^aNomenclature: U_L = superficial liquid velocity; U_G = superficial gas velocity; \bar{t} = mean residence time; σ^2 = dimensionless variance; N = number of CSTRs in series; P = Peclet number; E_T = void fraction measured for total reactor volume including transfer lines; $E_L = U_G/(U_L + U_G)$, based on the continuity of both liquid and gas flowing through the transfer lines under the plug flow conditions; E = void fraction of reactor excluding transfer lines, derived from E_T and E .

Table 7

Peclet Number and Number of CSTRs in
Series Derived from Correlations
(Basis: $U_G/U_L = 7.5$)

U_G	U_L	P	N
<u>For Methanol/N₂ System</u>			
0.02	0.002778	17.49	10.0
0.04	0.005556	26.75	13.89
0.06	0.008333	34.86	17.94
0.08	0.011111	42.35	21.69
0.10	0.013889	49.68	25.35
0.12	0.016667	56.79	28.90
0.14	0.019444	63.94	32.48
0.16	0.022222	71.12	36.07
0.18	0.025000	78.31	39.66
0.26	0.027778	85.54	43.28
<u>For Water/N₂ System</u>			
0.02	0.002778	24.05	12.55
0.04	0.005556	26.36	18.82
0.06	0.008333	47.33	24.17
0.08	0.011111	57.31	29.16
0.10	0.013889	66.77	33.89
0.12	0.016667	75.90	38.44
0.14	0.019444	84.85	42.92
0.16	0.022222	93.78	47.41
0.18	0.025000	102.81	51.89
0.20	0.027778	111.66	56.31

residence time can also be determined using the holdup correlation and nominal residence time.

From these results, the following empirical equations relating liquid dispersion coefficient and gas flow rate were developed:

Liquid dispersion coefficient for the methanol/nitrogen system:

$$E_{zL} = 0.0375U_G^{0.495} \quad (\text{correlation coefficient} = 0.94) \quad (6)$$

Liquid dispersion coefficient for the water/nitrogen system:

$$E_{zL} = 0.0279U_G^{0.492} \quad (\text{correlation coefficient} = 0.94) \quad (7)$$

Fractional gas holdup of the reactor section excluding the transfer lines for both systems:

$$E = 0.902U_G^{0.415} \quad (\text{correlation coefficient} = 0.98) \quad (1)$$

The correlation shows that the dispersion coefficient (with a high correlation coefficient at 0.94) can be reasonably assumed to be a sole function of gas velocity (for a given tube diameter). In contrast, the Peclet number strongly depends upon both gas and liquid velocities. Gas velocity is not a completely independent process variable, since gas flow rates in typical direct coal liquefaction processes will undoubtedly be locked into liquid flow rates within a certain narrow range of gas-to-liquid ratios, due to the hydrogen demand of the coal liquefaction process. This constraint provides a convenient way to tie the dispersion correlation (or Peclet number and number of CSTRs) with liquid velocity.

Typical demonstration plant reactor conditions are 30,000 standard cubic feet of hydrogen/ton of coal, 38 wt % coal slurry concentration, 840°F, and 2,000 psig. The ratio of hydrogen gas to liquid superficial velocities evaluated from these conditions turns out to be about 7.5. The Peclet number and number of CSTRs were derived using equations 4-8, based on a ratio of gas-to-liquid velocity of 7.5 (shown in Table 7 and plotted in Figures 18 and 19).

FIGURE 18
EFFECT OF FLOW RATES ON PECLET NUMBER

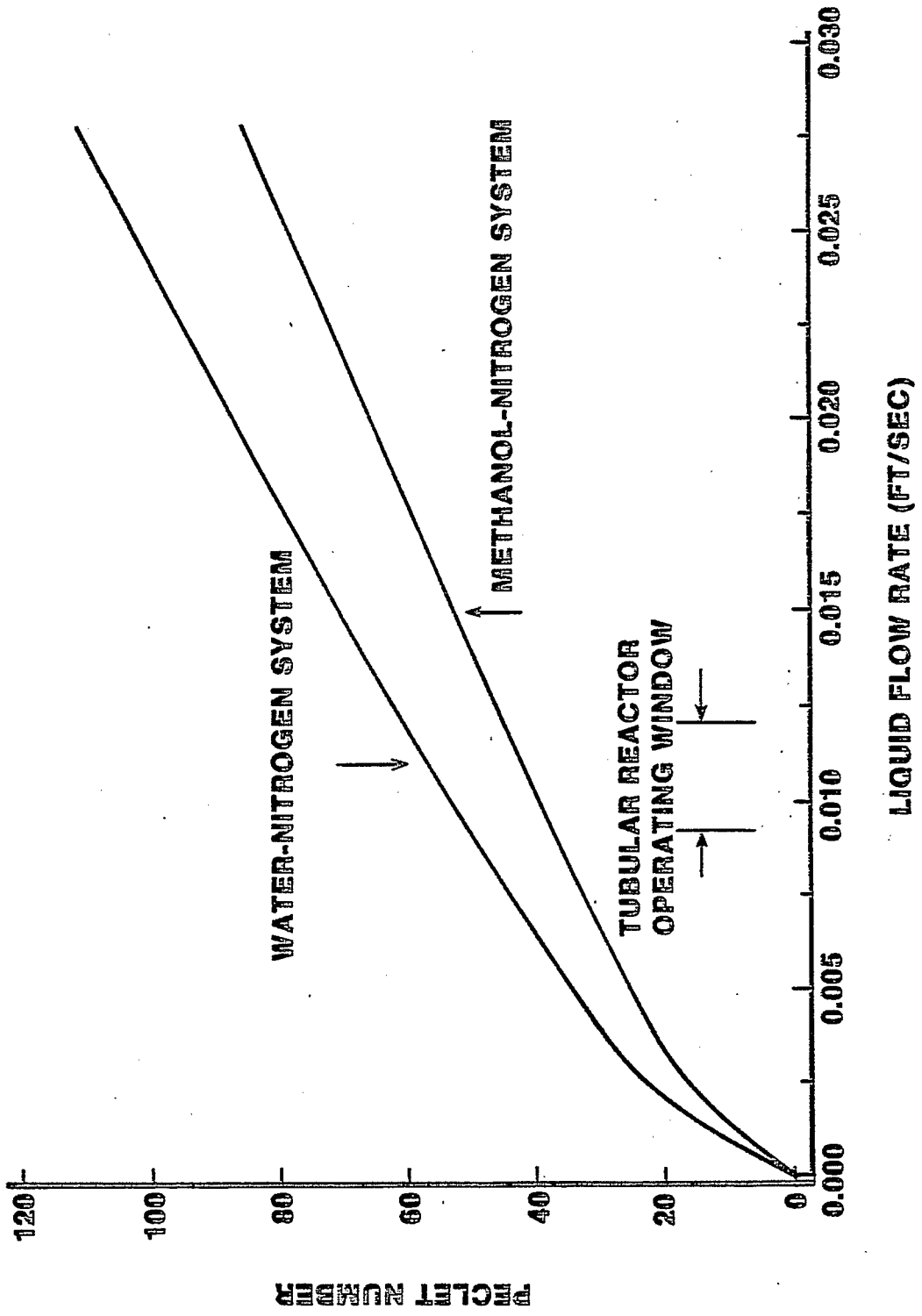
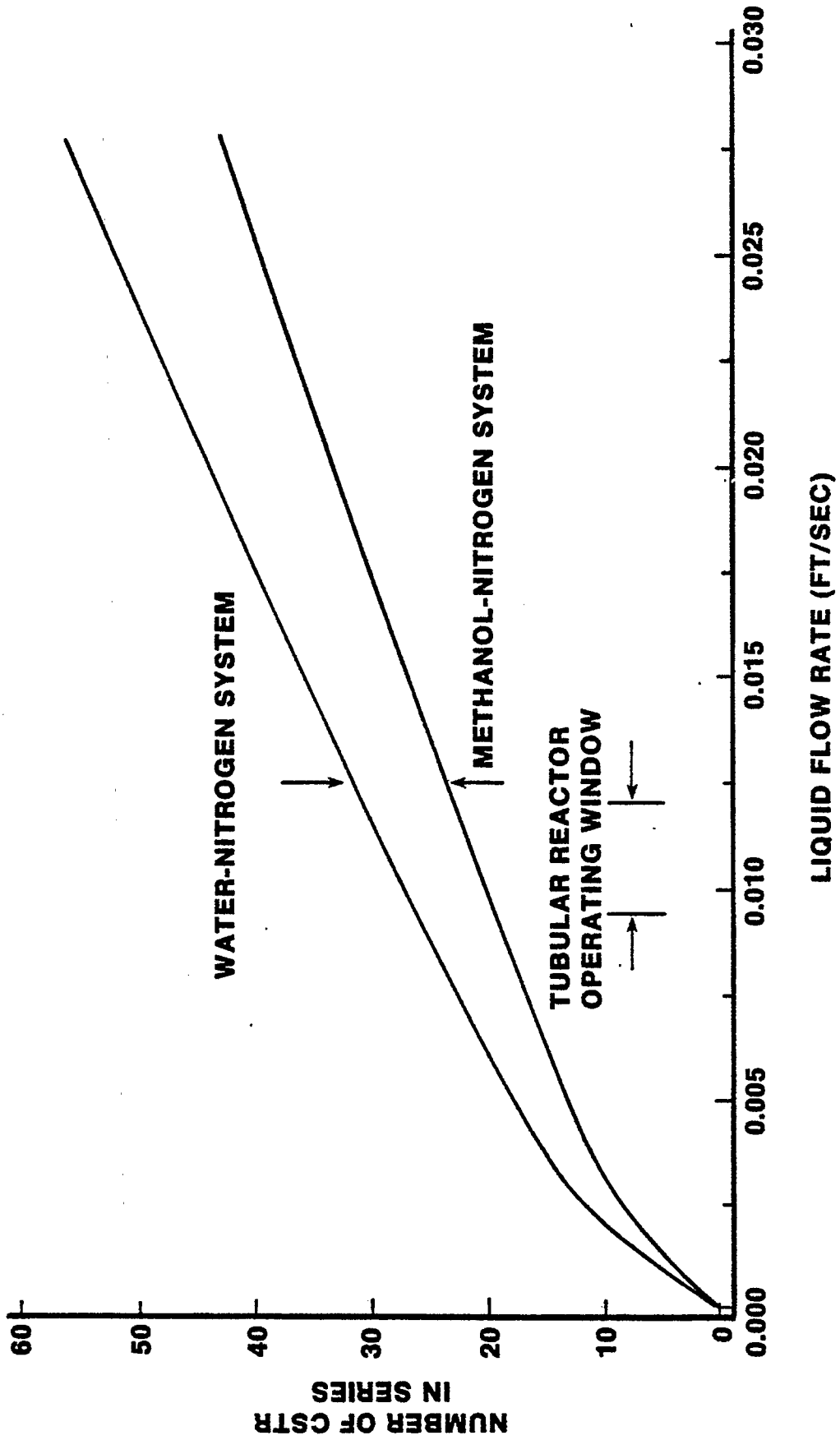


FIGURE 19
EFFECT OF FLOW RATES
ON NUMBER OF CSTR IN SERIES



Analysis of these results indicates that the Peclet numbers of the tubular reactor (based on the methanol/nitrogen system) would be about 36-44, and the performance of this reactor would be equivalent to 18-22 CSTRs in series within the planned experimental conditions (i.e., 22 and 18 CSTRs at 20- and 80-min nominal residence times, respectively).

Figure 20 compares residence time/distribution curves for solid particles and liquid obtained from the three-phase cold-flow simulation study using glass beads (-200 Tyler mesh, $-75\ \mu\text{m}$), methanol, and nitrogen at typical reactor operating conditions. The earlier appearance of the residence time curve for the solid particles compared to the liquid is an artifact, because liquid and solid flows started at different times. This artifact was corrected by shifting the residence time/distribution curve of the particles onto that of liquid, as shown in Figure 21. The differences between the two curves were then marginal. Analysis of these results indicates that the dispersion characteristics of solid particles in the tubular reactor closely resembled those of the liquid. On this basis, solids will probably not accumulate in the tubular reactor.

FIGURE 20
RESIDENCE TIME DISTRIBUTION
SOLID PARTICLES VS. LIQUID

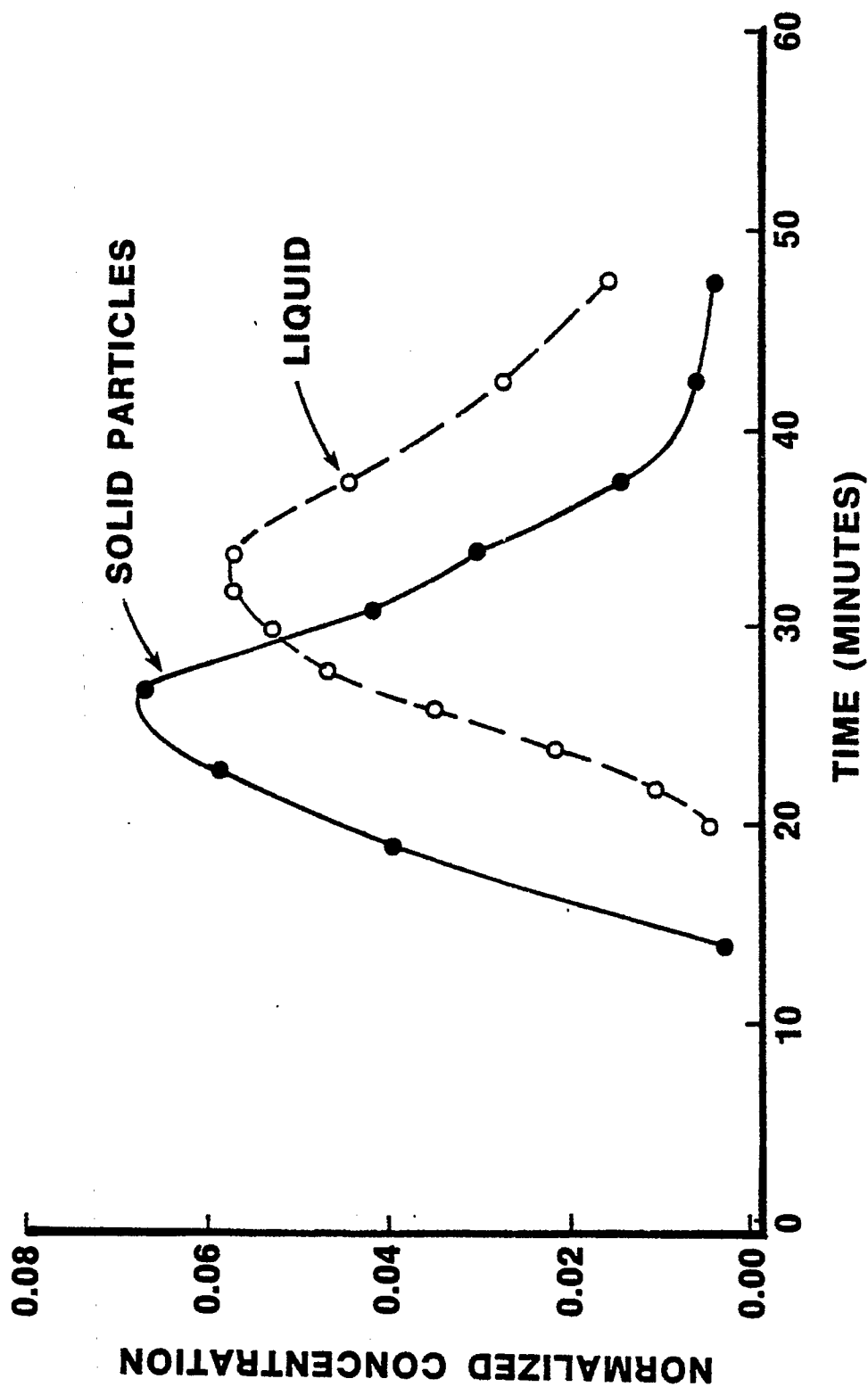
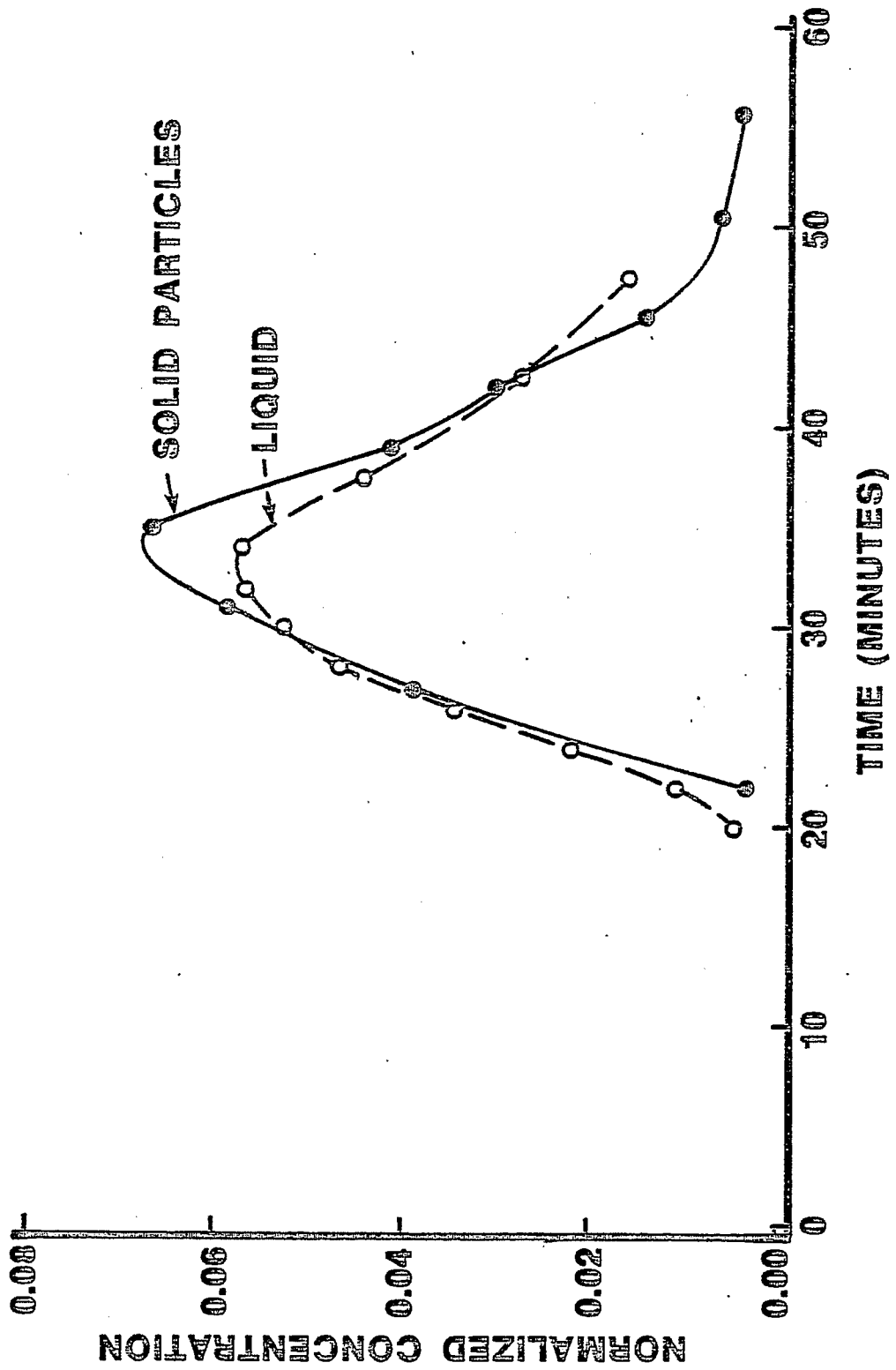


FIGURE 21
RESIDENCE TIME DISTRIBUTION
SOLID PARTICLES VS. LIQUID



LIQUEFACTION STUDY OF PLUG-FLOW TUBULAR REACTOR

PROCESS RUNS

Liquefaction runs were made in the tubular reactor with 38 wt % Kentucky #9 Mulford coal and recycle solvent from the Ft. Lewis pilot plant, while it was running in the SRC-I mode. Process conditions were:

Temperature	840°F
H ₂ pressure (psig)	2,000
H ₂ rate (scf/ton of coal)	3,000
Nominal residence time (min)	29 and 40
Coal space rate (lb of coal/ft ³ -hr)	40 and 30
Coal in solvent (wt %)	38

Other than residence times, process conditions were constant. Since the nominal residence time in the tubular reactor is a function of slurry flow rate, as detailed in the preceding section, the operating curve for the tubular reactor was developed using the equations derived from the cold-flow study.

The void fractions for tube segment and transfer lines of the reactor are from equations 1 and 2.

$$\text{Reactor segment: } E_R = 0.902U_G^{0.415} \quad (1)$$

$$\text{Transfer-line segment: } E_L = U_G/(U_L + U_G) = \frac{U_G/U_L}{1 + U_G/U_L} \quad (2)$$

where U_G/U_L is the ratio of superficial gas velocity to liquid velocity at reactor conditions. Therefore, the net available reactor volume for the liquid phase is:

$$V_N = V_R(1 - E_R) + V_L(1 - E_L) \quad (8)$$

$$= V_R(1 - 0.902U_G^{0.415}) + V_L \left[1 - \frac{U_G/U_L}{1 + (U_G/U_L)} \right] \quad (9)$$

where V_R = the tube segment reactor volume ($1,296 \text{ cm}^3$) and V_L = the transfer-line segment reactor volume (249 cm^3).

The ratio of slurry-to-gas volumetric flow rates in the reactor (at 840°F and $2,000 \text{ psig}$) is equal to the ratio of superficial liquid to gas velocity at the same conditions. An assumption is made that the gas flow rate is equal to hydrogen gas flow rate; then:

$$\frac{Q_{SL}}{Q_{H_2}} = \frac{U_L}{U_G} = \frac{Q_{SL} \times t}{Q_{H_2} \times t} = \frac{V_N \cdot A \cdot t}{U_G \cdot A \cdot t} \quad (10)$$

where Q_{SL} and Q_{H_2} are volumetric slurry and hydrogen flow rates, respectively, A is the cross-sectional area of the reactor tube, and t is the residence time.

$$\frac{U_G}{U_L} =$$

$$\frac{30,000 \text{ scf/ton of coal} \times 0.38 \text{ g of coal/g of slurry} \times 28,316.85 \text{ cm}^3/\text{scf}}{2,000 \text{ lb of coal/ton of coal} \times 453.6 \text{ g/lb} \times (1/1.13) \text{ cm}^3/\text{g of slurry}} \times$$

$$\frac{14.7 \text{ psia}}{2,014.7 \text{ psia}} \times \frac{460 + 840^\circ\text{R}}{460 + 70^\circ\text{R}} \times \frac{1.038}{1.006} = 7.465 \quad (11)$$

where $1.038/1.006$ is the compressibility correction factor term. Note that the slurry density used is 1.13 g/cm^3 , in order to relate to the nominal residence time:

$$\frac{V_N (\text{cm}^3)}{[U_G (\text{ft/sec}) \times 30.48 \text{ cm/ft}] \left[\left(\frac{9}{16} \times 2.54 \right)^2 \times \frac{\pi}{4} \right] \times t (\text{sec})} = \frac{1}{7.465}$$

Therefore,

$$U_G (\text{ft/sec}) = 0.1528 \left[\frac{V_N (\text{cm}^3)}{t (\text{sec})} \right] \quad (12)$$

Inserting equations (11) and (12) into equation (9) yields:

$$V_N = 1,296 \left[1 - 0.902 \left(0.1528 \frac{V_N}{t} \right)^{0.415} \right] + 29.4 \quad (13)$$

Rearranging equation (13) leads to:

$$t \text{ (sec)} = \frac{0.1528 V_N \text{ (cm}^3\text{)}}{\exp \left(\ln \left\{ \frac{1 - [(V_N - 29.4)/1,296]}{0.9017} \right\} / 0.4149 \right)} \quad (14)$$

The volumetric slurry flow rate at a nominal residence time t^1 is:

$$Q_{SLV} \text{ (cm}^3\text{/sec)} = \frac{V_N \text{ (cm}^3\text{)}}{t \text{ (sec)}} \quad (15)$$

and mass flow rate is:

$$Q_{SLM} \text{ (g/sec)} = 1.13(V_N/t) \quad (16)$$

Using equations (9), (13), and (15), reactor operating curves that relate slurry pumping rate, hydrogen flow rate, and nominal residence time can be plotted as shown in Figures 22 and 23 and Tables 8 and 9. In order to determine nominal residence time, we assigned the slurry density a value of 1.13 g/cm³ (at ambient temperature), whereas hydrogen flow rates were based on process conditions of 840°F, 2,000 psig, and 30,000 scf of hydrogen/ton of coal.

The operating curves in Figure 22 exclude the preheater tube volume from the net reactor volume, whereas those in Figure 23 include the first tube as an integral part of the useful reactor. Slurry and hydrogen rates required for the various residence times can be read from these operating curves. Likewise, these operating curves can be easily generated whenever process variables (temperature, pressure, and hydrogen rate) are changed.

At 840°F, 2,000 psig, and 30,000 scf of hydrogen/ton of coal, the following residence times and flow rates were determined from the figures:

¹Conversion of the nominal residence time to true residence time is correlated and illustrated in Appendix A-4.

FIGURE 22
PLUG FLOW REACTOR OPERATING CURVES
EXCLUDING THE PREHEATER

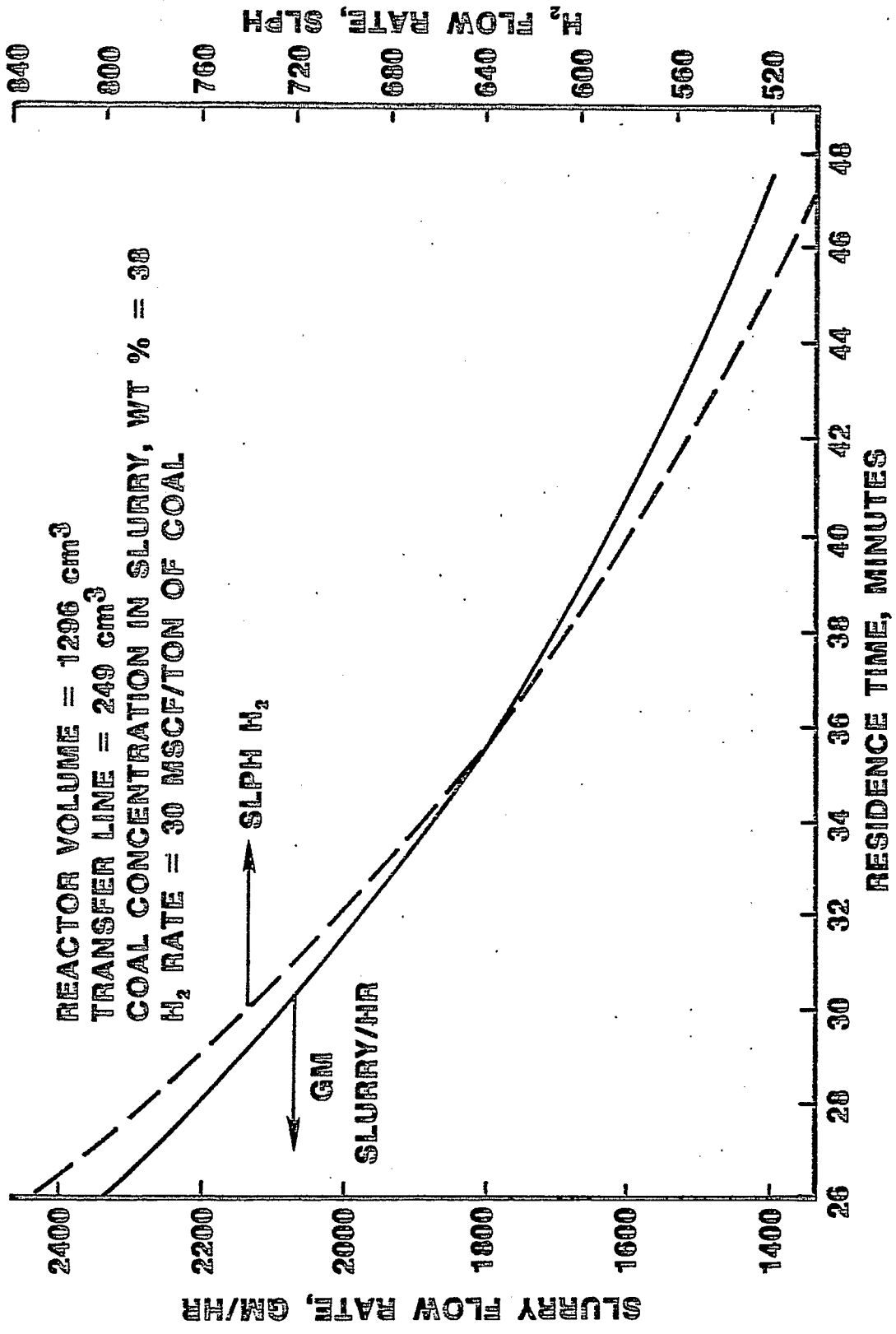


FIGURE 23
PLUG FLOW REACTOR OPERATING CURVES
INCLUDING THE PREHEATER AS AN INTEGRAL
PART OF USEFUL REACTOR

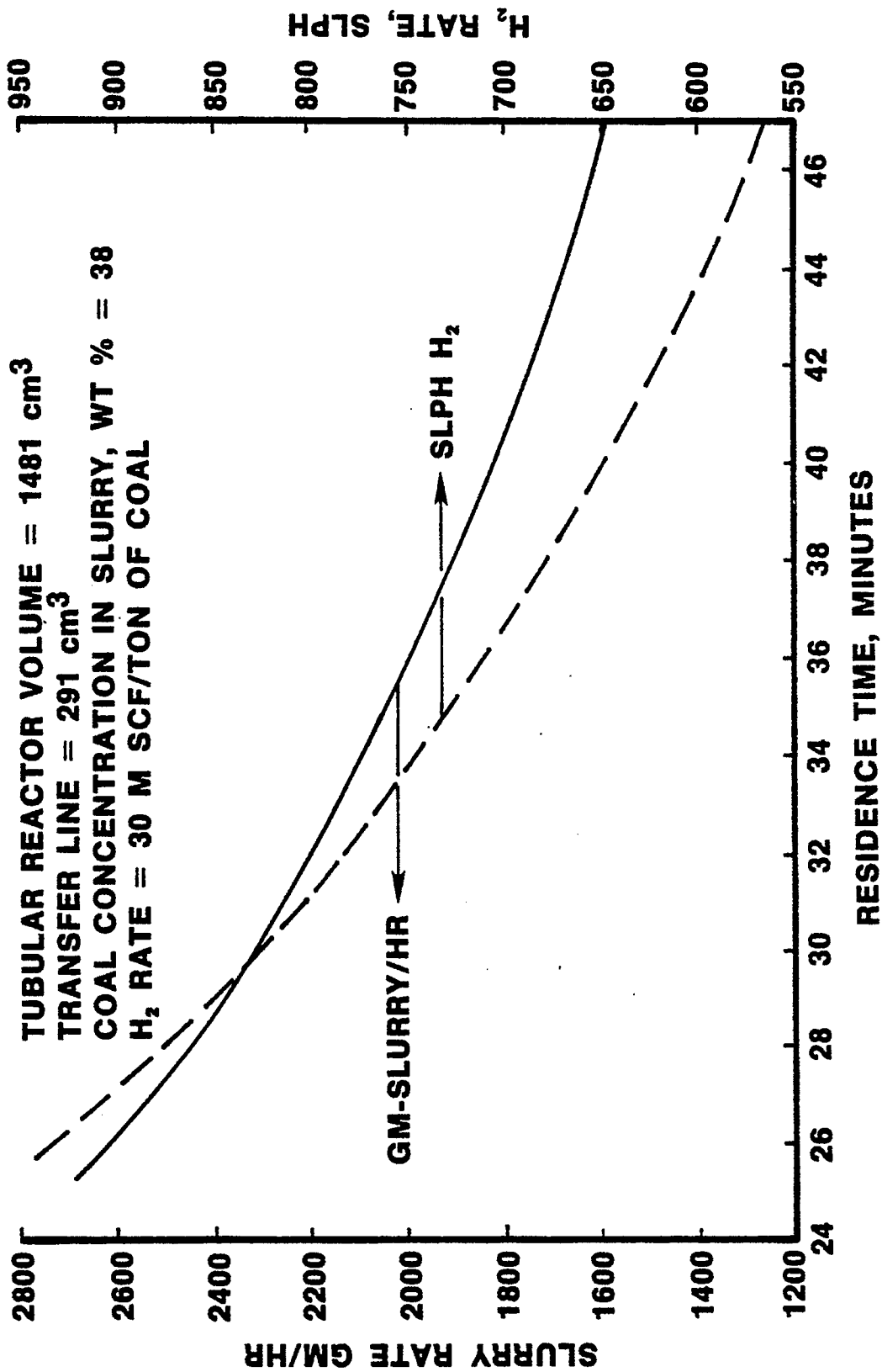


Table 8
 Operation Characterization Data for Plug-Flow Reactor,
 Excluding the Preheater

Net available reactor volume, V_n (cm ³)	Nominal residence time, t		Total void fraction, E_T	Slurry flow rate		H_2 rate (slph)	Superficial hydrogen velocity, U_G (ft/sec)
	sec	min		cm ³ /hr	g/hr		
900	1,570.86	26.16	0.328	2,062.6	2,330.74	829.36	0.0875
905	1,625.25	27.09	0.325	2,004.6	2,265.20	806.03	0.0851
910	1,682.04	28.034	0.321	1,947.6	2,200.83	783.13	0.0827
915	1,741.37	29.023	0.317	1,891.6	2,137.52	760.60	0.0803
920	1,803.49	30.057	0.313	1,836.54	2,074.29	738.46	0.0780
925	1,868.25	31.137	0.309	1,782.42	2,014.14	716.70	0.0757
930	1,936.10	32.268	0.305	1,729.25	1,954.05	695.32	0.0734
935	2,007.14	33.452	0.301	1,677.01	1,895.02	674.31	0.0712
940	2,081.55	34.693	0.297	1,625.71	1,837.05	653.68	0.0690
945	2,159.53	35.992	0.294	1,575.34	1,780.13	663.43	0.0669
950	2,241.31	37.355	0.290	1,525.89	1,724.26	613.55	0.0648
955	2,327.11	38.785	0.286	1,477.37	1,669.43	594.04	0.0627
960	2,417.19	40.287	0.282	1,429.76	1,615.63	574.90	0.0607
965	2,511.82	41.864	0.278	1,383.06	1,562.857	446.12	0.0587
970	2,611.30	43.522	0.274	1,337.26	1,511.108	537.70	0.0568
975	2,715.94	45.266	0.270	1,292.37	1,460.376	519.65	0.0549
980	2,826.09	47.102	0.267	1,248.37	1,410.655	501.96	0.0530
985	2,942.12	49.035	0.263	1,205.25	1,361.938	484.62	0.0512
990	3,064.42	51.074	0.259	1,163.03	1,314.220	467.64	0.0494
995	3,193.43	53.224	0.283	1,121.68	1,267.495	451.02	0.0476
1,000	3,329.63	55.494	0.251	1,081.20	1,221.756	434.74	0.0459

Table 9
 Operation Characterization Data for Plug-Flow Reactor,
 Including the Preheater

Net available reactor volume, V_n (cm ³)	Nominal residence time, t		Total void fraction, E_T	Slurry flow rate		H_2 rate (slph)	Superficial hydrogen velocity, U_G (ft/sec)
	sec	min		cm ³ /hr	g/hr		
900	889.90	14.83	0.416	3,640.86	4,114.17	1,463.96	0.155
910	936.03	15.60	0.409	3,499.89	3,954.87	1,407.27	0.149
920	985.08	16.42	0.402	3,362.17	3,799.25	1,351.90	0.143
930	1,037.28	17.29	0.395	3,227.67	3,647.26	1,297.82	0.137
940	1,092.89	18.21	0.389	3,096.37	3,498.90	1,245.03	0.131
950	1,152.19	19.20	0.382	2,968.25	3,354.12	1,193.51	0.126
960	1,215.49	20.26	0.375	2,843.29	3,212.91	1,143.26	0.121
970	1,283.12	21.39	0.368	2,721.46	3,074.25	1,094.28	0.116
980	1,355.50	22.59	0.362	2,602.74	2,941.09	1,046.54	0.111
990	1,432.99	23.88	0.355	2,487.11	2,810.43	1,000.04	0.106
1,000	1,516.09	24.27	0.348	2,374.54	2,683.22	954.78	0.101
1,010	1,604.30	26.75	0.341	2,265.00	2,559.45	910.74	0.096
1,020	1,701.19	28.35	0.335	2,158.49	2,439.09	867.91	0.092
1,030	1,804.42	30.07	0.328	2,054.96	2,322.10	826.28	0.087
1,040	1,915.68	31.93	0.321	1,954.39	2,208.46	785.84	0.0830
1,050	2,035.79	33.93	0.314	1,856.77	2,098.15	746.59	0.0788
1,060	2,165.65	36.09	0.308	1,762.06	1,991.13	708.51	0.0748
1,070	2,306.26	38.44	0.301	1,670.24	1,887.37	671.59	0.0709
1,080	2,458.77	40.98	0.294	1,581.28	1,786.84	635.82	0.0671
1,090	2,624.48	43.74	0.287	1,495.15	1,689.52	601.19	0.0635
1,100	2,804.86	46.75	0.281	1,411.84	1,595.38	567.69	0.0599
1,110	3,001.57	50.03	0.274	1,331.30	1,504.37	535.31	0.0565
1,120	3,216.54	53.61	0.267	1,253.52	1,416.48	504.03	0.0532
1,130	3,451.95	57.53	0.260	1,178.46	1,331.66	473.85	0.0500
1,140	3,710.32	61.84	0.254	1,106.11	1,249.90	444.76	0.0469
1,150	3,994.54	66.58	0.247	1,036.41	1,171.15	416.73	0.0440

	<u>Nominal residence time (min)</u>	
	<u>40</u>	<u>28.6</u>
With preheater, but not part of reactor		
Slurry rates (g/hr)	1,627	2,166
H ₂ rates (slph)	579	770
Preheater included as part of reactor		
Slurry (g/hr)	1,823	2,421
H ₂ rates (slph)	649	861

Details of the reactor operating data during the material-balance periods are summarized in Appendix A-3.

MATERIALS

Coal

Kentucky #9 Mulford coal was ground, dried before use to bring the moisture content below 2%, and sized to -200 mesh. Proximate and ultimate analyses of the coal are given in Table 10.

Solvent

The process solvent was a Ft. Lewis recycle solvent (Gulf P&M #1967), produced while that plant was running in the SRC-I mode. Elemental analyses, solvent separation, proton NMR, and simulated distillation data for the solvent are provided in Tables 11 and 12. The solvent contained 8.21 wt % hydrogen, which is typical of process solvent produced in the SRC-I mode. The proton NMR spectra of the solvent are shown in Figure 25.

RESULTS AND DISCUSSION

Table 13 summarizes yield data obtained from the plug-flow reactor at 840°F, 2,000 psig, and residence times of 29 and 40 min. Both targeted and actually achieved process conditions are given in the table.

Table 10
 Proximate and Ultimate Analyses of Coal
 (FSK #152/153)

		Proximate analysis determined by TGA ^a (wt %)		
	H ₂ O		2.10	
	Volatile matter		36.91	
	Fixed carbon		51.38	
	Ash		9.61	
		Ultimate analysis (wt %)		
		As received	Dry	Dry and ash free
	Carbon	71.86	73.40	80.96
	Hydrogen	5.02	4.89	5.39
	Oxygen	10.48	8.80	9.71
	Nitrogen	1.64	1.68	1.85
	Sulfur	3.07	3.14	--
	Organic	1.82	1.89	2.08
	Pyritic	1.25	1.25	--
	Ash (ASTM)	9.63	9.82	--

^aTGA, thermogravimetric analysis.

Table 11

Chemical Properties of the Process Solvent

	C	H	N	O	S	
Elemental composition (wt %)	87.76	8.24	0.85	2.95	0.36	
	Pentane-soluble oils		Benzene-soluble asphaltenes		Pyridine-soluble preasphaltenes	
Solvent extracts (wt %)	96.22		3.78		--	
	H_{α}		H_{β}		H_{T}	H_{ar}
	Cyclic	Alkyl	Cyclic	Alkyl	alkyl	Condensed Uncondensed
Proton NMR (%)	1.16	0.73	0.73	1.14	0.47	3.07 0.96

Table 12

Simulated GC Data of the Process Solvent

°F cut	% off (close to wt %)	
	Encapsulated GC APCI-modified ASTM D2886 ^a	Wilsonville method ^b
-350	0	0
350-450	6.32	5.16
450-550	25.77	23.94
550-650	27.04	20.59
650-750	19.77	16.97
750-850	10.65	20.45
850+	10.45	9.88
Nonvolatile	0	3.00 ^b

^aInjection temperature at 250°C with Dexsil 300 column.

^bAutomatically assumed to be 3 wt %, based on a preliminary study during method development at Wilsonville.

FIGURE 24
200.13 MHz ¹H SPECTRUM
FOR PROCESS SOLVENT (BCL-52)

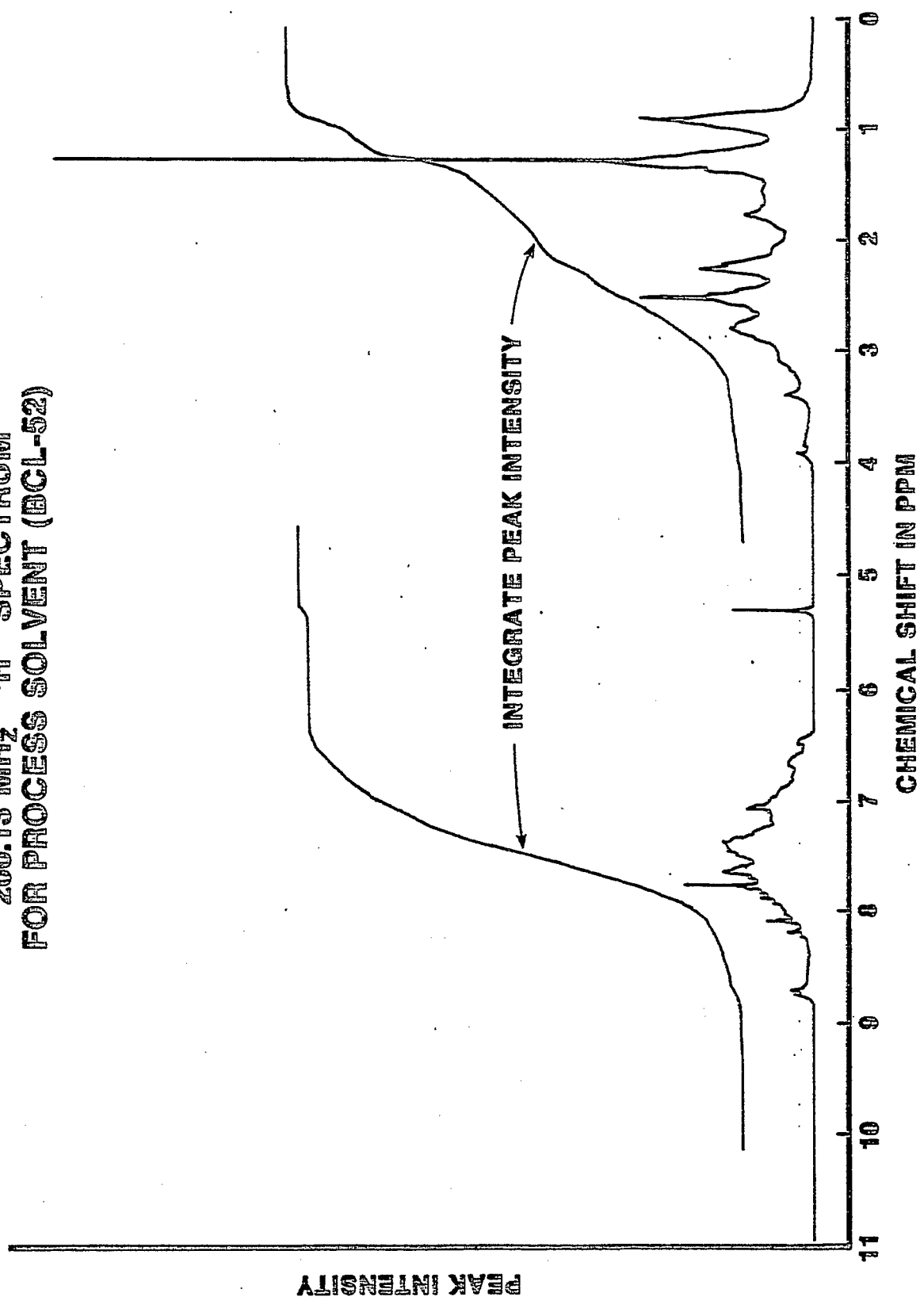


Table 13

Plug-Flow Reactor Yields Summary (Run BCL-52)

Sample i.d.	52-22	52-11	55-233	55-221	52-29 ^a	52-91	52-185	52-209	52-197	52-40 ^b
Temp (°F)	841	839	842	840	840	839	840	841	840	840
Pressure (psig)	2,005	2,006	2,008	2,004	2,006	2,004	2,004	2,003	2,004	2,004
Time (min): Target	29	29	29	29	29	40	40	40	40	40
Actual	30.36	29.74	27.54	28.79	29.11	41.29	41.27	36.37	38.13	39.27
Preheater	Yes	Yes	No	No	--	Yes	Yes	No	No	No
Conversion (wt % MAF coal)	94.25	94.24	94.13	94.10	94.18	94.70	96.10	94.62	94.34	95.19
H ₂ consumption (elemental balance) (wt % MAF coal)	2.95	2.84	3.27	3.24	3.08	3.86	4.40	3.67	3.87	3.95
From gas	2.33	2.22	2.85	2.82	2.56	3.66	4.20	3.09	3.29	3.56
From solvent	0.63	0.62	0.42	0.421	0.53	0.20	0.20	0.58	0.58	0.39
H ₂ consumption (process GC) (wt % MAF coal)	2.62	2.32	2.79	3.21*	2.74	3.21	40.07	3.68	3.54	3.63
C ₁ -C ₄ (wt %)	12.97	11.55	14.54	14.93	13.45	18.00	20.40	17.79	18.06	18.56
CO + CO ₂ (wt %)	2.22	2.29	2.73	2.66	2.48	2.27	2.34	2.70	2.26	0.39
H ₂ S + NH ₃ (wt %)	2.90	2.35	3.14	3.24	2.91	3.22	3.55	3.76	3.35	3.47
H ₂ O (process method) (wt %)	2.49	2.44	5.94	5.21	4.02	4.09	6.29	5.74	6.12	5.56
H ₂ O (oxygen balance) (wt %)	3.52	3.50	4.38	4.10	3.88	4.79	5.57	4.64	5.08	5.02
Oils (wt %)	31.75	33.40	28.67	27.62	30.36	32.31	29.59	30.12	31.06	30.77
SRC (wt %)	42.10	42.21	39.13	40.44	40.97	34.82	33.93	34.54	34.50	34.45
Asphaltenes (wt %)	19.76	22.27	22.75	24.63	22.36	21.15	20.58	19.83	19.94	20.38
Preasphaltenes (wt %)	22.34	19.93	16.38	15.81	18.62	13.67	13.35	14.68	14.57	14.07
Organic residue (wt %)	8.35	8.06	8.65	9.10	8.54	8.50	7.95	9.06	8.18	8.42
S in SRC (wt %)	0.65	0.65	0.59	0.59	0.62	0.55	0.55	0.49	0.49	0.52
H ₂ in: solvent in (wt %)	8.25	8.25	8.25	8.25	8.25	8.25	8.25	8.25	8.25	8.25
solvent out (wt %)	7.91	7.91	8.02	8.02	7.97	8.14	8.14	7.93	7.93	8.04

^aAverage of yields at 29-min residence.^bAverage of yields at 40-min residence.

As predicted, the slurry passing through the reactor reached the desired reaction temperature of 840°F within the preheater tube. Since the slurry temperatures in the preheater were transient, two sets of data were generated. In one (e.g., 52-233, 52-221), the assumption was made that the preheater did not contribute to coal conversion; in the other (e.g., 52-22, 52-11), the preheater was treated as an integral part of the reactor. The average yields with and without the preheater volume are also included in Table 13 (e.g., 52-29).

The average conversion of Mulford coal at 40-min residence was 95.2 wt % MAF coal, which was about 1% more than the 94.2 wt % conversion at 29-min residence. These are the highest conversion levels ever seen in the CPDU for any Kentucky #9 coal.

Comparison of oil, asphaltene, and preasphaltene yields showed that, in the plug-flow reactor, the residence-time effect was most significant for converting preasphaltenes, followed sequentially by asphaltenes and oils. The preasphaltene yield at 29 min was 18.6%, which decreased to 14.1% at 40 min, whereas the asphaltene and oil yields changed from 22.4 and 30.4% at 29 min to 20.4 and 30.8% at 40 min, respectively. The insignificant change in oil yield as the residence time increased, in contrast to the significant increase in gas yield, indicates that preasphaltenes and asphaltenes were the major contributors to the formation of light gaseous products.

Elementally balanced hydrogen consumption increased from 3.1 to 4.0 wt % MAF coal as the residence time increased from 30 to 40 min. This significant increase is not usually seen in the CSTR, and is also consistent with the large increase in light gases. For example, the yield of hydrocarbon gases (C_1-C_4) increased from 13.5 to 18.6% when the residence time increased from 29 to 40 min.

The effect of hydrodynamics on liquefaction can be better understood when the plug-flow yields are compared with CSTR yields (see Table 14). Yields from plug-flow reaction were enhanced considerably compared to the CSTR yields, especially at 29-min residence. The conversion of coal was 94%, 6% higher than that of the CSTR (88%). Conversion in the plug-flow reactor still increased to 95% at 40-min residence, in contrast to the absence of any apparent change in conversion observed in the CSTR for the same time change. Conversions of

Table 14

Comparison of Plug-Flow Reactor Yields with CSTR Yields

Reactor type	Plug flow ^a	CSTR ^b	Plug flow ^a	CSTR ^b	2 CSTRs ^b
Run i.d.	BCL	HCL	BCL	SCL	SCL
Sample i.d.	52-29	53-86	52-40	55-63	56-41
Temp (°F)	840	839	840	840	842
Pressure (psig)	2006	2001	2004	2000	2000
Residence time (min):	target	29	40	40	20+20 ³
	actual	29.1	39.3	40.4	41.5
Conversion (wt % MAF coal)	94.18	88.34	95.19	87.79	89.52
H ₂ consumption (elemental balance)	3.08	2.30	3.95	2.34	2.44
(wt % MAF coal)					
Yields (wt % MAF coal)					
C ₁ -C ₄	13.45	12.43	18.56	11.62	12.31
CO + CO ₂	2.48	1.68	2.39	1.64	1.70
H ₂ S + NH ₃	2.91	2.07	3.47	2.20	2.75
H ₂ (process method)	4.02	2.57	5.56	2.94	3.60
Oils	30.36	19.78	30.77	21.25	20.15
SRC	40.97	49.81	34.45	46.40	49.00
Asphaltenes	22.35	20.27	20.38	20.31	24.60
Preasphaltenes	18.62	29.55	14.07	26.09	24.40
Insoluble organic residue	8.54	14.12	8.42	14.07	12.48
S in SRC (wt %)	0.62	0.74	0.52	0.72	0.61
H in: solvent in (wt %)	8.25	8.25	8.25	8.25	8.25
solvent out (wt %)	7.97	8.02	8.04	7.84	7.91

^aAverage of four measurements.^bSingle measurement.^cTwo reactors in series.

insoluble organic matter are consistent with these results; the plug-flow reaction resulted in a net 5.6 and 5.7% decrease of IOM, from 14.1% to 8.5% and 8.4%, respectively.

Preasphaltene conversion was similar. With the plug-flow reactor, yields were 18.6% at 29 min and 14.1% at 40 min, a net 11 and 12% lower than the yields from the CSTR, respectively (29.6 and 26.1% at the same conditions).

In contrast to the large conversions seen in the yields of primary products (i.e., the insoluble organic matter and preasphaltenes), asphaltene yields differed very little between the two reactors. At 29 min, the plug-flow reactor yielded 22.4% asphaltenes, which was 2% more than that from the CSTR (20.3%). At 40 min, both reactors yielded 20.3% asphaltenes.

The plug-flow reactor also increased oil yields relative to the well-mixed CSTR system, parallel to its effect on coal conversion and preasphaltenes. Yields of 30.4% at 29 min and 30.8% at 40 min exceeded those from the CSTR by 10.6 and 9.5%, respectively (19.8 and 21.3% at 29 and 40 min, respectively). The data for both reactor systems show that residence time did not affect oil and asphaltene yields as much as the other products, especially preasphaltenes and gases. This indicates that the coal's initial reaction paths were pivotal to the final product destination, because these differences cannot be explained by the different mixing behaviors alone between the two reactor systems.

The effect of hydrodynamics on the light gases was strongly time-dependent. At 29-min residence, the C_1-C_4 yield from the plug-flow reactor was 1% higher than that from the CSTR (13.4% vs. 12.4%). In contrast, at 40-min residence, the plug-flow yield was significantly (7%) higher--18.6 vs. 11.6%. Comparison of plug-flow and CSTR data indicates that the primary products, i.e., IOM, preasphaltenes, and asphaltenes, were the major contributors to the formation of light gases. This is evidenced by the marginal increase of oil yields contrasted with considerable differences in the increases of gas yields between the two reactors as the residence time increased.

Hydrogen consumption differences between the two systems followed a similar pattern. At 29-min residence, the enhancement of conversion in the plug-flow reactor resulted in 0.8% more hydrogen consumed than in

the CSTR (an increase from 2.3 to 3.1%). At 40 min, the difference between the two reactors was even larger (1.6%; from 2.3 to 3.9%). The stronger effect of residence time on hydrogen consumption for the plug-flow reactor agreed with the trend noted for light gaseous products. Increasing the time from 29 to 40 min increased hydrogen consumption in the plug-flow reactor by nearly 0.9% (from 3.1 to 4.0%), whereas the change in the CSTR was insignificant (less than a 0.1% increase, from 2.30 to 2.34%).

Thus, the major difference in the performance of the two reactor systems is the mixing behavior of the reactants. However, the difference in gas residence times cannot be totally ignored, although we assume that our CSTR is not limited by gaseous hydrogen mass transfer within the operating window of our process study. Cold-flow studies conducted on the reactor simulators indicated that gas residence times may be about 7-10 times higher in the plug-flow reactor than in the CSTR. The impact of gas residence time on coal liquefaction yields has never been addressed.

PREDICTABILITY OF THE SEQUENTIAL REACTION MODEL FOR YIELD DISTRIBUTION

As discussed earlier, no two reactions have identical fluid dynamic characteristics. Therefore, data generated in different reactors will not have a common basis, because reaction rates of coal and its products depend on the hydrodynamics in each reactor system. This is why accurate reaction and hydrodynamic models must be developed in order to reduce the data bases from various sources to a common basis.

In order to check the predictability of APCI/ICRC's sequential kinetic model, the CSTR data on Kentucky #9 Mulford coal were transformed to plug-flow reactor yields using the model. In order to generate the most highly sensitive predictions from the reaction model, a single CSTR data point was used to predict the corresponding plug-flow reactor yields. In this way, temperature and residence time remained invariant, leaving the fluid dynamics for each reactor as the only variables. Thus, variations introduced in the predicted values by other process variables become minimal. Of course, measurement errors associated with experimental data were conveyed to the predicted data at the

same level of uncertainty. Overall, the prediction based on a single data point was sufficient for testing the model; incorporating additional data points would probably not significantly improve the prediction.

Tables 15 and 16 summarize results comparing the predicted and measured plug-flow yields. Also shown are the CSTR data measured at corresponding process conditions. Rate constants used for this evaluation are given in Table 17.

The sequential reaction model underestimated the oil yield of the plug-flow reactor at 29 min by about 7% (23.2 vs. 30.4%), and overestimated it at 40 min by 5% (35.9 vs. 30.8%). The most severe departures were in the prediction of asphaltene and preasphaltene yields: up to 14.4% differences in the asphaltene yields at 29 min (36.8% predicted vs. 22.4% measured) and 9.3% in the preasphaltene yields at 40 min (4.8% predicted vs. 14.1% measured).

The departure in the predicted gas yields grew larger at 40-min residence; e.g., the hydrocarbon gas yield was 10.7% predicted vs. 13.5% measured at 29 min, compared with 15.1% predicted vs. 18.6% measured at 40 min. Similarly, the predicted values of sulfur in SRC also differed significantly from the measured values: predicted vs. measured values were 0.14 and 0.62%, respectively, at 29 min, and 0.05 and 0.52%, respectively, at 40 min.

Good predictions of the coal conversions are not surprising in this time range. These values were biased by the assumption that 4% of the coal was unreactive, and the fast rate constants generated in the prediction were prejudiced by being near complete conversion.

Only three additional data points were available for Kentucky #9 Mulford coal, determined at 20-, 29-, and 40-min residence and 840°F. With these additional points, the fit of the model was reevaluated to see if any improvement had occurred. Tables 18 and 19 summarize the results, and rate constants determined using the sequential model are shown in Table 20.

The deviation of predicted from measured values follows essentially the same pattern seen in the previous point-to-point data evaluation, with no apparent improvement in predictability. An improved prediction for one component seemed to worsen the prediction for another component. Preasphaltenes and asphaltenes appeared to deviate more than others.

Table 15

Comparison of Predicted and Measured Plug-Flow Reactor
Yield Distribution Based on a Single Data Point:
29-Min Residence (840°F)

Products in wt % of MAF coal	CSTR, measured	Plug-flow reactor	
		Predicted	Measured
Oils	19.8	23.2	30.4
SRC	49.8	54.0	41.0
Asphaltenes	20.3	36.8	22.4
Preasphaltenes	29.5	17.2	18.6
Reactive residue	10.1	0.2	4.5
Unreactive residue	4.0 ^a	4.0 ^a	4.0 ^a
Hydrocarbon gases (C ₁ -C ₄)	12.4	10.7	13.5
Other gases (H ₂ O, H ₂ S, NH ₃ , CO, CO ₂)	6.3	7.9	9.4
Sulfur in SRC (wt % of SRC)	0.74	0.14	0.62
Conversion ^a	88.3	95.8 ^b	94.2

^aConversion is the summation of all the products measured.

^bAssumption was made that 4% of the coal is unreactive.

Table 16

Comparison of Predicted and Measured Plug-Flow Reactor
Yield Distribution Based on a Single Data Point:
40-Min Residence (840°F)

Products in wt % of MAF coal	CSTR, measured	Plug-flow reactor	
		Predicted	Measured
Oils	21.3	35.9	30.8
SRC	46.4	35.8	34.5
Asphaltenes	20.3	31.0	20.4
Preasphaltenes	26.1	4.8	14.1
Reactive residue	10.1	0.0	4.4
Unreactive residue	4.0 ^a	4.0 ^a	4.0 ^a
Hydrocarbon gases (C ₁ -C ₄)	11.6	15.1	18.6
Other gases (H ₂ O, H ₂ S, NH ₃ , CO, CO ₂)	8.1	9.2	11.4
Sulfur in SRC (wt % of SRC)	0.72	0.05	0.52
Conversion	87.8	96.0 ^a	95.2

^a Assumption was made that 4% of the coal is unreactive.

Table 17

Rate Constants (min^{-1}) Determined from
CSTR Data for Kentucky #9 Mulford Coal^a

	29 min	40 min	Reaction sequence
k_1	2.447×10^{-1}	1.761×10^{-1}	Coal to PA ^b
k_2	6.145×10^{-2}	5.074×10^{-2}	PA to A
k_3	3.842×10^{-2}	2.835×10^{-2}	A to oil
k_7	6.425×10^{-2}	4.883×10^{-2}	PA and A to sulfurous gases ^c
k_8	1.334×10^{-2}	2.715×10^{-2}	PA to oxide gases ^d
k_9	1.821×10^{-3}	1.227×10^{-3}	PA, A, and oil to C ₁ -C ₄ hydrocarbon gases

^aBased on one data point at 840°F.

^bPA, preasphaltenes; A, asphaltenes.

^cReaction rate = $k_7 \times (\text{PA concentration}) (\% \text{ S in PA})$.

^dReaction rate = $k_8 \times (\text{PA concentration}) (\% \text{ O in PA})$.

Table 18

Comparison of Predicted and Measured Plug-Flow Reactor
Yield Distributions Based on Three Data Points:
29-Min Residence (840°F)

Products in wt % of MAF coal	CSTR, measured	Plug-flow reactor	
		Predicted	Measured
Oils	19.8	26.2	30.4
SRC	49.8	54.0	41.0
Asphaltenes	20.3	36.8	22.4
Preasphaltenes	29.5	17.2	18.6
Reactive residue	10.1	0.2	4.5
Unreactive residue	4.0 ^a	4.0 ^a	4.0 ^a
Hydrocarbon gases (C ₁ -C ₄)	12.4	10.7	13.5
Other gases (H ₂ O, H ₂ S, NH ₃ , CO, CO ₂)	6.3	7.9	9.4
Sulfur in SRC (wt % of SRC)	0.74	0.14	0.62
Conversion ^b	88.3	95.8 ^a	94.2

^aAssumption was made that 4% of the coal is unreactive.

^bConversion is the summation of all the products measured.

Table 19

Comparison of Predicted and Measured Plug-Flow Reactor
Yield Distribution Based on Three Data Points:
40-Min Residence (840°F)

Products in wt % of MAF coal	CSTR, measured	Plug-flow reactor	
		Predicted	Measured
Oils	21.3	39.1	30.8
SRC	46.4	34.7	34.5
Asphaltenes	20.3	33.2	20.4
Preasphaltenes	26.1	1.5	14.1
Reactive residue	10.1	0.0	4.4
Unreactive residue	4.0 ^a	4.0 ^a	4.0 ^a
Hydrocarbon gases (C ₁ -C ₄)	11.6	14.4	18.6
Other gases (H ₂ O, H ₂ S, NH ₃ , CO, CO ₂)	8.1	7.7	11.4
Sulfur in SRC (wt % of SRC)	0.72	0.21	0.52
Conversion ^b	87.8	96.0 ^a	95.2

^aAssumption was made that 4% of the coal is unreactive.

^bConversion is the summation of all the products measured.

Table 20

Rate Constants (min^{-1}) Determined from
 CSTR Data for Kentucky #9 Mulford Coal,
 Based on Only Three Data Points (20, 29, and 40 Min) at 840°F

k_1	$= 2.669 \times 10^{-1}$	Coal to PA ^b
k_2	$= 6.753 \times 10^{-2}$	PA to A
k_3	$= 3.118 \times 10^{-2}$	A to oil
k_7	$= 5.568 \times 10^{-2}$	PA and A to sulfurous gases
k_8	$= 2.424 \times 10^{-2}$	PA to oxide gases
k_9	$= 1.447 \times 10^{-3}$	PA, A, and oil to C ₁ -C ₄ hydro- carbon gases

^aPA, preasphaltenes; A, asphaltenes.

UTILITY OF PLUG-FLOW REACTOR

Coal liquefaction conversion involves not only extremely complex reactions, but also a complicated reactor system. The system can easily result in incorrect data, often in subtle ways that are unnoticed by the researcher, which can overwhelm the intrinsic problems. For example, there are no known analytical methods to identify and define, in a universally acceptable manner, the feeds and products of coal liquefaction in a way that accurately relates to the process-defined materials. One of the problems for researchers in generating a data base for CSTR experiments was the channeling of hydrogen gas and concomitant depletion of vapor-phase reactants in the reactor, due to its characteristically low length-to-diameter (L/D) ratio. How these unduly shorter gas- and vapor-phase contact times and their impact on the consequential shifting of the liquid-to-vapor proportions in the CSTR would affect liquefaction yields is not well understood nor has it been studied. (The plug-flow reactor used in this study might have extended the gas residence time to about 7-10 times that of the CSTR.)

A plug-flow reactor study in conjunction with the CSTR can provide an excellent opportunity not only to look at the effect of hydrodynamics on coal liquefaction, but also to check the soundness of APCI/ICRC's reaction models, as discussed earlier. Because CSTR and plug-flow reactor hydrodynamics span the entire possible range of fluid dynamics, any data base generated from both reactors would allow us to interpolate the fluid dynamic effects in any specified reactor configuration, if the hydrodynamics of that reactor system were also known. Often, accurately determining a yield data base is very difficult and time-consuming, if not impossible. By providing the maximum fluid-dynamic variation in the reaction system, a comparison of CSTR and tubular reactor data maximizes the sensitivity of yield distribution to hydrodynamics. For the researcher, a basic rule is to avoid extrapolation of data, if possible. If either CSTR or plug-flow data alone are used to design a commercial reactor, extrapolation of the data base is an inevitable consequence. Evaluation of hydrodynamic effects using pilot-plant-scale reactors, such as that of the Wilsonville plant, is certainly uneconomical. Also,

the sensitivity of yields to the small fluid dynamic change was not great enough to yield a definitive conclusion.

The true reaction mechanism of coal must be the same, whether the reaction occurs in a CSTR or a plug-flow reactor. Interfacing the two data bases on a common fluid dynamic basis, through the transformation of one data base as exemplified earlier, should result in identical yield data, if the reaction model being tested is adequate. Therefore, generation of two data bases increases the chance of improving the reaction model. One of the advantages of paired data bases is that intermediate point-to-point checking of the reaction model is possible between the two data bases without the need for accumulating additional data. Another potential advantage of combining the data bases is that it can provide a way to determine gas residence time effects with a proper experimental design.

After an adequate reaction model has been developed with the benefit of the maximum sensitivity of the two data bases, the reactor can be optimized, including hydrodynamics (by optimizing the reactor configuration), by using various existing mathematical approaches. However, when sufficient data are gathered to tie up the domains of the two extreme reaction regimes, the optimal reactor may be searched explicitly even without the aid of a reaction model.

The generalized rate equations of an n-component reaction system for a CSTR and a plug-flow reactor are shown in equations (17) and (18). For the CSTR, the rate of the nth component, C_n , is:

$$\frac{C_n^m(\tau) - C_n^m(0)}{\tau} = - \sum_{j=1}^N k_{jn} C_n^m(\tau) + \sum_{j=1}^N k_{nj} C_j^m(\tau) \quad (17)$$

Depletion of C_n^m by forward reactions
Generation of C_n^m by reverse reactions

For the plug-flow reactor, the nth component C_n^P is:

$$\frac{dC_n^P(t)}{dt} = - \sum_{j=1}^N k_{jn} C_n^P(t) + \sum_{j=1}^N k_{nj} C_j^P(t) \quad (18)$$

Here, residence times are denoted by τ for a CSTR (mean residence time) and t for a plug-flow reactor (local residence time). The rate constant of the n th component converting to the j th component is denoted by k_{jn} , whereas k_{nj} is the reverse rate constant, converting from the j th to the n th component. $C_n(0)$ denotes the concentration of C_n at time zero, which, in other words, is the concentration of the n th component in the feed. The superscripts m and p distinguish the CSTR and plug-flow reactors, respectively.

Subtraction of the two equations leads to:

$$\frac{dC_n^p(t)}{dt} = \frac{C_n^m(\tau) - C_n^m(0)}{\tau} - \sum_{j=1}^N k_{jn} [C_n^p(t) - C_n^m(\tau)] + \sum_{j=1}^N k_{nj} [C_j^p(t) - C_j^m(\tau)] \quad (19)$$

If we let:

$$\delta(t, \tau) = C^p(t) - C^m(\tau) \quad (20)$$

then:

$$\frac{dC_n^p(t)}{dt} = \frac{C_n^m(\tau) - C_n^m(0)}{\tau} - \sum_{j=1}^N k_{jn} \delta_n(t, \tau) + \sum_{j=1}^N k_{nj} \delta_j(t, \tau) \quad (21)$$

$\delta_n(t, \tau)$ is the change in concentration of the n th component along the plug-flow reactor during the reaction compared to the concentration at the exit of the CSTR.

After data bases for both the CSTR and plug-flow reactor become available, equation (21) can be used to search for a reaction model using an appropriate computing technique in which the sensitivity of search is likely to be enhanced by the intrinsic fluid dynamic boundary conditions set by δ .

Solution of a combination of the above equations is deemed possible, whichever choice leads to the best sensitivity.

CONCLUSIONS

Laboratory-scale plug-flow reactor studies of coal liquefaction have been reported by others, but whether these studies were actually conducted in the plug-flow regime is questionable. We have attempted to determine the hydrodynamic effects of various reactor configurations on coal liquefaction, to help select the optimal reactor configuration and to provide additional understanding of coal liquefaction reaction kinetics, which cannot be definitively determined by a CSTR alone. Because of the many variables associated with coal liquefaction experiments, direct measurement of the hydrodynamic effects imposed upon coal liquefaction reactions has not been regularly practiced on a laboratory scale. Only a qualitative understanding of the fluid dynamic effects on product yields has been perceived by operating various sizes of open-column tubular reactors, because the fluid-dynamic characteristics of these reactors were not clearly understood and could not be varied significantly. Indirect studies, by cold-flow simulation, have been of little help in defining the fluid dynamic impact on coal liquefaction.

In this study, a laboratory plug-flow tubular reactor was developed. Based on cold-flow studies, the liquid residence time, mixing behavior, and void fraction in the reactor simulator showed that the performance of this reactor system would be equivalent to about 20 CSTRs in series. From a practical standpoint, this is essentially identical to that of a theoretical plug-flow reactor. A computer simulation using a kinetic model was conducted to support the design of the plug-flow reactor.

A three-phase experimental cold-flow study showed that the dispersion behavior of solid particles smaller than 200 Tyler mesh (74 μm) was nearly identical to that of liquids in this reactor system. (The critical particle size was not determined due to time constraints.) Overall, a three-phase system would behave similarly to a plug-flow reactor under this constraint. The three-phase system is anticipated to approach even closer to the plug-flow regime than the gas/liquid system, because of the solids' enhancement of apparent viscosity.

Comparison of actual coal liquefaction data from both the plug-flow reactor and the CSTR showed that the plug-flow configuration had various advantages. Reactor yields improved significantly, especially the primary product conversions. At 840°F and residence times of 29 and 40 min, coal and preasphaltene conversions were enhanced ~6 and 10%, respectively. At these conditions, the plug-flow reactor also yielded about 10% more oils than the CSTR. Significant increases of gas hydrogen utilization were also seen with the plug-flow reactor.

Also, this study provided an opportunity to examine the soundness of APCI/ICRC's sequential kinetic model, by interfacing the plug-flow and CSTR yield data. Transforming CSTR yields to plug-flow data showed that product yields deviated considerably from the measured plug-flow data, suggesting the need to improve the existing reaction model.

Having both CSTR and plug-flow reactor data bases is important for developing a sound coal reaction model and for determining hydrodynamic effects on coal liquefaction in a direct way. The results will lead to an optimized reactor configuration as well as optimized operation.

LITERATURE CITED

- Akita, K., and F. Yoshida. 1973. Gas holdup and volumetric mass transfer coefficient in bubble columns. I&EC Proc. Des. Develop. 12(1), 76.
- Hughmark, G. A. 1967. Holdup and mass transfer in bubble columns. I&EC Proc. Des. Develop. 6(2), 218.
- Levenspiel, O., and K. B. Bischoff. 1963. Patterns of flow in chemical process vessels. Pages 95-192 in Advances in chemical engineering, Vol. 4. Academic Press, New York.
- Martin, C. J. 1979. Kinetic model of the coal slurry reactor to evaluate mixing and residence time effects. SRC-I coal refinery preliminary demonstration plant design and cost estimates and long lead procurement planning - summary. Volume I, Chapter II, page 146, 31 July.
- Ying, D. H. S., R. Sivasubramanian, and E. N. Givens. October-December 1979. Gas/slurry flow in coal liquefaction process. Quarterly technical progress report to DOE. FE-14801-3.

APPENDIX A-1
DERIVATION OF THE TUBULAR REACTOR DESIGN CORRELATIONS

Peclet number is defined by:

$$P = \frac{UL}{E_{ZL}} = \frac{U_L L}{(1 - E_G)E_{ZL}} \quad (A-1)$$

where P = Peclet number
 U = average liquid velocity in column
 L = length of column
 E_{ZL} = liquid axial dispersion coefficient
 U_L = superficial liquid velocity
 E_G = void fraction by gas holdup in tube or column

Liquid dispersion coefficients for a vertical upflow bubble column can be predicted by the Ying correlation (1978), which was derived from extensive two-phase cold-flow study with various liquid/gas pairs using 2 to 5 in. i.d. columns.

$$E_{ZL} = 0.27DU_G \left(\frac{gD}{U_G^2} \right)^{0.32} \quad (A-2)$$

$$= 0.82D^{1.32} U_G^{0.36}$$

where E_{ZL} = liquid axial dispersion coefficient (ft²/sec)
 D = diameter of column (ft)
 U_G = superficial gas velocity (ft/sec)
 g = gravitational acceleration (32.2 ft/sec²)

Length of column when expressed with the volume and diameter of a column holds:

$$L = \frac{4V}{\pi D^2} \quad (A-3)$$

where L = column length
 V = column volume
 D = column diameter

The mean residence time for liquid flowing through a column is the ratio of column length to average liquid velocity:

$$\theta = \frac{L}{U_L / (1 - E_G)} = \frac{(1 - E_G)L}{U_L} \quad (A-4)$$

where L = column length
 U_L = superficial liquid velocity
 E_G = void fraction of gas

A new parameter R is defined, which is the ratio of superficial gas velocity to superficial liquid velocity:

$$R = \frac{U_G}{U_L} \quad (A-5)$$

Then:

$$U_G = R U_L \quad (A-6)$$

But combining equations (A-2) through (A-6) into equation (A-1), the following correlation of Peclet number as a function of void fraction (E_G), mean residence time (θ), reactor volume (V), and reactor diameter (D) can be derived:

$$P = \frac{1.812V^{1.64}}{(1 - E_G)^{0.36} R^{0.36} \theta^{0.64} D^{4.6}} \quad (A-7)$$

where V = reactor volume (ft³)
 θ = residence time (sec)
 D = diameter (ft)

Note that diameter is the most sensitive parameter affecting the Peclet number, followed by reactor volume, residence time, and the gas-to-liquid velocity ratio. Since $(1 - E_G)^{0.36} \cong 1$:

$$P = \frac{1.812V^{1.64}}{R^{0.36}\theta^{0.64}D^{4.6}} \quad (A-8)$$

Typical demonstration plant reactor conditions and additional assumptions can be given as follows:

Reactor conditions

Temperature	840°F
Pressure	2,014.7 psia
H ₂ rate	30,000 scf/2,000 lb of coal
Coal concentration in slurry	38 wt %

Assumptions

1. Hydrogen is grossly representative of the gas flowing through the reactor without solubilization; i.e., the gas velocity contributed by product gases and solvent vaporization is insignificant.
2. The slurry density in the reactor is assumed to be 0.8 g/cm³.
3. The compressibility of the gas mixture in the reactor is equal to that of hydrogen gas, which is 1.038 at 840°F and 2,014.7 psia.

Based on these conditions and assumptions, the ratio of gas to liquid velocity is:

$$\begin{aligned}
 R &= \frac{30,000 \text{ scf}/2,000 \text{ lb of coal}}{0.38 \text{ lb of slurry}/\text{lb of coal}} \\
 &= 0.38 \times 30,000 \times 28,316.85 \text{ cm}^3 \times \frac{14.7 \text{ psia}}{2,014.7 \text{ psia}} \times \frac{(460 + 840) \text{ }^\circ\text{R}}{(460 + 70) \text{ }^\circ\text{R}} \times \frac{1.038}{1.0006} \\
 &\quad \frac{(2,000 \times 453.6 \text{ g of slurry})/(0.8 \text{ g of slurry per cm}^3)}{} \\
 &= 5.28
 \end{aligned}$$

By the use of equation (A-8), Peclet numbers could be calculated for the various reactor tube diameters, for a fixed capacity of 1 L on the basis

of $R = 5.3$, $V = 0.0353 \text{ ft}^3$ (1 L), and $\theta = 20, 40, 60,$ and 80 min , as tabulated in Table A-1.

The relation between the tube diameter and Peclet number of a 1-L reactor at various residence times is plotted in Figure 7 in the text. More precise correlation between reactor geometry and Peclet number can be developed using the newly developed correlations for dispersion and void fraction (equations 6 and 1 in text). However, equation A-8 is good enough to guide the preliminary design criteria.

Table A-1

Relation of Reactor Diameter and
Peclet Number for a 1-L Reactor

Diameter (in.)	Length (ft)	Peclet numbers			
		20 min	40 min	60 min	80 min
0.4	40.47	275.33	176.68	136.30	113.38
0.5	25.90	98.64	63.30	48.83	40.62
0.6	17.99	42.64	27.36	21.11	17.56
0.7	13.21	20.98	13.47	10.39	8.64
0.8	10.12	11.35	7.29	5.62	4.68
0.9	7.99	6.60	4.24	3.27	2.72
1.0	6.47	4.07	2.61	2.01	1.67

APPENDIX A-2

COLD-FLOW FLUID-DYNAMIC DATA SUMMARY FOR
THE PLUG-FLOW REACTOR SIMULATOR

1.0 Residence Time - Tracer Response Data

1.1 Water-Nitrogen Flow System

a. U_l (Liquid Velocity) = 0.004265 ft/sec

U_g , ft/sec (gas Velocity)	0	.018	.028	.044	.080	.175	.315	.446
t_i (time, min)	C_i (Tracer Signal Intensity)							
15	-	-	-	-	-	-	-	2.0
18	-	-	-	-	-	-	1.0	-
20	-	-	-	-	-	-	3.2	13.7
22	-	-	-	-	-	-	7.3	-
23	-	-	-	-	-	0.9	-	-
24	-	-	-	-	-	-	11.8	-
25	-	-	-	-	-	-	-	31.0
26	-	-	-	-	-	2.5	17.3	-
28	-	-	-	-	0.2	-	22.5	-
29	-	-	-	-	-	8.0	-	-
30	-	-	-	-	-	-	34.7	52.0
32	-	-	-	-	1.9	15.3	47.3	-
34	-	-	-	-	-	-	56.8	-
35	-	-	0.2	0.9	-	24.6	-	76.0
36	-	-	-	-	5.0	-	62.3	-
38	-	-	-	-	-	32.8	67.3	-
40	-	0.2	0.9	3.1	11.1	-	71.2	91.0
41	-	-	-	-	-	38.1	-	-
42	-	-	-	-	-	-	71.9	-
44	-	-	-	-	19.5	44.0	70.2	-
45	-	1.6	3.0	9.4	-	-	-	85.5
46	-	-	-	-	-	-	66.1	-
47	-	-	-	-	-	47.4	-	-
48	-	-	-	-	29.5	-	63.8	-
50	-	7.0	7.6	20.0	-	52.3	58.0	77.1
52	-	-	-	-	38.6	-	54.0	-
53	-	-	-	-	55.8	-	-	-
54	-	-	-	-	-	48.8	-	-
55	-	15.8	13.3	31.4	-	-	-	58.1-
56	-	-	-	-	46.2	60.1	44.2	-
58	-	-	-	-	-	-	39.5	-
59	-	-	-	-	62.7	-	-	-
60	-	27.7	17.9	42.3	51.9	-	35.0	43.8
62	-	-	-	-	-	56.6	31.0	-
64	-	-	-	-	54.7	-	27.1	-
65	-	39.8	27.7	50.0	-	49.9	-	33.3
66	-	-	-	-	-	-	23.5	-
68	-	-	-	-	54.7	44.0	19.0	-
70	-	49.7	36.3	56.0	-	-	15.3	24.4
71	-	-	-	-	-	38.7	-	-

U_g , ft/sec (gas Velocity)	0	.018	.028	.044	.080	.175	.315	.446
t_i (time, min)	C_i (Tracer Signal Intensity)							
72	-	-	-	-	52.0	-	12.7	-
74	-	-	-	-	-	33.0	10.3	-
75	-	54.9	46.0	55.7	-	-	-	16.3
76	-	-	-	-	48.3	-	8.5	-
77	-	-	-	-	-	29.2	-	-
78	-	-	-	-	-	-	7.0	-
80	0.2	55.6	50.9	50.8	43.6	25.0	5.7	12.0
82	-	-	-	-	-	-	4.4	-
83	-	-	-	-	-	23.0	-	-
84	-	-	-	-	38.0	-	3.3	-
85	-	52.6	53.4	46.2	-	-	-	8.0
86	-	-	-	-	-	17.0	2.7	-
88	-	-	-	-	33.1	-	1.9	-
89	-	-	-	-	-	11.8	-	-
90	1.2	46.5	50.0	38.8	-	-	0.9	5.0
92	-	-	-	-	27.3	8.2	0.3	-
94	-	-	-	-	-	-	0	-
95	-	40.3	41.4	32.0	-	6.2	-	2.9
96	-	-	-	-	22.9	-	-	-
98	-	-	-	-	-	5.0	-	-
100	4.0	34.0	34.2	26.0	18.1	-	-	1.3
101	-	-	-	-	-	4.0	-	-
104	-	-	-	-	14.6	3.1	-	-
105	-	28.2	27.5	20.0	-	-	-	0.6
107	-	-	-	-	-	2.6	-	-
108	-	-	-	-	11.5	-	-	-
110	20.3	22.0	21.9	15.0	-	1.7	-	-
112	-	-	-	-	8.8	-	-	-
113	-	-	-	-	-	1.0	-	-
115	-	16.5	17.5	11.8	-	-	-	-
116	-	-	-	-	6.8	0.9	-	-
119	-	-	-	-	-	0.8	-	-
120	44.7	11.7	13.8	9.0	5.0	-	-	-
121	-	-	-	-	-	0.7	-	-
124	-	-	-	-	4.0	0.3	-	-
125	-	7.0	10.6	5.7	-	-	-	-
127	-	-	-	-	-	-	0	-
128	-	-	-	-	-	2.9	-	-
130	41.3	4.3	8.0	3.8	-	-	-	-
132	-	-	-	-	2.1	-	-	-
135	-	3.0	6.1	3.0	-	-	-	-
136	-	-	-	-	1.3	-	-	-
140	37.2	1.1	4.3	2.0	0.9	-	-	-
144	-	-	-	-	0.8	-	-	-
145	-	0.8	3.6	1.3	-	-	-	-
148	-	-	-	-	0.8	-	-	-
150	32.3	0.7	2.7	1.0	-	-	-	-
152	-	-	-	-	0.5	-	-	-
155	-	0.4	2.0	0.9	-	-	-	-
156	-	-	-	-	0.2	-	-	-
160	28.3	0.2	1.7	0.8	-	-	-	-

U_g , ft/sec (gas Velocity)	0	.018	.028	.044	.080	.175	.315	.446
t_i (time, min)	C_i (Tracer Signal Intensity)							
165	-	-	1.1	0.5	-	-	-	-
170	24.2	-	1.0	0.2	-	-	-	-
175	-	-	0.7	-	-	-	-	-
180	21.0	-	0.7	-	-	-	-	-
185	-	-	0.2	-	-	-	-	-
190	17.7	-	-	-	-	-	-	-
200	15.4	-	-	-	-	-	-	-
210	13.0	-	-	-	-	-	-	-
220	11.6	-	-	-	-	-	-	-
230	10.3	-	-	-	-	-	-	-
240	9.3	-	-	-	-	-	-	-
250	7.8	-	-	-	-	-	-	-
260	6.7	-	-	-	-	-	-	-
270	6.0	-	-	-	-	-	-	-
280	5.3	-	-	-	-	-	-	-
290	4.0	-	-	-	-	-	-	-
300	3.0	-	-	-	-	-	-	-
310	2.2	-	-	-	-	-	-	-
320	1.6	-	-	-	-	-	-	-
330	0.8	-	-	-	-	-	-	-

b. U_l (Liquid Velocity) = 0.007218 ft/sec

U_g , ft/sec (gas Velocity) t_i (time, min)	0	.018	.029	.042	.089	.179	.320	.483
	C_i (Tracer Signal Intensity)							
10	-	-	-	-	-	-	-	0.2
12	-	-	-	-	-	-	0.3	1.8
14	-	-	-	-	-	-	1.9	6.7
16	-	-	-	-	-	0.2	6.0	16.9
18	-	-	-	-	-	1.0	13.3	30.8
20	-	-	-	-	-	2.9	24.1	47.0
22	-	-	-	-	-	6.7	36.5	64.0
24	-	-	-	-	1.0	13.3	48.0	77.9
26	-	-	-	-	2.0	22.3	59.9	85.0
27	-	-	-	0.3	-	-	-	-
28	-	-	-	-	3.8	32.0	70.8	87.4
30	-	-	0.3	2.3	6.7	40.9	76.1	86.6
32	-	0.2	1.8	-	9.8	50.2	78.2	82.1
33	-	-	-	6.7	-	-	-	-
34	-	1.0	4.9	-	12.8	59.6	74.3	75.3
36	-	2.3	8.7	14.0	15.9	67.3	67.0	65.8
38	-	4.9	14.2	-	18.0	69.8	56.7	55.3
39	-	-	-	24.5	-	-	-	-
40	-	9.0	19.8	-	20.0	69.4	48.9	46.3
42	-	14.7	26.9	37.0	19.8	66.8	39.0	39.6
44	-	22.1	34.1	-	19.5	62.0	31.0	32.6
45	-	-	-	48.5	-	-	-	-
46	-	29.9	41.9	-	19.2	56.3	23.9	26.1
48	-	39.0	48.4	56.9	18.0	49.9	17.7	20.1
50	-	46.7	54.3	-	15.7	43.3	13.5	15.0
51	-	-	-	60.6	-	-	-	-
52	-	54.8	58.0	-	14.2	37.9	9.9	11.0
54	0.3	60.0	59.3	58.0	12.2	32.0	7.2	8.0
56	-	63.0	58.6	-	10.2	21.6	5.1	5.8
57	-	-	-	44.0	-	-	-	-
58	1.2	64.1	56.0	-	8.5	15.3	3.6	4.0
60	-	63.1	50.0	36.9	7.0	11.1	2.2	2.8
62	3.0	60.5	43.7	-	5.0	8.8	1.5	2.0
63	-	-	-	29.0	-	-	-	-
64	-	55.9	37.2	-	4.5	6.4	10.	1.2
66	7.6	50.2	31.7	22.6	3.2	4.8	0.5	0.9
68	-	45.0	26.5	-	2.6	3.5	0.1	0.5
69	-	-	-	17.0	-	-	-	-
70	22.9	38.9	22.1	-	1.8	2.6	-	0.3
72	-	32.7	17.6	12.7	1.2	1.8	-	-
74	28.2	27.4	14.0	-	1.0	1.0	-	-
76	-	22.7	-	9.0	-	-	-	-
78	28.0	18.0	8.1	6.0	0.2	0.4	-	-
80	-	14.0	6.2	-	-	0.2	-	-
81	-	-	-	4.0	-	-	-	-
82	27.0	11.0	4.9	-	-	-	-	-
84	-	8.3	3.7	2.7	-	-	-	-

U_g , ft/sec (gas Velocity)	0	.018	.029	.042	.089	.179	.320	.483
t_i (time, min)	C_i (Tracer Signal Intensity)							
86	25.0	6.3	2.7	-	-	-	-	-
87	-	-	-	1.7	-	-	-	-
88	-	-	4.9	1.9	-	-	-	-
90	23.1	3.7	1.1	1.0	-	-	-	-
92	-	-	0.9	-	-	-	-	-
93	-	-	-	0.8	-	-	-	-
94	21.9	-	0.3	-	-	-	-	-
96	-	-	0.1	0.3	-	-	-	-
98	20.3	-	-	-	-	-	-	-
102	18.7	-	-	-	-	-	-	-
106	17.0	-	-	-	-	-	-	-
110	15.3	-	-	-	-	-	-	-
114	14.0	-	-	-	-	-	-	-
118	12.6	-	-	-	-	-	-	-
122	11.3	-	-	-	-	-	-	-
126	11.0	-	-	-	-	-	-	-
130	10.1	-	-	-	-	-	-	-
134	9.0	-	-	-	-	-	-	-
138	7.7	-	-	-	-	-	-	-
142	6.5	-	-	-	-	-	-	-
146	5.9	-	-	-	-	-	-	-
150	4.9	-	-	-	-	-	-	-
154	4.1	-	-	-	-	-	-	-
158	3.0	-	-	-	-	-	-	-
162	2.2	-	-	-	-	-	-	-
166	2.8	-	-	-	-	-	-	-
170	2.1	-	-	-	-	-	-	-
178	2.0	-	-	-	-	-	-	-
182	1.0	-	-	-	-	-	-	-
186	0.5	-	-	-	-	-	-	-
190	0.2	-	-	-	-	-	-	-

c. U_l (Liquid Velocity) = 0.01083 ft/sec

U_g , ft/sec (gas Velocity)	0	.017	.030	.041	.078	.170	.311	.470
t_i (time, min)	C_i (Tracer Signal Intensity)							
10	-	-	-	-	-	-	-	0.9
11	-	-	-	-	-	-	-	1.8
12	-	-	-	-	-	-	1.0	3.0
13	-	-	-	-	-	-	2.0	4.9
14	-	-	-	-	-	-	3.7	6.5
15	-	-	-	-	-	0.9	5.9	8.1
16	-	-	-	-	-	-	8.9	9.5
17	-	-	-	-	-	3.0	11.5	11.0
18	-	-	-	-	-	-	14.9	12.0
19	-	-	-	-	1.1	7.2	16.9	12.5
20	-	-	-	0.9	-	-	19.0	10.5
21	-	-	-	-	6.0	12.0	20.8	9.5
22	-	-	-	4.0	-	-	21.0	9.5
23	-	-	-	-	16.0	16.8	20.8	8.0
24	-	1.0	12.0	-	-	20.0	6.9	-
25	-	-	-	-	31.2	17.5	19.0	5.5
26	-	-	4.8	23.8	-	-	17.3	4.6
27	-	0.6	-	-	52.0	18.5	16.0	3.7
28	-	-	13.0	40.5	-	-	14.0	2.8
29	-	-	-	-	70.5	16.5	12.0	2.0
30	-	3.7	25.5	57.2	-	-	10.5	1.3
31	-	-	-	-	83.4	14.0	9.0	1.0
32	-	-	41.5	67.7	-	-	7.4	0.4
33	-	13.1	-	-	89.7	11.0	6.0	0
34	-	-	56.0	73.6	-	-	5.1	-
35	-	-	-	-	88.1	8.5	-	-
36	-	32.5	66.5	72.1	-	-	3.4	-
37	-	-	-	-	-	81.1	6.5	2.7
38	-	-	-	70.1	68.1	-	2.0	-
39	-	53.5	-	-	69.8	4.0	1.5	-
40	0.7	-	68.0	50.0	-	-	1.5	-
41	-	-	-	-	49.8	2.2	0.9	-
42	-	69.3	60.9	49.6	-	-	0.7	-
43	-	-	-	-	28.3	1.8	0.4	-
44	3.7	-	51.7	38.7	-	-	0	-
45	-	73.5	-	-	16.0	0.8	-	-
46	-	-	40.1	29.5	-	-	-	-
47	-	-	-	-	10.0	-	-	-
48	16.9	66.0	29.5	21.2	-	-	-	-
49	-	-	-	-	6.0	-	-	-
50	-	-	20.8	15.0	-	-	-	-
51	-	48.0	-	-	2.0	-	-	-
52	32.6	-	14.3	10.8	-	-	-	-
54	-	15.0	-	-	-	-	-	-
56	32.0	-	6.8	5.1	-	-	-	-
57	-	15.3	-	-	-	-	-	-
58	-	-	4.2	3.8	-	-	-	-

U _g , ft/sec (gas Velocity) t _i (time, min)	C _i (Tracer Signal Intensity)							
	0	.017	.030	.041	.078	.170	.311	.470
60	29.7	0.9	2.7	2.7	-	-	-	-
62	-	-	1.5	1.9	-	-	-	-
63	-	4.3	-	-	-	-	-	-
64	26.8	-	1.0	-	-	-	-	-
66	-	2.0	-	-	-	-	-	-
68	24.0	-	-	-	-	-	-	-
69	-	1.0	-	-	-	-	-	-
70	-	-	-	-	-	-	-	-
72	21.7	0.5	-	-	-	-	-	-
76	18.9	-	-	-	-	-	-	-
80	16.8	-	-	-	-	-	-	-
84	14.6	-	-	-	-	-	-	-
88	12.3	-	-	-	-	-	-	-
92	10.8	-	-	-	-	-	-	-
96	8.9	-	-	-	-	-	-	-
100	7.3	-	-	-	-	-	-	-
104	6.2	-	-	-	-	-	-	-
108	5.3	-	-	-	-	-	-	-
112	4.3	-	-	-	-	-	-	-
116	3.3	-	-	-	-	-	-	-
120	2.4	-	-	-	-	-	-	-
124	1.9	-	-	-	-	-	-	-
128	1.1	-	-	-	-	-	-	-
132	0.9	-	-	-	-	-	-	-

d. U_l (Liquid Velocity) = 0.02198 ft/sec

U_g , ft/sec (gas Velocity) t_1 (time, min)	0	.017	.026	.041	.086	.180	.309	.450
	C_1 (Tracer Signal Intensity)							
5	-	-	-	-	-	-	-	0.1
6	-	-	-	-	-	0.2	0.7	-
7	-	-	-	-	-	-	2.5	15.6
8	-	-	-	-	-	0.1	12.0	39.0
9	-	-	-	-	-	1.5	32.5	63.0
10	-	-	-	-	0.5	6.9	55.4	73.7
11	-	-	-	-	2.7	19.6	68.1	68.6
12	-	-	0.4	-	9.8	36.2	67.0	54.5
13	-	-	0.6	1.0	27.0	53.2	55.3	37.0
14	-	0.4	1.0	4.0	51.8	61.1	40.4	23.7
15	-	1.8	3.6	11.5	75.2	59.7	26.7	13.5
16	-	7.0	10.5	26.9	87.3	50.8	16.2	7.6
17	-	20.0	23.9	46.0	87.2	38.5	9.0	3.9
18	0.1	39.6	42.0	60.2	75.6	26.7	4.9	2.0
19	-	58.0	58.7	66.5	60.3	16.7	2.4	1.0
20	1.8	66.0	65.5	63.0	44.0	10.2	1.2	0.4
21	-	60.0	62.0	51.5	29.5	5.4	0.8	0.2
22	9.7	44.0	51.0	37.0	18.0	3.0	0.3	-
23	-	31.0	36.0	23.5	9.8	1.5	0.1	-
24	19.8	18.0	20.5	13.5	5.5	0.9	-	-
25	-	9.0	11.0	7.0	2.6	0.4	-	-
26	22.2	4.5	6.2	3.3	1.3	0.1	-	-
27	-	2.2	3.5	1.8	0.7	-	-	-
28	21.4	0.9	2.0	1.0	0.3	-	-	-
29	-	0.4	1.0	0.5	-	-	-	-
30	20.0	0.1	0.9	0.2	-	-	-	-
32	18.7	-	-	-	-	-	-	-
34	17.0	-	-	-	-	-	-	-
36	15.4	-	-	-	-	-	-	-
38	13.7	-	-	-	-	-	-	-
40	11.9	-	-	-	-	-	-	-
42	10.0	-	-	-	-	-	-	-
44	8.5	-	-	-	-	-	-	-
46	7.2	-	-	-	-	-	-	-
48	5.9	-	-	-	-	-	-	-
50	4.8	-	-	-	-	-	-	-
52	4.0	-	-	-	-	-	-	-
54	3.0	-	-	-	-	-	-	-
56	2.6	-	-	-	-	-	-	-
58	1.5	-	-	-	-	-	-	-
62	1.0	-	-	-	-	-	-	-
64	0.9	-	-	-	-	-	-	-
66	0.7	-	-	-	-	-	-	-
68	0.4	-	-	-	-	-	-	-
70	0.2	-	-	-	-	-	-	-
72	0.1	-	-	-	-	-	-	-

e. U_l (Liquid Velocity) = 0.04364 ft/sec

U_g , ft/sec (gas Velocity) t_i (time, min)	0	.004	.010	.018	.029	.044	.079	.175	.166	.334
	Ci (Tracer Signal Intensity)									
2.1	-	-	-	-	-	-	-	-	-	-
2.6	-	-	-	-	-	-	-	-	-	-
3.1	-	-	-	-	-	-	-	-	-	-
3.4	-	-	-	-	-	-	-	-	0.1	-
3.5	-	-	-	-	-	-	-	-	-	6.0
3.6	-	-	-	-	-	-	-	-	-	-
3.9	-	-	-	-	-	-	-	-	4.7	-
4.0	-	-	-	-	-	-	-	2.0	-	51.0
4.1	-	-	-	-	-	-	-	-	-	36.0
4.4	-	-	-	-	-	-	-	-	28.2	-
4.5	-	-	-	-	-	-	16.0	-	87.0	-
4.6	-	-	-	-	-	-	-	-	-	-
4.9	-	-	-	-	-	-	-	-	72.5	-
5.0	-	-	-	-	-	0.3	45.0	-	67.0	-
5.1	-	-	-	-	-	-	-	-	-	-
5.4	-	-	-	-	-	-	-	-	83.5	-
5.5	-	-	-	-	-	0.8	4.0	61.5	-	29.0
5.6	-	-	-	-	-	-	-	-	-	-
5.9	-	-	-	-	-	-	-	-	55.0	-
6.0	-	-	-	-	-	6.0	25.0	50.0	-	7.0
6.4	-	-	-	-	-	-	-	-	19.0	-
6.5	-	0.8	-	-	4.0	27.5	51.0	39.0	-	1.5
6.9	-	-	-	-	-	-	-	-	4.0	-
7.0	-	4.5	-	2.0	6.0	25.0	51.0	58.0	10.0	-
7.4	-	-	-	-	-	-	-	-	-	1.1
7.5	-	11.5	-	7.0	32.0	60.0	70.0	51.0	2.8	-
7.9	-	-	-	-	-	-	-	-	0.2	-
8.0	-	18.3	-	41.0	63.0	70.0	44.0	32.0	-	-
8.5	21.0	4.0	80.0	54.0	45.0	39.0	15.0	-	-	-
9.0	20.2	52.0	55.0	26.0	14.0	12.0	4.0	-	-	-
9.5	18.1	95.0	18.0	12.0	4.0	5.0	1.5	-	-	-
10.0	15.3	62.0	5.0	2.0	1.5	1.8	-	-	-	-
10.5	13.0	11.0	2.5	-	-	1.0	-	-	-	-
11.0	11.0	0.5	1.0	-	-	-	-	-	-	-
11.5	9.3	-	-	-	-	-	-	-	-	-
12.0	8.1	-	-	-	-	-	-	-	-	-
12.5	7.8	-	-	-	-	-	-	-	-	-
13.0	5.8	-	-	-	-	-	-	-	-	-
13.5	5.8	-	-	-	-	-	-	-	-	-
14.0	4.3	-	-	-	-	-	-	-	-	-
14.6	3.7	-	-	-	-	-	-	-	-	-
15.0	3.2	-	-	-	-	-	-	-	-	-
15.5	2.6	-	-	-	-	-	-	-	-	-
16.0	2.1	-	-	-	-	-	-	-	-	-
16.5	1.7	-	-	-	-	-	-	-	-	-
17.0	1.3	-	-	-	-	-	-	-	-	-
17.5	1.0	-	-	-	-	-	-	-	-	-
18.0	0.5	-	-	-	-	-	-	-	-	-
18.5	0.5	-	-	-	-	-	-	-	-	-
19.0	0.2	-	-	-	-	-	-	-	-	-

1.2 Methanol-Nitrogen Flow System

a. U_l (Liquid Velocity) = 0.00674 ft/sec

<u>U_g, ft/sec (gas velocity)</u>	<u>.00341</u>	<u>.01023</u>	<u>.03411</u>	<u>.17053</u>
<u>t_j (time, min)</u>	<u>C_j (Tracer Signal Intensity)</u>			
16	-	-	-	0
18	-	-	-	0.2
20	-	-	-	0.8
22	-	-	-	1.7
24	-	-	-	3.7
26	-	-	0	7.1
28	-	-	-	12.0
30	-	-	0.5	18.4
32	-	-	-	25.5
33	-	0	1.0	33.0
34	-	-	-	-
36	-	0.5	2.9	40.5
38	-	-	-	48.0
39	-	1.6	5.8	-
40	-	-	-	54.0
42	-	2.3	10.9	59.8
44	-	-	-	64.0
45	-	4.0	16.5	-
46	-	-	-	67.0
48	0	8.0	22.7	69.0
50	0.6	-	-	69.0
51	-	14.0	29.6	-
52	-	-	-	68.0
53	1.8	-	-	-
54	-	21.2	34.6	67.0
56	4.3	-	-	64.0
57	-	29.3	38.8	-
58	-	-	-	60.0
59	9.7	-	-	-
60	-	37.0	41.7	56.5
62	17.0	-	-	52.5
63	-	42.5	42.6	-
64	-	-	-	48.0
65	26.5	-	-	-
66	-	46.0	42.4	44.0
68	36.5	-	-	39.5
69	-	47.8	41.5	-
70	-	-	-	46.2
71	46.0	-	-	-
72	-	47.5	39.0	32.6
74	52.7	-	-	28.8
75	-	45.7	39.0	-
76	-	-	-	25.5
77	56.2	-	-	-
78	-	42.9	32.7	22.5

b. U_l (Liquid Velocity) = 0.00614 ft/sec

U_g , ft/sec (gas velocity) t_i (time, min)	<u>.00341</u>	<u>.00682</u>	<u>.01023</u>	<u>.17053</u>	<u>.03411</u>	<u>.06821</u>	<u>.17053</u>
	C_i (Tracer Signal Intensity)						
14	-	-	-	-	-	-	0.2
16	-	-	-	-	-	-	2.8
18	-	-	-	-	0.3	0.7	6.7
20	-	-	-	-	1.0	2.4	14.0
22	-	-	-	-	3.2	6.0	24.7
23	-	-	-	0.4	-	-	-
24	-	-	-	-	7.5	11.2	34.9
26	-	-	-	2.4	15.7	18.9	43.0
28	-	0.7	0.4	-	28.5	27.1	49.5
29	-	-	-	8.1	-	-	-
30	-	-	1.5	-	39.3	34.1	53.0
31-	-	2.5	-	-	-	-	-
32	0.5	-	4.0	21.4	47.9	39.2	53.5
34-	-	9.1	9.5	-	61.0	42.9	52.0
35	4.8	-	-	33.5	-	-	-
36	-	-	17.3	-	66.8	43.2	42.8
37	-	21.5	-	-	-	-	-
38	20.7	-	26.0	42.8	67.6	42.0	42.8
40	-	38.0	34.9	-	64.2	39.0	37.2
41	48.0	-	-	46.5	-	-	-
42	-	-	41.5	-	58.3	35.3	31.8
43	-	55.0	-	-	-	-	-
44	68.5	-	46.7	44.4	51.9	30.2	26.2
46	-	65.0	48.6	-	43.7	25.2	21.0
47	70.0	-	-	38.5	-	-	-
48	-	-	47.5	-	36.0	19.0	13.2
49	-	61.5	-	-	-	-	-
50	71.0	-	43.9	30.5	29.2	13.0	7.1
52	-	49.5	39.4	-	23.4	9.5	5.1
53	49.5	-	-	22.7	-	-	-
54	-	-	34.0	-	18.1	6.0	3.9
55	-	38.0	-	-	-	-	-
56	28.0	-	27.5	15.9	14.1	5.3	2.9
58	-	25.0	22.7	-	11.1	4.0	2.0
59	13.0	-	-	10.5	-	-	-
60	-	-	-	-	8.5	2.9	1.7
61	-	17.0	-	-	-	-	-
62	5.0	-	14.3	6.4	6.6	2.0	1.0
64	-	10.8	10.6	-	5.0	1.3	0.9
65	1.6	-	-	3.8	-	-	-
66	-	-	7.7	-	3.7	0.7	0.7
67	-	6.2	-	-	-	-	-
68	0.5	-	5.7	2.0	2.6	0.2	0.4
70	-	3.9	3.9	-	1.9	-	0.2
71	-	-	-	1.1	-	-	-
72	-	-	2.7	-	1.1	-	-
73	-	2.0	-	-	-	-	-
74	-	-	1.8	0.5	0.8	-	-

b. U_l (Liquid Velocity) = 0.00614 ft/sec

U_g , ft/sec (gas velocity)	<u>.00341</u>	<u>.00682</u>	<u>.01023</u>	<u>.17053</u>	<u>.03411</u>	<u>.06821</u>	<u>.17053</u>
t_i (time, min)	C_i (Tracer Signal Intensity)						
76	-	1.0	1.1	-	0.4	-	-
77	-	-	-	0.2	-	-	-
78	-	-	0.7	-	0.3	-	-
79	-	0.5	-	-	-	-	-
80	-	-	0.4	0	-	-	-
82	-	0.1	0.3	-	-	-	-
84	-	-	0.1	-	-	-	-

c. U_l (Liquid Velocity) = 0.03649 ft/sec

U_g , ft/sec (gas velocity)	<u>.00341</u>
t_i (time, min)	C_i (Tracer Signal Intensity)
20	0
22	4.7
23	28.0
24	44.9
25	39.0
26	20.0
27	5.0
28	0.2
29	0

2.0 Reactor Configuration vs. Dispersion Experiment

2.1 Residence Time - Tracer Response Data for the configurations of One, Three, Five and Seven

Number of Tubes	<u>.002034</u>	<u>.006135</u>	<u>.010236</u>	<u>.014337</u>				
Length, ft	<u>.034121</u>	<u>.034121</u>	<u>0.034121</u>	<u>0.034121</u>				
U_L , ft/sec	<u>1 Tube</u>	<u>3 Tubes</u>	<u>5 Tubes</u>	<u>7 Tubes</u>				
U_G , ft/sec	<u>4.02</u>	<u>12.05</u>	<u>20.1</u>	<u>28.12</u>				
t_i	C_i	$\frac{C_i}{\Sigma C_i \Delta t_i}$	C_i	$\frac{C_i}{\Sigma C_i \Delta t_i}$	C_i	$\frac{C_i}{\Sigma C_i \Delta t_i}$	C_i	$\frac{C_i}{\Sigma C_i \Delta t_i}$
5	1.8	.00068	0	0	0	0	0	0
9	31.5	.01197	1.5	.00127	0	0	0	0
13	54.0	.02052	22.5	.01904	0.5	.00062	0	0
17	55.0	.02090	42.5	.03596	6.3	.00769	0.3	.00045
21	51.8	.01968	55.3	.04679	17.1	.02104	11.0	.01645
25	48.2	.01832	52.3	.04426	41.3	.05075	49.6	.07420
29	43.8	.01664	38.5	.03258	48.8	.05998	60.8	.09095
33	40.0	.01529	29.0	.02454	38.2	.04694	33.0	.04936
37	37.5	.01426	20.2	.01709	24.7	.03033	9.1	.01361
41	36.0	.01368	13.0	.01100	14.8	.01815	2.0	.00299
45	34.7	.01319	8.1	.06684	6.4	.00787	0.7	.00105
49	31.0	.01178	4.9	.00415	2.9	.00351	0.3	.00045
53	27.0	.01026	2.9	.00245	1.2	.00141	0.1	.00015
57	22.9	.00870	1.8	.00152	0.8	.00098	0	0
61	19.2	.00730	1.1	.00093	0.4	.00055	0	0
65	16.9	.00642	0.9	.00076	0.2	.00031	0	0
69	14.7	.00559	0.6	.00051	0	0	0	0
73	12.6	.00479	0.3	.00025	0	0	0	0
77	11.5	.00437	0.3	.00025	0	0	0	0
81	10.0	.00380	0.2	.00017	0	0	0	0
85	9.3	.00353	0	0	0	0	0	0
89	8.2	.00312	0	0	0	0	0	0
93	7.2	.00274	0	0	0	0	0	0
97	6.3	.00239	0	0	0	0	0	0
101	5.3	.00201	0	0	0	0	0	0
105	4.5	.00171	0	0	0	0	0	0
109	3.7	.00141	0	0	0	0	0	0
113	3.1	.00118	0	0	0	0	0	0
117	2.7	.00103	0	0	0	0	0	0
121	2.1	.00080	0	0	0	0	0	0
125	2.0	.00076	0	0	0	0	0	0
129	1.6	.00061	0	0	0	0	0	0

Nomenclature Used in Table 2.1

U_L = liquid Velocity

U_G = gas Velocity

t_i = residence time in minutes

Δt_i = time interval of summation (four minutes)

C_i = tracer signal intensity

$\frac{C_i}{\sum C_i \Delta t}$ = dimensionless concentration

3.0 Three Phase Flow System

3.1 Methanol-Glass Beads-Nitrogen Flow System

U_L (Slurry Flow Rate) = 0.281 cm/sec (0.009219 ft/sec)

U_G (Gas Flow Rate) = 2.079 cm/sec (0.068209 ft/sec)

Size Distribution of the Glass Beads Charged

<u>Tyler Mesh</u>	<u>wt. gm</u>	<u>Bulk density (gm/cm³)</u>
200/270	8.5	0.1166
270/325	3.95	0.1583
325/400	2.2	0.3427
Total	<u>14.65</u>	

<u>Sampling Time Interval (min.)</u>	<u>Sample, wt. (gm)</u>	<u>Glass Beads</u>		<u>KCl Tracer Signal Intensity</u>
		<u>weight, gm</u>	<u>wt. %</u>	
0-5	--	--		0
5-7	--	--		0
7-9	--	--		0
9-13	--	--		0
13-15	97.08	0.18	0.19	0
15-17	--	--	--	0
17-19	44.71	0.72	1.61	0
19-21	40.89	1.33	3.25	0.5
21-23	39.87	1.83	4.59	1.2
23-25	79.27	2.44	3.08	2.5
25-27	7.72	0.41	5.31	--
27-29	78.83	3.12	3.96	5.4
29-31	3.97	0.17	4.28	--
31-33	59.55	1.43	2.40	6.6
33-35	37.30	0.68	1.82	6.6
35-40	129.95	1.10	0.85	5.1
40-45	82.57	0.28	0.34	3.15
45-50	88.86	0.19	0.21	1.8
Total		<u>13.88</u>		
% Recovery		<u>94.7</u>		

Glass Beads				
t_i	Δt_i	C_i	$C_i \Delta t_i$	$\frac{C_i}{\Sigma C_i \Delta t_i}$
14	2	.00185	.0037	.00302
19	4	.02395	.0958	.03906
23	4	.03594	.14336	.05945
27	4	.04079	.16316	.06553
31	4	.02519	.10076	.04108
34	2	.0182	.03640	.02568
37.5	5	.00846	.0423	.01380
42.5	5	.0039	.0195	.00553
47.5	5	.00214	.01070	.00349
Σ			<u>.61313</u>	

KCl Tracer				
t_i	Δt_i	C_i	$C_i \Delta t_i$	$\frac{C_i}{\Sigma C_i \Delta t_i}$
20	2	0.5		
22	2	1.2		
24	2	2.5		
26	2	(4.0)*		
28	2	5.4		
30	2	(6.1)*		
32	2	6.6		
34	2	6.6		
37.5	5	3.15		
42.5	5	3.15		
47.6	5	1.8		

t_i = median time chosen

C_i = concentration: gram solid/gram sample for glass beads
 signal intensity for KCl tracer, respectively

Δt = time interval

$\frac{C_i}{\Sigma C_i \Delta t_i}$ = dimensionless concentration

* = interpolated data

3.2 Water/Glass Beads-Nitrogen System

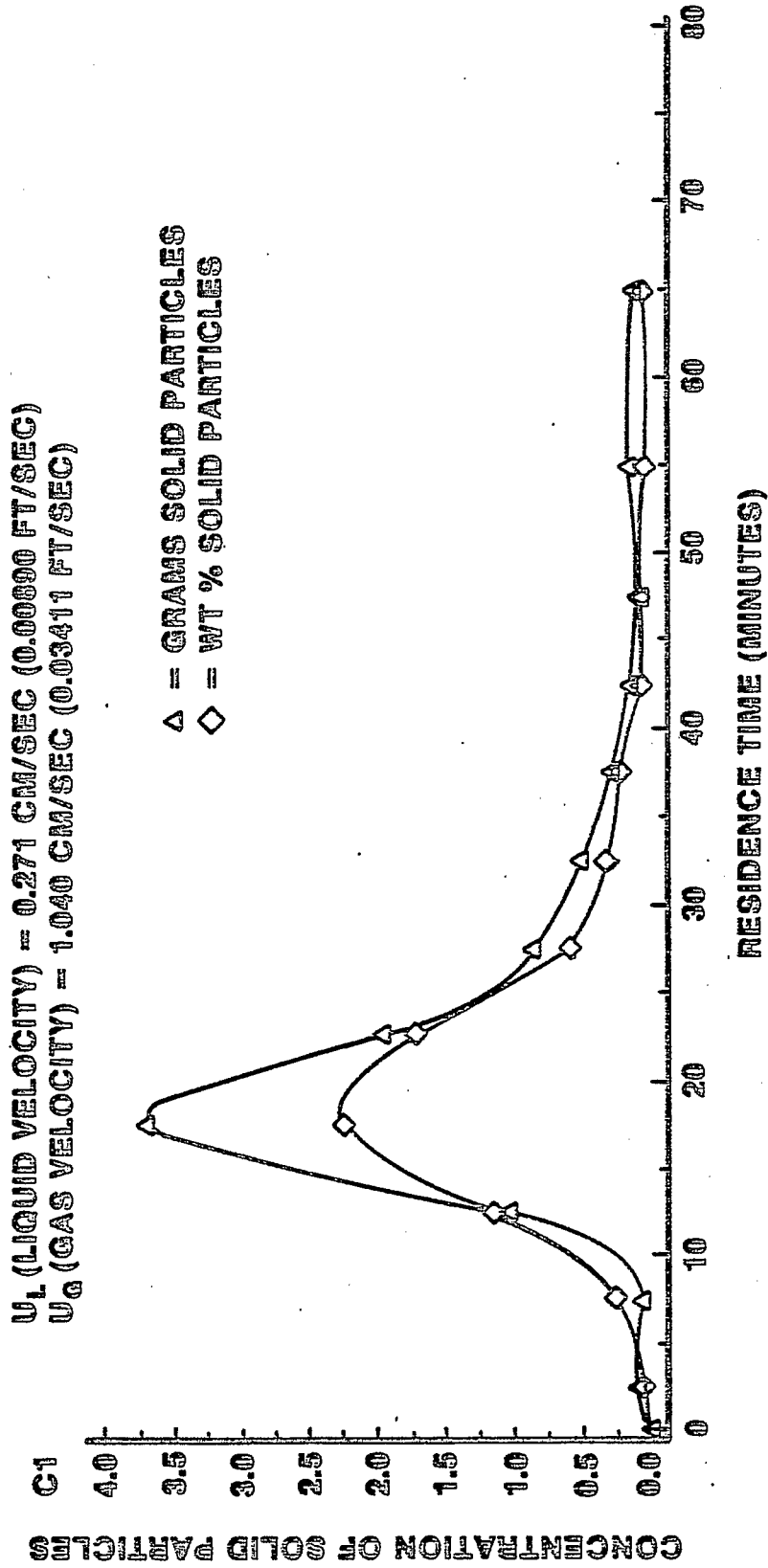
Glass beads = 140/400 mesh (8.45 grams charged)

U_L (Liquid Velocity) = 0.271 cm/sec (0.00890 ft/sec)

U_G (Gas Velocity) = 1.040 cm/sec (0.03411 ft/sec)

<u>Sampling Time Interval (min)</u>	<u>Water/Glass Beads Sample Weight</u>		<u>Glass Beads</u>		
	<u>in gm.</u>	<u>in gm.</u>	<u>wt% in sample</u>	<u>% Distribution</u>	
0-5	208.23	.09	0.04	.59	
5-10	23.59	.06	0.25	3.68	
10-15	92.38	1.05	1.14	16.97	
15-20	165.79	3.69	2.23	32.84	
20-25	116.30	1.96	1.69	24.89	
25-30	140.46	.86	0.61	8.98	
30-35	148.12	.51	0.34	5.01	
35-40	125.58	.28	0.22	3.24	
40-45	150.01	.12	0.08	1.18	
45-50	102.40	.10	0.10	1.47	
50-60	319.29	.16	0.05	0.74	
60-70	280.11	.10	0.04	0.59	
Σ		<u>8.98</u>			
<u>Recovery, %</u>				<u>106.3</u>	

FIGURE A.3.1
RESIDENCE TIME OF GLASSBEADS
IN WATER/NITROGEN SYSTEM
GLASS BEADS = 0.45 GM, SIZE OF 140/400 MESH,
INLET PRESSURE = 10 PSIG



APPENDIX A-3

OPERATING AND MATERIAL-BALANCE DATA SUMMARY
FOR THE PLUG-FLOW REACTOR

1. Run BCL-52 Operating Data Summary

Date Hr/Day/Mo/Yr	Balance Period	Reactor Temp. °F		System Pressure psig	Slurry Rates gm/hr		Gas Rates SLPH		Condensate Rates, gm/hr		Remarks
		In	Out		Feed	Product	Feed	Products	Organic	H ₂ O	
1900 3-2-28	5A	832	837	2009.5	2305	2230	779	584.9	3.40	5.34	Batches #1 & 2
2000	6	835	841	2007.5	2288	2200	777	580			
2100	7	841	847	2007.5	2299	1160	802	588			
2300	8	837	841	2008	2236	2200	767	589			
2300	9	833	840	2009	2299	2060	756	573			d = 1.1153
2400	10	834	839	2013	2280	2840	743	564	5.42	7.92	Sampling
0100 3-3-82	11	856	842	2010	2221	1925			11.3	5.6	Batch #2
0200	12	837	842	2003	2331	1440	772	538			
0300	13	840	845	2006	2315	2000	755	576			
0400	14	839	845	2007	2284	1820	767	576			
0500	15	840	835	2001	2037	2140	755	572			
0600	16	839	845	2008	2283	4040	761	569	4.22	13.82	
0700	17	838	841	NA	2243	1980	759	535			Batch #3
0800	18	839	841	2007	2299	2180	766	566			
0900	19	837	841	2012	2266	1940	745	555			
1000	20	839	840	2007	2248	1980	778	564			d = 1.141
1100	21	836	841	2010	2233	2840	775	578	3.74	13.50	Sampling
1200	22	835	840	2009	2219	1191	771	554	7.8	11.6	

Part I

Run BCL 52 Operating Data Summary

(continued)

Date Hr/Day/Mo/Yr	Reactor Temp. °F		System Pressure psig	Slurry Rates gm/hr		Gas Rates SLPH		Condensate Rates, gm/hr		Remarks
	Inl	Out		Feed	Product	Feed	Products	Organic	H ₂ O	

Part II

1300	836	840	2008	2124	1880	589	441			
1400										Rupture Disk Blown
1500										
1600	838	841	2013	1694	3260	526	373	5.40	11.975	
1700	838	840	2018	1672	1840	526	321			
1800	838	840	2018	1643	480	527	366			Batch #4
1900	838	841	2018	1643	1720	587	410			
2100	838	840	12014	1638	1380	576	420	3.82	8.28	
2200	838	839	2022	1655	940	584	342			

Due to erratic G/C separator control level detector probe was replaced.

0900	830	834	2010	1935	1860	578	404			Resume run
1000	829	834	2008	1718	1580	571	417			
1100	831	834	2008	1715	1520	550	401			
1200	831	837	2002	1682	1600	535	400			
1300	832	835	1992	--	2840	510	332	0.44	0.28	
1400	830	835	2011	1664	1060	573	465			
1500	831	835	2011	1655	240	553	386			
1600	836	840	12014	1664	1660	552	386			
1700	837	840	2002	1655	0	517	386			d = 1.151
1800	836	835	2014	1643	2320	576	391	0.26	1.52	

Run BCL 52 Operating Data Summary

(continued)

Date Hr/Day/Ho/Yr	Balance Period	Reactor Temp. °F		System Pressure psig	Slurry Rates gm/hr		Gas Rates SLPH		Condensate Rates, gm/hr		Remarks
		In	Out		Feed	Product	Feed	Products	Organic	H ₂ O	
1900	43	837	838	2009	1683	0	586	385	0.90	4.4	
2000	44	836	830	2012	1647	1020	558	394			
2100	45	837	840	2014	1655	1540	595	398			
2200	46	836	834	2015	1626	1400	501	410			
2300	47	834	833	2005	1626	1560	561	418			
2400	48	840	845	2023	1638	1360	612	422	0.68	2.82	
0110	3-7-82	840	845	2015	1626	1400	581	410			
0200	50	837	839	2007	1643	1680	574	209			
0300	51	835	841	1998	1591	200	564	474			
0400	52	836	841	2009	1599	1270	567	389			d = 1.1194
0500	53	835	838	2009	1643	1880	551	406	1.30	3.22	
0600	54	835	836	2023	1655	0	569	372	5.2	2.3	
0700	55	833	839	2025	1626	1600	553	400			
0800	56			1250	---	2680					
0900	57	833	840	2012	1622	580	570	433			

Run BCL 52 Operating Data Summary

(continued)

Date Hr/Day/Mo/Yr	Balance Period	Reactor Temp. °F		System Pressure psig	Slurry Rates gm/hr		Gas Rates SLPH		Condensate Rates, gm/hr		Remarks
		In	Out		Feed	Product	Feed	Products	Organic	H ₂ O	
1000	58	832	835	2015	1639	1520	553	406			
1100	59	834	839	2007	1634	1700	552	391	1.30	3.32	
1200	60	834	839	2013	1868	540	554	358			
1300	61	834	839	2014	1626	1300	611	445			
1300	62	835	837	2016	1626	1440	587	440			
1400	62	835	837	2016	1626	1440	587	440			
1500	63	833	832	2017	1617	1500	588	407			
1600	64	835	840	2018	1618	1420	605	418	1.02	2.06	Batch #5
1700	65	835	839	2015	1592	1320	592	419			
1800	66	833	838	2015	1581	1360	577	420			
1900	67	833	838	2015	1680	1520	854	315			
2000	68	835	840	2016	1655	1440	571	420			
2100	69	836	839	2017	1630	1400	588	401	1.02	4.90	
2200	70	835	840	2014	1622	1460	615	432			
2300	71	834	839	2015	1643	1540	602	435			
2400	72	837	841	2012	1664	1360	594	414			
0100	73	839	841	2031	1599	1380	548	378			
0200	74	837	840	2017	1623	1500	584	416	1.02	3.34	Coal Samples 153 & 154
0300	75	838	837	2009	1615	1500	582	425			
0400	76	839	841	2000	1635	1420	593	403			

Run BCL 52 Operating Data Summary

(continued)

Date Hr/Day/Mo/Yr	Balance		Reactor Temp. °F		System Pressure psig	Slurry Rates gm/hr		Gas Rates SLPH		Condensate Rates, gm/hr		Remarks
	Period	In	Out	In		Out	Feed	Product	Feed	Products	Organic	
0500	77	839	840	2013		1626	1380	573	390			
0600	78	840	840	1993		1623	1400	563	384			
0700	79	834	840	2010		1671	1380	580	411	1.98	5.36	
0800	80	833	833	2009		1647	1460	566	389			G/L separation control
0900	81	832	840	2013		1648	1420	574	395			span 25%
1000	82	832	841	2012		1659	1420	566	406			d = 1.11684
1100	83	836	840	2012		1626	1520	567	409			Batch #6
1200	84	833	840	1975		1617	2300	557	431	1.72	6.66	Sampling
1300	85	838	838	2016		1655	691.3	563	352	3.7	13.1	G/L control problem
1400	86	835	841	2005		1643	640	564	392			
1500	87	833	841	2012		1639	2080	570	410			
1600	88	833	840	1998		1651	1600	570	389			
1700	89	831	839	2006		1630	620	566	392			
1800	90	836	839	2007		1647	2240	577	402	3.30	11.10	Sampling
1900	91	833	840	2007		1858	---	574	395	7.1	8.5	
2000	92	833	840	2007		16634	1780	573	404			
2100	93	833	840	2007		1663	620	571	381			
2200	94	833	840	2005		1520	1480	569	393			
2300	95	830	387	2006		1655	1340	570	391			No air supply to sand bath
2400	96	834	838	2005		1578	1460	562	388			

Run BCL 52 Operating Data Summary

(continued)

Date Hr/Day/Mo/Yr	Balance Period	Reactor Temp. °F		System Pressure psig	Slurry Rates gm/hr		Gas Rates SLPH		Condensate Rates, gm/hr		Remarks
		In	Out		Feed	Product	Feed	Products	Organic	H ₂ O	
0100 3-9-82	97	836	838	2005	1578	1450	562	388			
0200	98	838	8409	2003	1626	1400	565	399			
0300	99	837	841	2005	1610	1420	574	402			
0400	100	837	842	2006	1635	1460	576	409			
0500	101	835	842	2003	1594	1360	572	402	5.68	16.06	
0600	102	835	840	2005	1639	1420	575	395			
0700	103	834	840	2005	1634	1360	576	405			
0800	104	833	838	2007	1626	1400	583	405			
0900	105	833	840	2006	1635	1380	590	417			Batch #7
1000	106	836	838	2005	1651	1400	858	414	10.78	25.38	
1100	107	832	838	2002	1643	1420	577	j401			
1200	108	832	840	2003	1618	1380	586	413			
1300	109	833	840	2005	1655		578	404	12.97	26.33	d = 1.1214
1400	110	832	839	2004	1643	--	573	391	13.3	21.2	
1500	111	832	840	2011	1643	460	575	401			
1600	112	831	839	2007	1626	1460	579	4032			
1700 3-9-82	113	833	840	2006	1625	1380	582	404			
1800	114	832	840	2005	1638	1420	578	402			
1900	115	831	839	2007	1617	1380	582	402	6.96	27.02	
2000	116	830	839	2006	1639	1400	584	396			
2100	117	830	839	2006	1617	1380	572	409			
2200	118	832	840	2005	1643	1460	622	401			
2300	119	831	840	2006	1647	1380	578	407			
2400	1120	832	838	2006	1833	1400	576	400	6.40	26.28	

Run BCL 52 Operating Data Summary

(continued)

Date Hr/Day/Mo/Yr	Balance Period	Reactor Temp. °F		System Pressure psig	Slurry Rates gm/hr		Gas Rates SLPH		Condensate Rates gm/hr		Remarks
		In	Out		Feed	Product	Feed	Products	Organic	H ₂ O	
0100 3-10-82	121	833	839	2008	1635	1360	570	392			
0200	122	833	838	2007	1649	1460	570	393			
0300	123	832	839	2007	1630	1460	569	389			
0400	124	832	840	2004	1583	1340	568	390			
0500	125	834	840	2007	1610	1420	567	379	12.80	30.16	
0600	126	833	839	2006	1618	1380	576	398			
0700	127	832	840	2003	1610	1460	577	392			
0800	128	832	836	2012	1626	1320	567	388			
0900	129	832	839	2012	1626	1320	567	388			Batch #8
1000	130	831	839	2009	1659	1360	570	402	11.54	28.64	
1100	131	832	840	2013	1639	1400	577	395			
1200	132	830	838	2012	1634	1420	576	388			
1300	133	831	839	2014	1610	1380	577	401			d = 1.1271
1400	134	830	838	2009	1590	2120	582	403	10.90	28.08	
1500	135	830	838	2012	1651	220	582	392	12.6	24.2	
1600	136	830	830	2015	1635	540	582	382			
1700	137	830	837	2013	1630	1400	580	400			
1800	138	830	837	2012	1626	1420	588	399			
1900	139	830	835	2015	1630	1420	587	388			
2000	140	834	840	2012	1614	1420	579	397	7.14	27.46	

Run BCL 52 Operating Data Summary
(continued)

Date Hr/Day/Mo/Yr	Balance Period	Reactor Temp. °F		System Pressure psig	Slurry Rates gm/hr		Gas Rates SLPH		Condensate Rates, gm/hr		Remarks
		In	Out		Feed	Product	Feed	Products	Organic	H ₂ O	
2100 3-11-82	141	832	840	2014	1630	1360	582	298			
2200	142	830	840	2014	1630	1440	582	398			
2300	143	831	840	2012	1622	1380	582	405			
2400	144	832	840	2015	1647	1420	586	395			
0100 3-11-82	145	836	842	2013	1615	1440	581	398	11.16	29.54	
0200	146	833	841	2011	1643	1400	594	394			
0300	147	832	841	2008	1618	1420	585	403			
0400	148	833	840	2010	1623	1400	586	393			
0500	149	833	841	2006	1635	1380	590	400			
0600	150	833	840	2006	1623	1420	584	394	12.36	28.72	
0700	151	831	839	1626	1400	587	386				
0800	152	831	839	2006	1651	1420	584	385			
0900	153	831	840	2009	1643	700	580	400			
1000	154	831	839	2008	1651	1340	588	371			Sample Solvent
1100	155	832	840	2006	1643	700	580	400	9.38	28.67	
1200	156	831	839	2001	1626	1420	577	391			
1300	157	830	838	1996	1635	1500	588	388			
1400	158	830	839	2009	1626	1480	578	391			d = 1.1236
1500	159	824	838	2006	1660	--	579	386	9.70	31.60	
1600	160	829	838	2008	1635	--	584	386	11.3	17.5	
1700	161	829	835	2006	--	1160	585	393			Pump stopped for 32 min.

Run BCL 52 Operating Data Summary

(continued)

Date Hr/Day/Mo/Yr	Balance Period	Reactor Temp. °F		System Pressure psig	Slurry Rates gm/hr		Gas Rates SLPH		Condensate Rates, gm/hr		Remarks
		In	Out		Feed	Product	Feed	Products	Organic	H ₂ O	
1800	162	830	837	2005	1570	880	560	434			
1900	163	830	837	2006	1589	2840	586	357			
2000	164	830	839	2008	1597	1080	588	374			
2100	165	830	836	2006	1610	1760	586	308	5.86	18.46	
2200	166	830	839	2009	1610	0	586	394			
2300	157	829	837	2005	1635	1460	583	391			
2400	168	834	840	2005	1639	1400	592	379			
0100	169	832	841	2008	1623	1360	585	388			
0200	170	836	841	2007	1647	1380	587	378			
0300	171	834	841	2007	1647	1380	587	378			
0400	172	833	841	2006	1647	1400	585	382			
0500	173	831	841	1005	1535	1380	589	385			
0600	174	831	840	2003	1615	1420	589	382			
0700	175	831	840	2006	1591	1440	585	392	7.08	22.20	
0800	176	830	841	2008	1655	1420	588	387			
0900	177	831	841	2008	1683	1440	577	388			
1000	178	832	841	2003	1535	1440	579	378			
1100	179	832	841	1999	1643	1360	579	378			
1200	180	830	840	1014	1641	1400	578	371	7.86	25.90	
1300	181	832	841	2002	1655	1380	575	377			

Run BCL 52 Operating Data Summary

(continued)

Date Hr/Day/Mo/Yr	Balance Period	Reactor Temp. °F		System Pressure psig	Slurry Rates gm/hr		Gas Rates SLPH		Condensate Rates, gm/hr		Remarks
		In	Out		Feed	Product	Feed	Products	Organic	H ₂ O	
1400	182	832	840	2003	1635	1420	580	370			
1500	183	830	839	2006	1643	1420	580	370			d = 1.138
1600	184	830	840	2008	1630	1380	588	387	6.80	27.58	Sampling
1700	185	834	841	2010	1605	---	582	376	9.9	22.50	
1800	186	832	840	2009	1721	1580	630	431			
1900	187	829	839	2007	1729	1500	631	441			
2000	188	828	837	2007	1830	1620	691	482			
2100	189	829	840	2006	1835	1580	684	482			
2200	190	831	840	2005	1809	1660	671	467	6.82	29.84	
2300	191	830	837	2008	1820	1520	658	449			
2400	192	830	387	2008	1836	1540	663	452			
0100	3-13-82	830	840	2007	1750	1580	654	450			Batch #10
0200		829	840	2009	1806	1600	658	441			
0300		829	839	2006	1782	1540	650	440			
0400		830	840	2008	1777	1560	648	433	7.07	26.70	d = 1.1355 Sampling
0500		829	839	2006	1774	---	647	436	12.2	24.7	
0600	3-13-82	830	840	2004	1825	1780	643	439			
0700		829	839	2005	1837	1580	644	438			Batch #11
0800		827	837	2007	1806	1500	637	424			
0900		828	838	2005	1790	1600	633	427			

Run BCL 52 Operating Data Summary

(continued)

Date Hr/Day/Mo/Yr	Balance Period	Reactor Temp. °F		System Pressure psig	Slurry Rates gpm/hr		Gas Rates SLPH		Condensate Rates, gpm/hr		Remarks
		In	Out		Feed	Product	Feed	Products	Organic	H ₂ O	
1000	202	829	838	2007	1029	1620	636	412	6.54	28.38	
1100	203	826	839	2006	1036	1620	625	409			
1200	204	828	839	2008	1053	1580	629	415			
1300	205	828	837	2015	1077	1560	632	413			
1400	206	828	840	2005	1061	1660	625	417			
1500	207	829	838	2006	1069	1600	627	405			d = 1.1290
1600	208	830	841	2003	1060	1600	626	422	8.18	28.52	
1700	209	829	839	1977	2225	1860	860	591			
1800	210	829	839	1997	2225	1860	860	591			
1900	211	830	839	2009	2225	1960	867	618			
2000	212	829	840	2010	2267	2000	861	621			
2100	213	832	842	2011	2380	2100	853	602			
2200	214	831	842	2005	2388	2080	853	603	6.94	33.54	
2300	215	831	841	2009	2412	2140	853	601			
2400	216	832	840	2009	2299	2100	853	597			
0100	3-14-82	830	841	2007	2347	2120	850	604			
0200	218	833	841	2007	2371	2120	860	614			
0300	219	830	841	2008	2379	2140	864	570			d = 1.128
0400	220	830	840	2007	2369	2140	843	599	8.83	31.45	

Run BCL 52 Operating Data Summary

(continued)

Date Hr/Day/Mo/Yr	Balance Period	Reactor Temp. °F		System Pressure psig	Slurry Rates gm/hr		Gas Rates SLPH		Condensate Rates, gm/hr		Remarks
		In	Out		Feed	Product	Feed	Products	Organic	H ₂ O	
0500	221	830	840	2008	2363	1040	853	585	10.1	28.8	
0600	222	833	842	2006	2421	2160	849	604			
0700	223	829	840	2009	2388	2140	860	575			Batch #12
0800	224	829	841	2007	2418	2180	851	611			
0900	225	831	840	2007	2363	2140	851	600	7.125	33.70	
1000	3-14-82	832	840	2005	2462	2180	852	601			
1100	227	830	842	2005	2436	2140	847	594			
1200	228	830	840	2015	2454	2180	851	597	6.60	35.03	
1300	229	829	840	2018	2437	2160	851	594			
1400	230	829	839	2012	2487	2180	854	592			
1500	231	832	842	2140	2454	2140	845	598			d = 1.1210
1600	232	833	842	2015	2488	220	847	608	6.93	33.60	Sampling
1700	233	832	843	2016	2445	920	849	596	12.4	30.0	
1800				2015		1820					
1900						1580					
2000				2009	1680	1400	584	384			
2100					1637	1420					

Material Balance Data Summary

Key For Raw Data Matrix

Column #	1	2	3	4	5	6	7	8	9
Run Conditions	Run # Temp ¹	Sample # Temp ²	Month Pressure	Day H ₂ Feed ¹	Year Slurry Rate ²	Hr Start	Hr End		
Gas	Receiver ²	H ₂ O ²	Lights ²	Gas Produced ¹					
Analysis (%)	C ₃	C ₃ ²	IC ₄	H ₂ S	nC ₄	C ₄ ²	H ₂	CO ₂	
Solvent Breakdown In Slurry	C ₂ ²	C ₂	NH ₃	O ₂	N ₂	C ₁	CO	C ₅ ⁺	H ₂ O
Coal	Lights	C	H	N	S	0			
Added SRC	Oils	C	H	N	S	0			
	Asph.	C	H	N	S	0			
	Preash.	C	H	N	S	0			
	Wt.%	C	H	N	S	0	Ash	H ₂ O	
	Lights	C	H	N	S	0			
	Oils	C	H	N	S	0			
	Asph.	C	H	N	S	0			
	Preash.	C	H	N	S	0			
	Residue	C	H	N	S	0			
Not Utilized	Lights	C	H	N	S	0			
	Oils	C	H	N	S	0			
	Asph.	C	H	N	S	0			
	Preash.	C	H	N	S	0	Ash		
	Residue	C	H	N	S	0	Ash		

¹ SLPH
² gm/hr

All pressures in PSIG, All Temperatures, °F All Fractions Wt.%

THIS ARRAY CONTAINS INITIAL DATA

52.00	11.00	3.00	2.00	1982.00	2300.00	2400.00	0.0	0.0
839.00	839.00	2006.00	750.00	2280.00	0.0	0.0	0.0	0.0
2074.00	25.49	5.42	671.00	0.0	0.0	0.0	0.0	0.0
0.87	0.09	0.10	1.54	0.45	0.01	82.00	0.96	0.0
0.04	2.78	0.41	0.0	0.05	7.58	0.56	0.16	0.56
0.0	86.71	9.39	0.27	1.09	2.54	0.0	0.0	0.0
59.66	87.76	8.24	0.85	0.36	2.95	0.0	0.0	0.0
2.34	87.76	8.24	0.85	0.36	2.95	0.0	0.0	0.0
0.0	87.73	8.47	0.78	0.43	2.91	0.0	0.0	0.0
38.00	72.54	4.96	1.66	1.87	9.75	10.97	1.18	0.0
0.0	86.71	9.39	0.27	1.09	2.54	0.0	0.0	0.0
0.0	88.09	8.32	0.74	0.51	2.83	0.0	0.0	0.0
0.0	86.09	5.68	2.17	1.03	4.11	0.18	0.0	0.0
0.0	0.0	0.0	0.0	0.0	0.0	0.0	0.0	0.0
0.0	0.0	0.0	0.0	0.0	0.0	0.0	0.0	0.0
0.0	0.0	0.0	0.0	0.0	0.0	0.0	0.0	0.0
0.0	0.0	0.0	0.0	0.0	0.0	0.0	0.0	0.0
0.0	0.0	0.0	0.0	0.0	0.0	0.0	0.0	0.0
0.0	0.0	0.0	0.0	0.0	0.0	0.0	0.0	0.0
2.52	86.71	9.39	0.27	1.09	2.54	0.0	0.0	0.0
73.52	87.69	8.00	1.00	0.19	3.02	0.0	0.0	0.0
10.66	86.33	5.61	2.60	0.67	4.80	0.0	0.0	0.0
7.29	85.11	4.80	2.94	0.63	6.52	0.0	0.0	0.0
6.02	37.73	1.98	0.75	1.00	7.53	56.25	0.0	0.0
0.0	0.0	0.0	0.0	0.0	0.0	0.0	0.0	0.0
0.0	0.0	0.0	0.0	0.0	0.0	0.0	0.0	0.0

THIS ARRAY CONTAINS INITIAL DATA

52.00	22.00	3.00	3.00	1982.00	1100.00	1200.00	0.0	0.0
840.00	841.00	2005.00	773.00	2233.00	0.0	0.0	0.0	0.0
1970.00	31.75	3.98	669.00	0.0	0.0	0.0	0.0	0.0
1.46	0.10	0.11	1.75	0.49	0.01	83.60	0.87	0.0
0.03	2.61	0.59	0.0	0.05	7.04	0.54	0.16	0.56
0.0	86.71	9.39	0.27	1.09	2.54	0.0	0.0	0.0
59.66	87.76	8.24	0.85	0.36	2.95	0.0	0.0	0.0
2.34	87.76	8.24	0.85	0.36	2.95	0.0	0.0	0.0
0.0	87.76	8.24	0.85	0.36	2.95	0.0	0.0	0.0
38.00	71.90	5.02	1.65	1.85	10.47	10.86	2.08	0.0
0.0	86.71	9.39	0.27	1.09	2.54	0.0	0.0	0.0
0.0	88.09	8.32	0.74	0.51	2.83	0.0	0.0	0.0
0.0	86.09	5.68	2.17	1.03	4.11	0.18	0.0	0.0
0.0	0.0	0.0	0.0	0.0	0.0	0.0	0.0	0.0
0.0	0.0	0.0	0.0	0.0	0.0	0.0	0.0	0.0
0.0	0.0	0.0	0.0	0.0	0.0	0.0	0.0	0.0
0.0	0.0	0.0	0.0	0.0	0.0	0.0	0.0	0.0
0.0	0.0	0.0	0.0	0.0	0.0	0.0	0.0	0.0
0.0	0.0	0.0	0.0	0.0	0.0	0.0	0.0	0.0
0.0	0.0	0.0	0.0	0.0	0.0	0.0	0.0	0.0
2.52	86.71	9.39	0.27	1.09	2.54	0.0	0.0	0.0
73.36	87.69	8.00	1.00	0.19	3.02	0.0	0.0	0.0
9.74	86.33	5.61	2.60	0.67	4.80	0.0	0.0	0.0
8.15	85.11	4.80	2.94	0.63	6.52	0.0	0.0	0.0
6.22	37.73	1.98	0.75	1.00	7.53	56.25	0.0	0.0
0.0	0.0	0.0	0.0	0.0	0.0	0.0	0.0	0.0
0.0	0.0	0.0	0.0	0.0	0.0	0.0	0.0	0.0

THIS ARRAY CONTAINS INITIAL DATA

52.00	91.00	3.00	8.00	1982.00	1800.00	1900.00	0.0	0.0
839.00	839.00	2004.00	572.00	1642.00	0.0	0.0	0.0	0.0
1449.00	29.70	3.50	469.00	0.0	0.0	0.0	0.0	0.0
0.89	0.10	0.14	2.04	0.06	0.01	79.95	0.94	0.0
0.04	3.21	0.82	0.0	0.03	9.70	0.62	2.19	0.56
0.0	86.71	9.39	0.27	1.09	2.54	0.0	0.0	0.0
59.66	87.76	8.24	0.85	0.36	2.95	0.0	0.0	0.0
2.34	87.76	8.24	0.85	0.36	2.95	0.0	0.0	0.0
0.0	87.73	8.47	0.78	0.43	2.91	0.0	0.0	0.0
38.00	72.26	4.99	1.65	1.86	10.07	10.92	1.58	0.0
0.0	86.71	9.39	0.27	1.09	2.54	0.0	0.0	0.0
0.0	88.09	8.32	0.74	0.51	2.83	0.0	0.0	0.0
0.0	86.09	5.68	2.17	1.03	4.11	0.18	0.0	0.0
0.0	0.0	0.0	0.0	0.0	0.0	0.0	0.0	0.0
0.0	0.0	0.0	0.0	0.0	0.0	0.0	0.0	0.0
0.0	0.0	0.0	0.0	0.0	0.0	0.0	0.0	0.0
0.0	0.0	0.0	0.0	0.0	0.0	0.0	0.0	0.0
0.0	0.0	0.0	0.0	0.0	0.0	0.0	0.0	0.0
0.0	0.0	0.0	0.0	0.0	0.0	0.0	0.0	0.0
0.0	0.0	0.0	0.0	0.0	0.0	0.0	0.0	0.0
2.76	86.71	9.39	0.27	1.09	2.54	0.0	0.0	0.0
75.01	88.21	8.24	1.07	0.0	2.86	0.0	0.0	0.0
10.51	87.82	5.62	2.57	0.54	3.45	0.0	0.0	0.0
5.12	86.43	4.56	2.73	0.57	5.71	0.0	0.0	0.0
6.61	37.50	1.90	0.67	0.99	7.10	58.94	0.0	0.0
0.0	0.0	0.0	0.0	0.0	0.0	0.0	0.0	0.0
0.0	0.0	0.0	0.0	0.0	0.0	0.0	0.0	0.0

THIS ARRAY CONTAINS INITIAL DATA

52.00	185.00	3.00	12.00	1982.00	1600.00	1700.00	0.0	0.0
835.00	840.00	2004.00	586.00	1643.00	0.0	0.0	0.0	0.0
1388.00	38.50	7.33	447.00	0.0	0.0	0.0	0.0	0.0
1.43	0.12	0.16	2.30	0.07	0.02	76.50	0.95	0.0
0.04	3.61	0.96	0.0	0.04	10.30	0.74	2.59	0.56
0.0	86.71	9.39	0.27	1.09	2.54	0.0	0.0	0.0
59.66	87.76	8.24	0.85	0.36	2.95	0.0	0.0	0.0
2.34	87.76	8.24	0.85	0.36	2.95	0.0	0.0	0.0
0.0	87.73	8.47	0.78	0.43	2.91	0.0	0.0	0.0
38.00	72.54	4.96	1.66	1.87	9.75	10.97	1.18	0.0
0.0	86.71	9.39	0.27	1.09	2.54	0.0	0.0	0.0
0.0	88.09	8.32	0.74	0.51	2.83	0.0	0.0	0.0
0.0	86.09	5.68	2.17	1.03	4.11	0.18	0.0	0.0
0.0	0.0	0.0	0.0	0.0	0.0	0.0	0.0	0.0
0.0	0.0	0.0	0.0	0.0	0.0	0.0	0.0	0.0
0.0	0.0	0.0	0.0	0.0	0.0	0.0	0.0	0.0
0.0	0.0	0.0	0.0	0.0	0.0	0.0	0.0	0.0
0.0	0.0	0.0	0.0	0.0	0.0	0.0	0.0	0.0
0.0	0.0	0.0	0.0	0.0	0.0	0.0	0.0	0.0
0.0	0.0	0.0	0.0	0.0	0.0	0.0	0.0	0.0
2.76	86.71	9.39	0.27	1.09	2.54	0.0	0.0	0.0
75.27	88.21	8.24	1.07	0.0	2.86	0.0	0.0	0.0
10.53	87.82	5.62	2.57	0.54	3.45	0.0	0.0	0.0
5.12	86.43	4.56	2.73	0.57	5.71	0.0	0.0	0.0
6.33	37.50	1.90	0.67	0.99	7.10	58.94	0.0	0.0
0.0	0.0	0.0	0.0	0.0	0.0	0.0	0.0	0.0
0.0	0.0	0.0	0.0	0.0	0.0	0.0	0.0	0.0

THIS ARRAY CONTAINS INITIAL DATA

52.00	197.00	3.00	13.00	1982.00	400.00	500.00	0.0	0.0
835.00	840.00	2004.00	649.00	1778.00	0.0	0.0	0.0	0.0
1551.00	41.41	6.95	515.00	0.0	0.0	0.0	0.0	0.0
1.29	0.11	0.13	2.12	0.06	0.02	80.35	0.89	0.0
0.04	3.05	0.79	0.0	0.04	9.05	0.66	2.08	0.56
0.0	86.71	9.39	0.27	1.09	2.54	0.0	0.0	0.0
59.66	87.76	8.24	0.85	0.36	2.95	0.0	0.0	0.0
2.34	87.76	8.24	0.85	0.36	2.95	0.0	0.0	0.0
0.0	87.73	8.47	0.78	0.43	2.91	0.0	0.0	0.0
38.00	72.59	4.96	1.66	1.87	9.69	10.97	1.18	0.0
0.0	86.71	9.39	0.27	1.09	2.54	0.0	0.0	0.0
0.0	88.09	8.32	0.74	0.51	2.83	0.0	0.0	0.0
0.0	86.09	5.68	2.17	1.03	4.11	0.18	0.0	0.0
0.0	0.0	0.0	0.0	0.0	0.0	0.0	0.0	0.0
0.0	0.0	0.0	0.0	0.0	0.0	0.0	0.0	0.0
0.0	0.0	0.0	0.0	0.0	0.0	0.0	0.0	0.0
0.0	0.0	0.0	0.0	0.0	0.0	0.0	0.0	0.0
0.0	0.0	0.0	0.0	0.0	0.0	0.0	0.0	0.0
0.0	0.0	0.0	0.0	0.0	0.0	0.0	0.0	0.0
0.0	86.71	9.39	0.27	1.09	2.54	0.0	0.0	0.0
77.73	87.91	8.03	1.08	0.23	2.89	0.0	0.0	0.0
10.16	87.49	5.41	2.60	0.47	4.03	0.0	0.0	0.0
5.52	87.01	4.58	3.04	0.54	4.83	0.0	0.0	0.0
6.60	34.79	1.72	0.57	0.96	8.95	62.03	0.0	0.0
0.0	0.0	0.0	0.0	0.0	0.0	0.0	0.0	0.0
0.0	0.0	0.0	0.0	0.0	0.0	0.0	0.0	0.0

THIS ARRAY CONTAINS INITIAL DATA

52.00	209.00	3.00	13.00	1982.00	1600.00	1700.00	0.0	0.0
835.00	841.00	2003.00	626.00	1864.00	0.0	0.0	0.0	0.0
1592.00	41.45	7.36	489.00	0.0	0.0	0.0	0.0	0.0
1.08	0.11	0.14	2.45	0.06	0.01	76.85	1.17	0.0
0.04	3.37	1.18	0.0	0.06	10.00	0.81	2.25	0.56
0.0	86.71	9.39	0.27	1.09	2.54	0.0	0.0	0.0
59.66	87.76	8.24	0.85	0.36	2.95	0.0	0.0	0.0
2.34	87.76	8.24	0.85	0.36	2.95	0.0	0.0	0.0
0.0	87.73	8.47	0.78	0.43	2.91	0.0	0.0	0.0
38.00	72.41	4.98	1.66	1.86	9.90	10.94	1.37	0.0
0.0	86.71	9.39	0.27	1.09	2.54	0.0	0.0	0.0
0.0	88.09	8.32	0.74	0.51	2.83	0.0	0.0	0.0
0.0	86.09	5.68	2.17	1.03	4.11	0.18	0.0	0.0
0.0	0.0	0.0	0.0	0.0	0.0	0.0	0.0	0.0
0.0	0.0	0.0	0.0	0.0	0.0	0.0	0.0	0.0
0.0	0.0	0.0	0.0	0.0	0.0	0.0	0.0	0.0
0.0	0.0	0.0	0.0	0.0	0.0	0.0	0.0	0.0
0.0	0.0	0.0	0.0	0.0	0.0	0.0	0.0	0.0
0.0	0.0	0.0	0.0	0.0	0.0	0.0	0.0	0.0
0.0	86.71	9.39	0.27	1.09	2.54	0.0	0.0	0.0
77.12	87.91	8.03	1.08	0.23	2.89	0.0	0.0	0.0
10.08	87.49	5.41	2.00	0.47	4.03	0.0	0.0	0.0
5.54	87.01	4.58	3.04	0.54	4.83	0.0	0.0	0.0
7.27	34.79	1.72	0.57	0.96	8.95	62.03	0.0	0.0
0.0	0.0	0.0	0.0	0.0	0.0	0.0	0.0	0.0
0.0	0.0	0.0	0.0	0.0	0.0	0.0	0.0	0.0

THIS ARRAY CONTAINS INITIAL DATA

56.00	41.00	6.00	5.00	1982.00	1900.00	2000.00	0.0	0.0
840.00	842.00	2000.00	849.00	2332.00	0.0	0.0	0.0	0.0
2163.00	46.30	16.95	809.00	0.0	0.0	0.0	0.0	0.0
1.23	0.09	0.11	1.87	0.61	0.01	81.20	0.54	0.0
0.05	2.59	0.0	0.0	2.70	6.60	0.56	0.0	0.56
0.0	86.71	4.39	0.27	1.09	2.54	0.0	0.0	0.0
57.73	87.76	8.24	0.85	0.36	2.95	0.0	0.0	0.0
2.27	87.76	8.24	0.85	0.36	2.95	0.0	0.0	0.0
0.0	87.73	8.47	0.78	0.43	2.91	0.0	0.0	0.0
40.00	71.86	5.02	1.04	1.82	10.48	10.88	2.10	0.0
0.0	86.71	9.39	0.27	1.09	2.54	0.0	0.0	0.0
0.0	88.09	8.32	0.74	0.51	2.83	0.0	0.0	0.0
0.0	86.09	5.68	2.17	1.03	4.11	0.18	0.0	0.0
0.0	0.0	0.0	0.0	0.0	0.0	0.0	0.0	0.0
0.0	0.0	0.0	0.0	0.0	0.0	0.0	0.0	0.0
0.0	0.0	0.0	0.0	0.0	0.0	0.0	0.0	0.0
0.0	0.0	0.0	0.0	0.0	0.0	0.0	0.0	0.0
0.0	0.0	0.0	0.0	0.0	0.0	0.0	0.0	0.0
0.0	0.0	0.0	0.0	0.0	0.0	0.0	0.0	0.0
0.0	0.0	0.0	0.0	0.0	0.0	0.0	0.0	0.0
0.0	0.0	0.0	0.0	0.0	0.0	0.0	0.0	0.0
3.20	86.71	9.39	0.27	1.09	2.54	0.0	0.0	0.0
60.80	88.26	8.00	1.06	0.41	3.36	0.0	0.0	0.0
12.00	87.08	5.71	2.46	0.62	4.97	0.0	0.0	0.0
9.40	85.47	4.64	2.88	0.60	6.91	0.0	0.0	0.0
8.60	43.79	2.25	0.98	1.17	7.99	46.88	0.0	0.0
0.0	0.0	0.0	0.0	0.0	0.0	0.0	0.0	0.0
0.0	0.0	0.0	0.0	0.0	0.0	0.0	0.0	0.0

THIS ARRAY CONTAINS INITIAL DATA

55.00	63.00	5.00	25.00	1982.00	1130.00	1230.00	0.0	0.0
839.00	840.00	2000.00	424.00	1194.00	0.0	0.0	0.0	0.0
1166.00	25.50	9.72	396.00	0.0	0.0	0.0	0.0	0.0
1.42	0.10	0.12	1.40	0.24	0.01	84.80	0.85	0.0
0.04	2.51	0.0	0.04	2.29	0.53	0.49	0.01	0.56
0.0	86.71	9.39	0.27	1.04	2.54	0.0	0.0	0.0
57.73	87.76	8.24	0.85	0.36	2.95	0.0	0.0	0.0
2.27	87.76	8.24	0.85	0.36	2.95	0.0	0.0	0.0
0.0	87.73	8.47	0.78	0.43	2.91	0.0	0.0	0.0
40.00	71.86	5.02	1.64	1.82	10.48	10.88	2.10	0.0
0.0	86.71	9.39	0.27	1.04	2.54	0.0	0.0	0.0
0.0	88.09	8.32	0.74	0.51	2.83	0.0	0.0	0.0
0.0	86.09	5.68	2.17	1.03	4.11	0.18	0.0	0.0
0.0	0.0	0.0	0.0	0.0	0.0	0.0	0.0	0.0
0.0	0.0	0.0	0.0	0.0	0.0	0.0	0.0	0.0
0.0	0.0	0.0	0.0	0.0	0.0	0.0	0.0	0.0
0.0	0.0	0.0	0.0	0.0	0.0	0.0	0.0	0.0
0.0	0.0	0.0	0.0	0.0	0.0	0.0	0.0	0.0
0.0	0.0	0.0	0.0	0.0	0.0	0.0	0.0	0.0
3.06	86.71	9.39	0.27	1.04	2.54	0.0	0.0	0.0
67.16	88.12	7.92	0.85	0.43	3.03	0.0	0.0	0.0
10.33	85.28	5.71	2.63	0.71	5.69	0.0	0.0	0.0
10.11	83.61	4.66	2.56	0.73	8.24	0.0	0.0	0.0
9.34	44.38	2.35	1.07	1.22	9.28	49.48	0.0	0.0
0.0	0.0	0.0	0.0	0.0	0.0	0.0	0.0	0.0
0.0	0.0	0.0	0.0	0.0	0.0	0.0	0.0	0.0

THIS ARRAY CONTAINS INITIAL DATA

52.00	233.00	3.00	14.00	1982.00	1600.00	1700.00	0.0	0.0
838.00	842.00	2008.00	846.00	2462.00	0.0	0.0	0.0	0.0
2140.00	53.10	6.77	713.00	0.0	0.0	0.0	0.0	0.0
0.74	0.10	0.10	1.98	0.04	0.01	82.95	1.09	0.0
0.04	2.60	0.68	0.0	0.05	7.55	0.74	1.67	0.56
0.0	86.71	9.39	0.27	1.09	2.54	0.0	0.0	0.0
59.66	87.76	8.24	0.85	0.36	2.95	0.0	0.0	0.0
2.34	87.76	8.24	0.85	0.36	2.95	0.0	0.0	0.0
0.0	87.73	8.47	0.78	0.43	2.91	0.0	0.0	0.0
38.00	72.69	4.95	1.66	1.87	9.58	10.98	0.97	0.0
0.0	86.71	9.39	0.27	1.09	2.54	0.0	0.0	0.0
0.0	88.09	8.32	0.74	0.51	2.83	0.0	0.0	0.0
0.0	86.09	5.68	2.17	1.03	4.11	0.18	0.0	0.0
0.0	0.0	0.0	0.0	0.0	0.0	0.0	0.0	0.0
0.0	0.0	0.0	0.0	0.0	0.0	0.0	0.0	0.0
0.0	0.0	0.0	0.0	0.0	0.0	0.0	0.0	0.0
0.0	0.0	0.0	0.0	0.0	0.0	0.0	0.0	0.0
0.0	0.0	0.0	0.0	0.0	0.0	0.0	0.0	0.0
0.0	0.0	0.0	0.0	0.0	0.0	0.0	0.0	0.0
2.92	86.71	9.39	0.27	1.09	2.54	0.0	0.0	0.0
73.07	88.33	8.11	0.97	0.13	2.75	0.0	0.0	0.0
11.10	86.07	5.73	2.59	0.58	5.03	0.0	0.0	0.0
6.14	85.50	4.54	2.80	0.60	6.56	0.0	0.0	0.0
6.77	36.75	1.80	0.76	0.99	7.60	58.93	0.0	0.0
0.0	0.0	0.0	0.0	0.0	0.0	0.0	0.0	0.0
0.0	0.0	0.0	0.0	0.0	0.0	0.0	0.0	0.0

THIS ARRAY CONTAINS INITIAL DATA

52.00	221.00	3.00	14.00	1982.00	400.00	500.00	0.0	0.0
835.00	840.00	2004.00	854.00	2355.00	0.0	0.0	0.0	0.0
2100.00	49.65	7.89	691.00	0.0	0.0	0.0	0.0	0.0
0.92	0.10	0.10	2.03	0.04	0.01	82.30	1.08	0.0
0.04	2.69	0.77	0.0	0.03	7.75	0.71	1.65	0.56
0.0	86.71	9.39	0.27	1.09	2.54	0.0	0.0	0.0
59.66	87.76	8.24	0.85	0.36	2.95	0.0	0.0	0.0
2.34	87.76	8.24	0.85	0.36	2.95	0.0	0.0	0.0
0.0	87.73	8.47	0.78	0.43	2.91	0.0	0.0	0.0
38.00	72.41	4.98	1.66	1.87	9.90	10.95	1.37	0.0
0.0	86.71	9.39	0.27	1.09	2.54	0.0	0.0	0.0
0.0	88.09	8.32	0.74	0.51	2.83	0.0	0.0	0.0
0.0	86.09	5.68	2.17	1.03	4.11	0.18	0.0	0.0
0.0	0.0	0.0	0.0	0.0	0.0	0.0	0.0	0.0
0.0	0.0	0.0	0.0	0.0	0.0	0.0	0.0	0.0
0.0	0.0	0.0	0.0	0.0	0.0	0.0	0.0	0.0
0.0	0.0	0.0	0.0	0.0	0.0	0.0	0.0	0.0
0.0	0.0	0.0	0.0	0.0	0.0	0.0	0.0	0.0
0.0	0.0	0.0	0.0	0.0	0.0	0.0	0.0	0.0
2.92	86.71	9.39	0.27	1.09	2.54	0.0	0.0	0.0
72.38	88.33	8.11	0.97	0.13	2.75	0.0	0.0	0.0
11.74	86.07	5.73	2.59	0.58	5.03	0.0	0.0	0.0
5.89	85.50	4.54	2.80	0.60	6.56	0.0	0.0	0.0
7.08	36.75	1.80	0.76	0.99	7.60	58.93	0.0	0.0
0.0	0.0	0.0	0.0	0.0	0.0	0.0	0.0	0.0
0.0	0.0	0.0	0.0	0.0	0.0	0.0	0.0	0.0

THIS ARRAY CONTAINS INITIAL DATA

53.00	86.00	2.00	20.00	1981.00	1820.00	1930.00	0.0	0.0
839.00	839.00	2001.00	556.00	1674.00	0.0	0.0	0.0	0.0
1563.00	77.40	6.90	466.00	0.0	0.0	0.0	0.0	0.0
1.15	0.09	0.80	1.74	0.37	0.08	83.40	0.86	0.0
0.04	2.12	0.01	0.09	3.21	5.37	0.37	1.10	0.56
0.0	85.23	10.01	0.27	1.09	2.54	0.0	0.0	0.0
57.73	87.41	8.25	0.84	0.45	2.94	0.0	0.0	0.0
2.27	87.41	8.25	0.84	0.45	2.94	0.0	0.0	0.0
0.0	87.73	8.47	0.78	0.43	2.91	0.0	0.0	0.0
40.00	71.86	5.02	1.64	1.62	10.48	10.88	2.10	0.0
0.0	86.71	9.39	0.27	1.09	2.54	0.0	0.0	0.0
0.0	88.09	8.32	0.74	0.51	2.83	0.0	0.0	0.0
0.0	86.09	5.68	2.17	1.03	4.11	0.18	0.0	0.0
0.0	0.0	0.0	0.0	0.0	0.0	0.0	0.0	0.0
0.0	0.0	0.0	0.0	0.0	0.0	0.0	0.0	0.0
0.0	0.0	0.0	0.0	0.0	0.0	0.0	0.0	0.0
0.0	0.0	0.0	0.0	0.0	0.0	0.0	0.0	0.0
0.0	0.0	0.0	0.0	0.0	0.0	0.0	0.0	0.0
0.0	0.0	0.0	0.0	0.0	0.0	0.0	0.0	0.0
0.0	0.0	0.0	0.0	0.0	0.0	0.0	0.0	0.0
0.50	86.14	11.25	0.17	0.38	1.62	0.0	0.0	0.0
68.85	88.32	8.28	0.75	0.38	2.82	0.0	0.0	0.0
10.20	85.25	5.86	2.36	0.77	5.86	0.0	0.0	0.0
11.27	84.25	4.84	2.76	0.71	7.72	0.0	0.0	0.0
9.10	45.08	2.32	1.14	1.25	9.55	47.25	0.0	0.0
0.0	0.0	0.0	0.0	0.0	0.0	0.0	0.0	0.0
0.0	0.0	0.0	0.0	0.0	0.0	0.0	0.0	0.0

APPENDIX A-4

RELATIONSHIP OF NOMINAL LIQUID RESIDENCE TIME TO TRUE LIQUID RESIDENCE TIME

Ultimately, reaction yield behavior has to be correlated with true reactor residence time in order to improve insertion of reactor yield data into a kinetic correlation, and vice versa. Estimation of true residence time requires an adequate thermophysical correlation that can accurately predict phase behavior in the reactor.

Currently, available correlations for coal liquids are still under development, and these may require significant improvement before meaningful predictions are seen. Despite these uncertainties, however, the existing NGPA thermocorrelations* can be used to determine how much nominal residence times deviate from true residence times.

Nominal liquid residence time thus far defined can be related to true liquid residence time by the following equation:

$$\tau = \frac{(1 - E)}{(1 - E_0)} \frac{\rho_{SL}}{\rho_{SL}^0 \phi_{SL}} t \quad (A4-1)$$

- where
- τ = true slurry residence time
 - t = nominal residence time with entrance slurry conditions in the plug-flow reactor
 - E = true reactor void fraction
 - E_0 = reactor void fraction based on entrance slurry conditions in the plug-flow reactor
 - ρ_{SL} = slurry-phase density at reaction conditions
 - ρ_{SL}^0 = slurry-phase density at entrance conditions
 - ϕ_{SL} = slurry-phase weight fraction in the reactor at reaction conditions based on the weight of feed slurry

*The VLE correlation commonly known as NGPA (Natural Gas Processor's Association) in ICRC and APCI is otherwise known as the Vapor-Liquid Equilibrium Model of Chao Seader, as modified by Grayson and Streed (Chao, K. C., and J. D. Seader. 1961. AIChE J. 7:598; Grayson, H. G., and C. W. Streed. June 1963. The 6th World Petroleum Congress, Frankfurt-Mein. Section VII, paper 20).

The void fraction of the plug-flow reactor expressed as a function of superficial gas velocity (equation 1 on page 34) is:

$$E = 0.902U_G^{0.415}$$

Therefore:

$$E/E_0 = (U_G/U_H^0)^{0.415} \quad (A4-2)$$

and:

$$\tau = \left[\frac{1 - (U_G/U_H^0)^{0.415} E_0}{1 - E_0} \right] \times \left(\frac{\rho_{SL}}{\rho_{SL}^0 \phi_{SL}} \right) \times t \quad (A4-3)$$

Various physical parameters affecting the residence time correlation were evaluated for actual plug-flow liquefaction yield data based on flash calculations using the NGPA thermocorrelation; these are listed in Table A4-1. The results indicate that the true residence times for runs 52-22 and 52-91 would be 7 and 16% longer than the nominal residence times of 30 and 41 min at the specified process conditions, respectively.

The ratio $(1 - E)/(1 - E_0)$ is close to unity, with no more than about 1% deviation. Therefore, equation (A4-3) may be reasonably approximated as:

$$\tau = (\rho_{SL}/\rho_{SL}^0 \phi_{SL}) t \quad (A4-4)$$

The above equation indicates that the deviation of true residence time from nominal residence time should be mainly due to $(\rho_{SL}/\rho_{SL}^0 \phi_{SL})$. The degree of precision that the existing thermoprograms can provide for the parameters should be evaluated in the future, but it is beyond the scope of the current study.

Table A4-1

Typical Plug-Flow Reactor Phase Properties Estimated by
the NGPA Thermocorrelation^a

	Sample no.	
	55-22	55-91
Temp (°F)	840	840
t (min)	30.4	41.3
P_{H_2}/P	0.712	0.650
ρ_V (lb/ft ³)	2.913	3.495
ρ_{SL} (lb/ft ³) ^b	53.948	53.763
U_H^0/U_{SL}^0	7.465	7.465
U_G/U_{SL}	8.453	8.854
U_G/U_H^0	0.961	0.948
$(U_G/U_H^0)^{0.415}$	0.983	0.978
ϕ_{SL} (lb/lb of feed slurry)	0.709	0.655
$\rho_{SL}/(\rho_{SL}^0 \phi_{SL})$	1.079	1.164
E_0	0.409 ^c (0.318) ^d	0.379 ^c (0.283) ^d
E	0.417 ^c (0.325) ^d	0.384 ^c (0.285) ^d
$(1 - E)/(1 - E_0)$	0.987	0.992
τ/t	1.065	1.155
τ (min)	32.4	47.7

^a ρ_V = vapor density; U_H^0/U_{SL}^0 = ratio of volumetric flow rates of hydrogen to slurry in the reactor based on the entrance mass flow rates.

^b Evaluation of slurry density is based on the assumption that the average specific gravity of coal mineral matter is 2.7 g/cm³.

^c Based on the tube section of the reactor volume, excluding transfer-line volume.

^d Based on total reactor volume.